RECONSTRUCTING FLORIDA LACUSTRINE ENVIRONMENTS FROM THE LATE PLEISTOCENE TO THE PRESENT

By

THOMAS ELLIOTT ARNOLD

A DISSERTATION PRESENTED TO THE GRADUATE SCHOOL
OF THE UNIVERSITY OF FLORIDA IN PARTIAL FULFILLMENT
OF THE REQUIREMENTS FOR THE DEGREE OF
DOCTOR OF PHILOSOPHY

UNIVERSITY OF FLORIDA

2017

To my committee

ACKNOWLEDGMENTS

I would like to thank the entire Geological Sciences Department: professors, staff, students, and lab technicians. I am especially indebted to Mark Brenner, Jason Curtis, and William Kenney. These three “raised” me in the field of limnology and chemistry. Their assistance was invaluable, and will never be forgotten. I would also like to thank Tom Bianchi for unbridled access to his organic geochemistry lab, and Kate Freeman and Aaron Diefendorf for training in lab methods. Funding from the University of Florida was provided by the Land Use and Environmental Change Institute (LUECI) and the Water Institute. Additional support for this research was provided by the Inter-university Training in Continental-scale Ecology (ITCE Project) under Award Numbers EF-1137336 and EF-1240142 from the National Science Foundation

TABLE OF CONTENTS

page

LIST OF TABLES

LIST OF FIGURES

Abstract of Dissertation Presented to the Graduate School
of the University of Florida in Partial Fulfillment of the
Requirements for the Degree of Doctor of Philosophy

RECONSTRUCTING FLORIDA LACUSTRINE ENVIRONMENTS FROM THE LATE PLEISTOCENE TO THE PRESENT

By

Thomas Elliott Arnold

May 2017

Chair: Mark Brenner
Major: Geology

I analyzed bulk geochemical and biomarker data from subtropical lakes in Florida to determine how environmental change and anthropogenic effects are recorded in lacustrine sediments. On short (i.e. centennial) time scales, anthropogenic impacts are apparent in more recent sediments from three Florida lakes, and manifest themselves as increased algal lipid biomarker concentrations, more enriched $\delta^{13}C$ values, and lower TOC:TN ratios. Across millennial time scales in Lake Harris, biomarker concentrations and their carbon isotopic values respond to regional hydrological changes in the early Holocene that were triggered by eustatic sea level rise. The carbon ($\delta^{13}C$) and hydrogen (δD) isotope ratios of lipid biomarkers extracted from a Lake Tulane sediment core serve as paleohydrology proxies across stadial/interstadial time scales during the late Pleistocene. $\delta^{13}C$ and δD lipid values of specific *n*-alkane chain lengths, demonstrate that subtropical Florida responded out of phase with high-latitude environmental changes during at least three of the late Pleistocene stadial-interstadial transitions. The region remained warm and wet, when the North Atlantic was cold and dry, because of oceanic/atmospheric patterns that limited northward export of warm, saline water. All three studies presented within, broadly agree with published literature on similar topics

spanning identical timeframes. Thus, we are confident in the application of lacustrine biomarker data to measure regional change across highly variable time scales.

CHAPTER 1
INTRODUCTION

In the following three research papers, I present the results of biomarker studies from five Florida lakes. The first paper compares up-core changes in bulk geochemical data, as well as alkyl lipid concentrations to estimate the sources of organic matter and the changes in trophic status to three Florida lakes over the past ~150 years. Bulk geochemical variables including: organic carbon percentages, organic carbon to nitrogen ratios, and carbon isotope values of total organic carbon ($\delta^{13}C_{TOC}$), can be applied as general techniques to measure productivity, vascular versus non-vascular plants sources, and autochthonous carbon assimilation, respectively. Although they only represent a small fraction of bulk organic matter, alkyl lipids, including *n*-alkanes and fatty acids, provide greater source specificity. Alkanes are hydrocarbons, a class of organic compounds that consist of the elements carbon and hydrogen (Bianchi and Canuel, 2011). Alkanes with fewer than 20 carbon atoms are typically synthesized by algae. Alkanes with intermediate numbers of carbon atoms, i.e. between 20-25 carbon atoms, are typically, but not exclusively, synthesized by aquatic macrophytes. Long-chain alkanes, i.e. > 25 carbon atoms, are most abundant in the leaves of woody, terrestrial plants. Fatty acids are lipid biomarkers that consist of variable chain-length hydrocarbon units, bound to a carboxyl functional group. Similar to alkanes, fatty acids can be subdivided into bacterial, algal, and terrestrial sources. As a group, fatty acids are less source specific than *n*-alkanes: long-chain lengths are synthesized by vascular plants, polyunsaturated varieties by algae, and branched fatty acids by bacteria. We measured concentrations of these biomarkers to assess temporal changes in organic matter source to each lake.

The second paper uses identical bulk geochemical variables to assess changes in organic matter sources to Lake Harris, Florida, USA, but introduces the $\delta^{13}C$ analyses of individual alkane chain lengths, known as compound-specific isotope analyses (CSIA). With the CSIA approach I document complex changes in regional hydrology over millennial scales. I hypothesize that the sources of organic matter (i.e. allochthonous vs. autochthonous) to the lake's sediments changed in concert with regional hydrologic and environmental events that occurred as the earth's climate stabilized in the mid-Holocene. Shifts in alkane biomarkers should correspond to fluctuations in the regional water table that were caused by these hydrological changes.

The final paper documents shifts in sub-tropical climate during Heinrich Events (HE) in the North Atlantic. HE are recorded in the sediment record of the North Atlantic as layers of ice-rafted debris (IRD), lithic fragments from rocks of continental origin, which were derived from the calving and melting of large continental ice sheets (Bond et al., 1993). During Earth's last glacial interval, these periodic iceberg discharges perturbed global heat transport via reduction in the Atlantic meridional overturning circulation (AMOC) (Lynch-Stieglitz et al., 2014). CSIA of carbon and hydrogen in *n*-alkanes extracted from the sedimentary record of Lake Tulane were analyzed to provide an approximation of precipitation changes, or more specifically aridity levels, in the subtropics during these extreme cold periods in the North Atlantic.

CHAPTER 2
SOURCES OF ORGANIC MATTER TO THREE LAKES OF DIFFERENT TROPHIC STATUS

Introduction: Sheelar, Wauberg, and Apopka

There are nearly 8,000 lakes in the state of Florida with surface area >10 ha. Most are relatively shallow dissolution features (mean depth <5 m, maximum depth <20 m). From a geological perspective, these lakes are relatively recent additions to the landscape. Most began to accumulate lacustrine sediment in the early Holocene (~8,000 yrs BP), as water table elevations rose and climate became wetter (Watts, 1980). Florida lakes span the entire trophic state continuum, from ultra-oligotrophic in the quartz sands of the Lake Wales Ridge, to hyper-eutrophic in some low-lying urbanized and agricultural areas. Furthermore, many naturally eutrophic lakes are located in regions characterized by deposits of the phosphorus-rich Hawthorn Group. The trophic status of lakes in close proximity to Hawthorn sediments is strongly correlated to regional geology, and these systems may have a long history of having been eutrophic (Brenner et al., 1999).

The consequences of natural and anthropogenic eutrophication of fresh water bodies have been well documented since the early 20th century (e.g., Hasler, 1947). More recently, studies have verified the correlation between excessive nutrient loading (primarily nitrogen and phosphorus) and harmful algal blooms (Correll, 1998; Anderson et al., 2002), fish kills (Landsberg et al., 2009), and reductions in biological diversity (Craft et al., 1995; Craft and Richardson, 1997). A recent analysis of surface water quality in Florida classified 8% of rivers and streams, 26% of lakes, and 21% of estuaries in the state as impaired because of excessive nitrogen and/or phosphorus concentrations (Florida Department of Environmental Protection, 2008).

Lakes function as natural repositories for organic matter derived from aquatic (autochthonous) and terrestrial (allochthonous) primary and secondary productivity. Thus, lake sediments serve as archives of past changes in the water column and watershed. In Florida, numerous studies have tracked past changes in lacustrine productivity (e.g. Gu et al., 1996; Riedinger-Whitmore et al., 2005). Organic and inorganic elemental concentrations in dated sediment cores, including N, P, C and Si, have been used to infer temporal trends in cultural eutrophication (Bianchi and Canuel, 2011). More recently, $\delta^{13}C$ and $\delta^{15}N$ measurements on bulk organic matter (OM) (Torres et al., 2012) and photosynthetic pigments in sediments (Waters et al., 2015) have been employed to reconstruct past lacustrine trophic status and identify the primary producer communities.

Most previous work on eutrophication in Florida lakes relied on analysis of bulk sediment or bulk OM, which limited the ability to identify the source(s) of the analyzed material. In other studies, for which biomarkers were assayed, one had to be cognizant of the fact that such molecules may represent a small fraction of the total organic matter preserved within the lake. Determination of the biogeochemical processes that occur in the water column and in deposited sediments remains a challenge. Combined use of bulk sediment and biomarker data, however, can help answer general questions about such processes in elemental pools, as well as specific questions about the sources of these elements to the overall pool. The primary goals of this study were to investigate the source(s) of organic carbon to the sediment in three subtropical Florida lakes, evaluate recent changes in lacustrine productivity of the water bodies, and better understand recent human impacts on these aquatic ecosystems. I used a multi-

biomarker approach that included *n*-alkanes and fatty acids, as well as bulk sediment isotopic analyses, to examine recent changes in autochthonous and allochthonous carbon inputs to the three lakes.

Study Sites

Lake Sheelar is a small (0.07 km^2), relatively deep (mean depth = ~8 m, z_{max} = ~21 m) lake in Mike Roess Goldhead Branch State Park, north of Keystone Heights, FL. It is underlain by quartz sands and is a poorly buffered system, with low pH (5.4), low conductivity (18 µS/cm), and low total alkalinity (0.8 mg/L as $CaCO_3$). It is also an oligotrophic (total phosphorus = 4 µg/L, total nitrogen = 86 µg/L, chlorophyll *a* = 1.7 µg/L), clear-water (Secchi depth = 7.5 m) system (Florida Lakewatch, 2003), which receives some hydrologic input from shallow groundwater seeps along its northwest shoreline.

Lake Wauberg is located south of Gainesville, FL and is primarily surrounded by hardwood pine and oak forests. The lake has a surface area of 1.5 km^2, and is shallow, with a maximum depth of ~3.7 m (Florida Lakewatch, 2003). Wauberg receives water mainly from groundwater and direct rainfall, and has a shallow outflow into Sawgrass Pond. Unlike Sheelar, Wauberg is eutrophic, with mean concentrations of total phosphorus = 112 µg/L, total nitrogen = 1670 µg/L, chlorophyll *a* = 82.1 µg/L, and a Secchi depth of 0.6 m (Florida Lakewatch, 2003). Near-surface geologic deposits around the lake are derived from the phosphate-rich Hawthorn Formation, and high phosphorus concentrations have been measured in groundwater entering the lake. Gu et al. (2006) reported that phytoplankton is the dominant primary producer group in the lake, with limited macrophyte abundance, possibly a consequence of light limitation.

The phytoplankton populations have been a dominant feature of Lake Wauberg's flora since at least the 1930s (Carr, 1934).

Lake Apopka, central Florida, is the largest (124 km^2) and shallowest (mean depth = 1.7 m) of the three study lakes. It is a hyper-eutrophic system with a mean total phosphorus concentration of 192 µg/L, mean total nitrogen concentration of 3906 µg/L, mean chlorophyll-*a* concentration of 96 µg/L, and a Secchi depth of 0.3 m. Water from the lake flows out to Beauclair Canal, which is hydrologically linked to other lakes in the Harris Chain of Lakes. Apopka shifted from a clear-water, macrophyte-dominated system, to a phytoplankton-dominated water body in the middle of the twentieth century (Waters et al., 2015). This shift has been attributed to high phosphorus loading and inputs of dissolved color from muck farms that operated along the north shore (Schelske et al., 2005).

Organic Matter Sources of *n*-Alkyl Lipids

The major sources of alkanes to lacustrine sediments are algae, bacteria, submerged and emergent macrophytes, and woody terrestrial plants. Because these sources generally synthesize unique alkane homologues, alkanes can be used to identify the source of organic matter in lake sediments. Algae and bacteria primarily synthesize short-chain *n*-alkanes, including *n*-$C_{17\text{-}19}$ (Cranwell, 1987). Macrophytes synthesize a broad range of *n*-alkanes, but *n*-$C_{21\text{-}25}$ predominate among the submerged varieties (Ficken et al., 2000). Odd-numbered, long-chain hydrocarbons (*n*-$C_{27\text{-}33}$) are characteristic of higher terrestrial plants, and are stable over the longest time periods (Muri and Wakeham, 2006).

Aliphatic, or acyclic, hydrocarbons are "defunctionalized" lipids and are therefore least susceptible to post-depositional degradation (Meyers, 2003). Studies on

hydrocarbon preservation in lakes demonstrated that these compounds are stable over at least decadal time scales (Wakeham et al., 2004). Other studies have reported stability of hydrocarbons over much longer, i.e. geologic timescales (Castañeda and Schouten, 2011). This does not imply that *n*-alkanes are immune from decomposition/alteration, as biodegradation does occur in both aerobic and anaerobic environments, and preferentially targets low-molecular weight molecules (Wakeham et al., 2004; Bianchi and Canuel, 2011).

Unlike hydrocarbons, fatty acids are more susceptible to diagenesis and alteration. A study from a single lake demonstrated that fatty acids degraded twice as fast as alkanes in oxic sediments (Muri and Wakeham, 2006). Another study of a 0.5-m-long lake sediment core showed that fatty acids were sensitive to post-depositional alteration, but hydrocarbons were not (Ho and Meyers, 1994). Nevertheless, these lipids (fatty acids) have been used successfully to track sources of organic matter in many aquatic systems (Meyers, 2003; Zhang et al., 2015). Freshwater algae synthesize C_{16} and C_{18} saturated fatty acids (chain lengths that are ubiquitous among higher lifeforms), as well as polyunsaturated ($C_{18:2}$ and $C_{18:3}$) and monounsaturated ($C_{16:1\omega7}$) varieties. Odd-numbered (C_{15}, C_{17}) and branched short-chain fatty acids (*iso*- and *anteiso*-C_{15}) are typically synthesized by bacteria, and even-numbered, long-chain fatty acids ($\geq C_{24}$) are from higher plants (Palomo and Canuel, 2010).

Ratios of long-chain-length to short-chain-length lipids can be used to assess the relative contributions of terrestrial and aquatic organic matter to the sediments (Meyers, 2003). For fatty acids (TAR_{FA}) this is calculated as:

$$TAR_{FA} = (C_{24} + C_{26} + C_{28})/(C_{12} + C_{14} + C_{16}) \quad (1\text{-}1)$$

and for hydrocarbons (TAR_{HC}) as:

$$TAR_{HC} = (C_{27} + C_{29} + C_{31})/(C_{15} + C_{17} + C_{19}) \quad (1\text{-}2)$$

Furthermore, the proportional contribution of submerged aquatic vegetation, relative to emergent and terrestrial vegetation, P_{aq} (Ficken, 2000), is calculated as:

$$P_{aq} = (C_{23} + C_{25})/(C_{23} + C_{25} + C_{29} + C_{31}) \quad (1\text{-}3)$$

These equations are broadly applicable, but must be used with caution as shorter-chain-length *n*-alkyl lipids are preferentially degraded.

Core Collection and Sampling

We collected a sediment-water interface core from each of the three lakes using a piston corer designed to retrieve undisturbed sediments (Fisher et al., 1992). In Lake Sheelar, 80 cm of sediment was retrieved, in Lake Wauberg, 90 cm, and in Lake Apopka, 100 cm. Cores were kept vertical and the poorly consolidated deposits were extruded upward and sampled into labeled containers at 2-4-cm intervals. Samples were frozen, freeze-dried, and ground with a mortar and pestle in preparation for geochemical analyses. Total carbon and total nitrogen (TN) were measured on a Carlo Erba NA1500 CNS elemental analyzer. Inorganic carbon was measured on a UIC Coulometrics 5012 CO_2 coulometer coupled with an AutoMate automated carbonate preparation device (AutoMateFX.com). Total organic carbon (TOC) was calculated as the difference between total carbon and inorganic carbon. TOC:TN values are expressed on a (wt/wt) basis. Dried sediment for $\delta^{13}C_{TOC}$ analyses was pretreated with 1N HCl to remove inorganic carbon, and then measured on a Carlo Erba NA1500 CNS

elemental analyzer interfaced with a Thermo Scientific Delta V Advantage isotope-ratio mass spectrometer. Isotopic compositions were normalized to the VPDB scale, and reported in standard delta notation as follows:

$$\delta^{13}C = [(({}^{13}C/{}^{12}C)\ \text{sample}/({}^{13}C/{}^{12}C)\ \text{standard})) - 1] \times 1000 \qquad (1\text{-}1)$$

Chronology

Cores were dated by ^{210}Pb, using gamma counting methods described by Schelske et al. (1994). Sediment ages were calculated using the constant rate of supply model (Appleby and Oldfield, 1983). Age errors were propagated using first-order approximations and calculated according to Binford (1990). ^{210}Pb dates could not be calculated for Lake Apopka, because the lake surface area was altered in the middle of the 20th century, thus violating an assumption of the constant rate of supply model. A ^{210}Pb-based age model developed by Schelske (1997) for a core from the same site, however, showed that unsupported ^{210}Pb activity (dpm/g) was negligible below 70 cm core depth, suggesting an age at that depth of ~110 years, i.e. five ^{210}Pb half-lives.

Lipid Extraction, Purification, and Quantification

Lipids were extracted from 1 g of freeze-dried sediment with an Accelerated Solvent Extractor ASE200 (Dionex), using 2:1 (v/v) dichloromethane(DCM):methanol through three extraction cycles at 10.3 MPa (1500 psi) and 100°C. Total lipid extracts (TLE) were concentrated under a gentle stream of nitrogen, and the neutral and acidic lipid fractions were separated via base saponification of the TLE with 0.5 M KOH in methanol at 70 C for 2 h. Neutral lipids were extracted from the aqueous solution with hexane, and after acidification with concentrated HCl, the acidic fraction was extracted

using 4:1 (v/v) hexane:DCM. The acidic fraction was blown to dryness and derivatized with BF_3 in methanol, and extracted again with DCM as fatty acid methyl-esters (FAMES). Neutral lipids were further separated, based on polarity, into compound classes, by column chromatography, using 5% deactivated silica gel, according to methods modified from Nichols (2011). Hydrocarbons were eluted from the silica gel column with 4.5 ml of 9:1 Hexane:DCM, and saturated hydrocarbons were separated from alkenes on 5% Ag-impregnated silica gel (w/w) with 4 ml of hexane and ethyl acetate, respectively. Branched and cyclic saturated hydrocarbons were isolated from *n*-alkanes with triple urea adduction.

Alkane and fatty acid concentrations were measured and identified on a Thermo Scientific Trace 1310 gas chromatograph with a Supelco Equity 5 column, interfaced to a Thermo Scientific TSQ 8000 triple quadrupole mass spectrometer with electron ionization. For the hydrocarbons, the inlet was operated in splitless mode at 280°C. The column flow rate was set to 2.0 ml/min and the oven was programmed to an initial temperature of 60°C and held for 1 minute, then ramped to 320°C at 6°C/min and held for 20 minutes. Quantification was based on the calibration curves generated from the peak areas of external standards (C_7-C_{40}) with concentrations ranging from 5-250 μg/ml. Androstane was used as an internal standard, and recovery rates for *n*-alkanes were >80%. For fatty acids, the split/splitless inlet was operated in split mode, at 280°C with a split ratio of 10:1. The column flow rate was 1.5 ml/min and the oven started at an initial temperature of 60°C and was held for 1 minute, followed by a ramp to 140°C at 15°C/min, and finally to 320°C and held at that temperature for 20 min.

Bulk Geochemical Data: Lakes Sheelar, Wauberg, Apopka

TOC, TOC/TN, and $\delta^{13}C_{TOC}$ are shown in Figure (2-1). Highest average TOC percentages were found in Lake Wauberg sediments, followed by the sediments of Lake Apopka. Lowest average TOC values were measured in the Lake Sheelar core. Average TOC:TN was similar for Wauberg and Apopka, with values of 10.67 and 11.58, respectively, but was substantially higher in Sheelar (15.40). In Sheelar, the TOC:TN values decrease up-core, from a maximum value of 18.69 at 80 cm depth, to a minimum value of 12.03 at 5 cm depth. Ranges for TOC:TN values are less extreme in Wauberg and Apopka, with standard deviations of only 0.5 and 0.4, respectively. Mean $\delta^{13}C_{TOC}$ values across the three lakes become more positive with increasing trophic status, from -29.11‰ (Sheelar), to -22.82‰ (Wauberg), to -20.32‰ (Apopka). Carbon stable isotope values became enriched in ^{13}C up-core in the Wauberg and Apopka sediments, whereas Sheelar $\delta^{13}C_{TOC}$ values remained relatively constant throughout the core.

Alkane Concentrations: Lakes Sheelar, Wauberg, Apopka

ACL, P_{aq}, and TAR_{HC} values for each lake are displayed in Tables 2-1, 2-2, and 2-3. Average ACL values for all three lakes were similar (~28) and varied only slightly throughout each core. Average P_{aq} values for the three lakes were also relatively similar, ranging from 0.44 to 0.49. Average TAR_{HC} values in Lake Sheelar (39.41), however, were approximately 4-fold and 10-fold higher than TAR_{HC} values in Wauberg (10.98) and Apopka (3.49).

Alkanes were grouped by their most probable biological source: algae (*n*-$C_{17\text{-}19}$), macrophyte (*n*-$C_{23\text{-}25}$), and terrestrial (*n*-$C_{27\text{-}31}$). Representative homologues are shown in Figure 2-2. In Sheelar, there was no discernible stratigraphic trend in the concentrations of *n*-alkanes within the three groups. Of note, however, are the low

concentrations of algal-derived hydrocarbons, which never exceed 15 µg/g OC throughout the core, and high concentrations of the terrestrial alkane, *n*-C_{29}, throughout the entire core. In contrast to Sheelar, *n*-C_{17} concentration in the Wauberg and Apopka cores increases by an order of magnitude at ~40 cm core depth, reaching maximum concentrations in the upper 10 cm. This is the most abundant chain-length in the top 20 cm of sediment in both lakes. The increasing up-core trend in *n*-C_{17} concentration in Wauberg and Apopka is accompanied by a decrease in terrestrial-derived alkanes, by 119.3 µg/g OC and 37.8 µg/g OC, respectively.

Fatty Acid Concentrations: Lakes Sheelar, Wauberg, Apopka

Fatty Acids were grouped based on their primary source, in a manner similar to the *n*-alkane data. These data, along with TAR_{FA} values for each lake, are displayed in Tables 2-1, 2-2, and 2-3. Terrestrial, long-chain fatty acids (LCFA) represent the sum of even-carbon fatty acids from C_{24} to C_{30}. Algae-derived polyunsaturated fatty acids (PFA) are the sum of $C_{18:2}$ and $C_{18:3}$. Bacteria produce a wide array of fatty acids (BFA), and are represented in this study by the following chain lengths: branched *iso* and *anteiso*-$C_{15:0}$, monounsaturated $C_{16:1\omega7}$, $C_{18:1\omega7}$, $C_{18:1\omega9}$, and the odd-carbon-number saturated fatty acids, $C_{15:0}$ and $C_{17:0}$.

Long-chain, saturated fatty acids dominated the record in all three lakes, with $C_{12:0}$, $C_{16:0}$, $C_{24:0}$, $C_{26:0}$, $C_{28:0}$ being the most abundant homologues. Each of the lakes displays large up-core concentration increases in algae- and bacteria-derived fatty acids, and to a lesser magnitude, decreases in LCFA concentrations (Figure 2-3, 2-4, 2-5). Of note are distinct patterns of bacteria-derived fatty acid (BDFA) abundances in the sediment records. In Sheelar, two groups of BDFA display similar concentration

patterns throughout the core: group 1 (saturated, branched *iso* and *anteiso*-$C_{15:0}$, $C_{16:1\omega7}$, and $C_{18:1\omega9}$), group 2 ($C_{17:0}$ and $C_{18:1\omega7}$). The two groups of BDFA from Wauberg that vary correspondingly in concentrations are: group 1 (saturated, branched *iso* and *anteiso*-$C_{15:0}$, $C_{17:0}$), and group 2 ($C_{16:1\omega7}$, $C_{18:1\omega9}$, and $C_{18:2\omega7}$). In Apopka, all the BDFA follow similar up-core patterns of abundance.

Interpreting Bulk Geochemical Data: Lakes Sheelar, Wauberg, Apopka

The three lakes in this study can be loosely grouped into trophic state categories using the bulk geochemical data. The Sheelar core has the lowest TOC concentrations, highest TOC:TN values, and most depleted $\delta^{13}C_{TOC}$ signatures throughout, whereas the Lake Apopka and Wauberg cores have higher OC levels, lower TOC:TN, and less negative carbon isotope values. The values of these three variables in the Sheelar core are indicative of lower trophic status, and in Apopka and Wauberg of higher productivity (Meyers, 1997; Brenner et al., 1999). There are, however, limitations to using only bulk sediment data to infer trophic status, which are apparent when comparing up-core changes in sediment TOC:TN and $\delta^{13}C_{TOC}$ values. In Lake Sheelar, TOC:TN exhibits the largest up-core decrease, suggestive of increasing relative algal contributions to the sediment. Across the same interval, $\delta^{13}C_{TOC}$ signatures remain essentially unchanged, which implies no change in primary productivity. Furthermore, the carbon isotope values (-30.39‰ to -28.44‰) are characteristic of a constant, and primarily C_3, terrestrial carbon source to the sediments (Peterson and Fry, 1987; Magill et al., 2013). TOC:TN may display an up-core decrease in the Sheelar core because of N processing in the sediments. The plot of %N and %C (Figure 2-6) shows that the lower TOC:TN values near the surface are a consequence of relatively higher %N values up-core, not greater

TOC concentrations. Nitrogen removal from sediments and re-deposition into the near-surface sediments of this low-nutrient system could be responsible for the stratigraphic distribution of TN in the sediments. In Apopka, TOC:TN values decrease slightly up-core while $\delta^{13}C_{TOC}$ values increase substantially, from -23.24‰ to -17.45‰. A similar pattern occurs in Lake Wauberg, where $\delta^{13}C_{TOC}$ increases by nearly 4‰, from -25.93‰ to -22.03‰ and TOC:TN varies by <2. Although the TOC:TN values and $\delta^{13}C$ signatures in Apopka and Wauberg both indicate primarily algal sources of organic carbon in the sediment (Filley et al., 2001), negligible changes in TOC:TN fail to capture the increasing algal contributions that are indicated by the up-core decrease in carbon isotope values. A possible explanation for this discrepancy may lie in the historic concentrations of algal and aquatic macrophyte communities. If substantial populations of both phytoplankton and submerged macrophytes with similar TOC:TN values (see review of TOC:TN values in Bianchi and Canuel, 2011) were already well established in both lakes, a further increase in trophic state would cause an increase in $\delta^{13}C_{TOC}$ values, but not significantly affect TOC:TN levels.

Based on $\delta^{13}C_{TOC}$ alone, we infer relatively stable, oligotrophic conditions in Lake Sheelar throughout the time period represented by the core. The ^{210}Pb dates extend to a depth of only 24 cm (1885 AD), indicating relatively low mean sedimentation rate, thereby further confirming the lake's status as a historically oligotrophic system. Carbon isotope studies on a sediment core from Lake Annie, another oligotrophic Florida lake, similarly conclude that low $\delta^{13}C_{TOC}$ values are the result of primarily allochthonous contributions to the sediments (Torres et al., 2012). The up-core trend in $\delta^{13}C_{TOC}$ values in the Wauberg and Apopka cores suggests the trophic status of both lakes increased

from the bottom of the core to the most recent sediments. The up-core increase in $\delta^{13}C_{TOC}$ values is most likely associated with greater phytoplankton abundance that results in reduced discrimination against ^{13}C and/or active uptake of HCO_3^- (Brenner et al., 1999). This phenomenon was documented in Lake Wauberg by Gu et al. (2006), who measured ^{13}C enrichment in particulate organic matter during periods of high productivity and carbon limitation. In the Apopka core, both average $\delta^{13}C_{TOC}$ values and the rate of ^{13}C enrichment were greater than in the Wauberg core. Some of this enrichment is almost certainly a consequence of high $\delta^{13}C$ values of dissolved inorganic carbon (DIC). Carbon-13 enrichment of the DIC pool in Lake Apopka (average DIC = 9.0‰) was documented by Gu et al. (2004), and attributed to methanogenesis in the sediments. Methanogenesis produces isotopically depleted CH_4, and isotopically enriched CO_2 (Whiticar, 1999). Utilization of this enriched carbon source by primary producers elevates their $\delta^{13}C$ signatures. Over time, as the lake becomes more productive, and incorporation of ^{13}C-enriched CO_2 increases, the carbon isotope value of the sedimented organic matter consequently becomes more enriched.

The bulk geochemical data enable us to reach the following conclusions about each of the three lakes: 1) Lake Sheelar is, and historically has been an oligotrophic water body, with primarily allochthonous, but some autochthonous inputs to its sediment carbon pool. TOC:TN values decrease up-core, possibly indicating an increase in algal input relative to terrestrial input, but the $\delta^{13}C_{TOC}$ values remain well within the terrestrial range throughout the entire core. The Wauberg and Apopka cores both show evidence for recent increases in primary productivity and contributions of algal biomass, as evidenced by higher $\delta^{13}C_{TOC}$ and lower TOC:TN values. The up-core increase in

$\delta^{13}C_{TOC}$ in both cores is the result of carbon limitation and/or uptake of HCO_3^-. In Apopka, $\delta^{13}C_{TOC}$ is very high because of methanogenesis, which led to ^{13}C-enriched DIC.

Interpreting Alkyl Lipid Data: Lakes Sheelar, Wauberg, Apopka

Concentrations of *n*-alkanes in the Sheelar core suggest little change in organic matter sources through time. From the bottom of the core to the top, *n*-C_{17} concentrations remain low, while *n*-C_{23-25} and *n*-C_{27-31} concentrations, although variable, are the most abundant homologues. Furthermore, we see no evidence for cultural eutrophication in the hydrocarbon record (i.e. increasing *n*-C_{17} concentrations, higher $\delta^{13}C_{TOC}$ values). In addition, hydrocarbon proxy ratios TAR_{HC} and P_{aq} both indicate primarily terrestrial and submerged/emergent macrophyte contributions to the sediment organic carbon pool. These data, however, conflict with bulk TOC:TN data, which decrease upcore, implying relatively greater algal contributions to the sediment, and hence increased lacustrine productivity. TOC:TN values, however, can be misleading and are susceptible to *in situ* alteration (Meyers, 2003), and the large range in ratios results in overlapping values for terrestrial and aquatic sources (Bianchi and Canuel, 2011). Furthermore, the TOC:TN data from sediments are at odds with modern lake water phosphorus (4 µg/L), nitrogen (86 µg/L) and chlorophyll *a* (1.7 µg/L) concentrations, all of which imply very low limnetic production.

From the bottom of the Lake Wauberg core (88 cm) to ~40 cm core depth, vascular plant *n*-alkanes (*n*-C_{23-31}) dominate the hydrocarbon record. Above 40 cm (AD 1986), algal-derived *n*-alkanes increase, and higher-plant biomarkers decrease. This shift is concurrent with an up-core rise in sedimentary organic carbon, a decrease in TOC:TN ratios, and higher $\delta^{13}C_{TOC}$ values. Interestingly, substantial development of the

Lake Wauberg watershed began after 1980, and the rise in *n*-C_{17} concentration, a 9-fold increase since 1980, is concurrent with this development. Despite this increase in the algae biomarker, vascular plant biomarkers remain the most abundant chain lengths throughout the Wauberg core, and although TAR_{HC} values indicate a decline in macrophyte abundance up-core, values never drop below the threshold value of <1, indicative of primarily algal input. Furthermore, all P_{aq} values fall within the range reported for submerged macrophytes, meaning that for the entirety of the Wauberg record, chain lengths > *n*-C_{21} are primarily derived from aquatic sources (Ficken et al., 2000).

The interpretation of the Wauberg *n*-alkane record contrasts with inferences based on cyanobacterial pigment data and diatom analysis of another core from the lake, which appeared to show persistent eutrophic conditions and stable primary producer populations since at least ca. AD 1894 (Riedinger-Whitmore et al., 2005). I propose that some of the variability in the pigment record of Riedinger-Whitmore et al. (2005) is the result of post-depositional alteration of pigment concentrations. Pigment biomarkers are unsaturated compounds, and are thus more likely to degrade than saturated compounds such as *n*-alkanes. The authors reported that native chlorophyll abundance declined by 50% from the base of the core (10%) to the surface (5%). Percent native chlorophyll is a metric used to quantify preservation of photosynthetic pigments in sediments (Swain, 1985). The significant up-core reduction in preservation of pigments would probably have resulted in an underestimation of cyanobacterial abundance in the most recent sediments.

As in the Wauberg core, the most striking trend in the Lake Apopka lipid concentration data is the rapid increase in algal-derived biomarkers beginning at ~40 cm core depth (Figure 2-2.). Multiple studies (Shumate et al., 2002; Waters et al., 2005; Waters et al., 2015) have documented that Lake Apopka transitioned from a macrophyte-dominated system to an algal-dominated system in the 1940s. The increase in algal biomarker concentration at 40 cm likely represents this shift. Another study on Lake Apopka presented *n*-alkane concentration data from a core raised from the same location as our core (Silliman and Schelske, 2003). In that study, TAR_{HC} values indicated a shift from macrophyte-dominated organic matter at 65 cm core depth, to mixed macrophyte/phytoplankton sediments at 50 cm, and finally to phytoplankton-rich sediments at 30 cm. In our core, the concentrations of macrophyte-derived *n*-C_{23} dominated the *n*-alkane record beginning at ~60 cm core depth, before their decline at 50 cm, and eventual replacement by *n*-C_{17} as the dominant chain length at 40 cm. The TAR_{HC} values are consistent with this trend, and their decrease at 40 cm indicates a switch to organic matter dominated by phytoplankton remains. Our P_{aq} results confirm that terrestrial leaf waxes were never a significant source of *n*-alkanes to Lake Apopka sediment. Rather, long-chain *n*-alkanes in sediments from this lake were primarily derived from aquatic macrophytes. Reliable ^{210}Pb dates for the Apopka core could not be obtained, but the age of the sediments is well-constrained by the disappearance of unsupported ^{210}Pb at 70 cm, and we are confident that the rapid rise in phytoplankton hydrocarbon concentrations at 40 cm represents the primary producer shift that occurred in the 1940s.

Several authors have reported on the long-term stability of aliphatic hydrocarbons (Ho and Meyers, 1994; Meyers, 2003; Eglington and Eglington, 2008). We argue that both long-chain and short-chain *n*-alkanes were stable over the time frames represented by our cores. The carboxylic acids, however, show evidence of bacterial degradation. Previous work demonstrates that bacteria commonly produce the following fatty acids: branched *iso* and *anteiso*-$C_{15:0}$, monounsaturated $C_{16:1\omega7}$, $C_{18:1\omega7}$, $C_{18:1\omega9}$, and the odd-carbon-number saturated fatty acids, $C_{15:0}$ and $C_{17:0}$ (Palomo and Canuel, 2010). In our study lakes, the BDFA concentrations follow two distinct trends (with all BDFA from Apopka following a single trend), implying two bacteria communities are synthesizing distinct fatty acids. This has also been reported in studies from estuaries (Zhang et al., 2015) and marine sediments (Parkes and Taylor, 1983). Presence of multiple bacteria communities in lakes is not surprising, given the range of redox conditions in the water column and sediments, and studies have demonstrated that under anaerobic and aerobic settings, bacteria produce different fatty acids (Parkes and Taylor, 1983). Saturated fatty acids that are probably, but not exclusively, of autochthonous origin (i.e. $C_{12\text{-}16}$), also follow the up-core trends of the BDFA, but the LCFA do not (Figures 2-3, 2-4, 2-5). I hypothesize that these two groups track one another because the BDFA used the short-chain fatty acids SCFA ($C_{12\text{-}16}$) as a carbon source, and/or both groups increased simultaneously, albeit independently, as a consequence of an external forcing such as increased nutrient loading. If the former hypothesis is correct, then SCFA are not reliable indicators of organic matter source, as their labile nature makes them susceptible to bacterial consumption. If the latter is correct, then each of the three lakes displays increased bacterial (likely cyanobacteria)

and algal concentrations that are tied to anthropogenic nutrient inputs. Whatever the case, concentrations of BDFA and SCFA are linked in the cores, and from this, we conclude that: 1) two separate groups of bacteria have created and/or consumed fatty acids in our study lakes, and 2) short-chain fatty acids are susceptible to bacterial reworking, but LCFA are not. The ability to differentiate between the ultimate sources of these FA will require additional research

Biomarker data from each of the three lakes confirms that organic matter in the lacustrine sediments came from terrestrial and aquatic sources. In oligotrophic Lake Sheelar, low *n*-C_{17} concentrations throughout the core imply negligible algal input to the sediments. The dominance of *n*-$C_{23\text{-}31}$ in the sediments confirms that organic matter in the sediment of Lake Sheelar is of primarily vascular plant origin, and that it has been a low-productivity system throughout historic times. The Lake Wauberg and Apopka sediment cores both display increases in *n*-C_{17} in response to cultural activities. In Wauberg this increase occurred very recently, after watershed development in the 1980s. Non-vascular plants, however, never became the dominant source of organic carbon to Wauberg, and P_{aq} values, in conjunction with TAR_{HC} values, demonstrate that submerged aquatic vegetation contributes the most *n*-alkanes. In Lake Apopka, the transition from a macrophyte-dominated to a phytoplankton-dominated state in the 1940s is documented by the *n*-alkane concentration data. Over the last several decades, algae have contributed the majority of hydrocarbons to the sediment record. Fatty acid biomarkers show evidence of bacterially mediated diagenesis, which may be post-depositional. We cannot use SCFA data to definitively establish the source of these compounds in sediments, but future work on fatty acid biomarkers, especially

compound-specific isotope analyses, should provide insights into the extent of post-depositional changes.

Conclusions: Sheelar, Wauberg, and Apopka

Bulk and biomarker data from sediment cores indicate that Lake Sheelar has remained a low productivity system dominated by macrophyte and terrestrial inputs since at least the early 19th century. Increases in algal contributions, measured as *n*-C_{17} concentrations, in Lake Wauberg in the 1980s and Lake Apopka in the 1940s, demonstrate the detrimental impacts of anthropogenic influences on lacustrine systems. Both systems increased in trophic status and transitioned from macrophyte to algal dominated systems after human alteration of the landscape. In all three lakes, BDFA concentrations suggest increased bacterial contributions to the modern sediments, however, this trend may be the result of post depositional degradation of fatty acid biomarkers. Bulk elemental and isotopic data, while somewhat diagnostic, are plagued by myriad issues (see overview in Bianchi and Canuel, 2011). Overall, the hydrocarbon data represents the most source specific and stable biomarker, and therefore concentrations of *n*-alkane chain lengths can be used for reconstructions of organic matter sources and trophic status over decadal to centennial timescales.

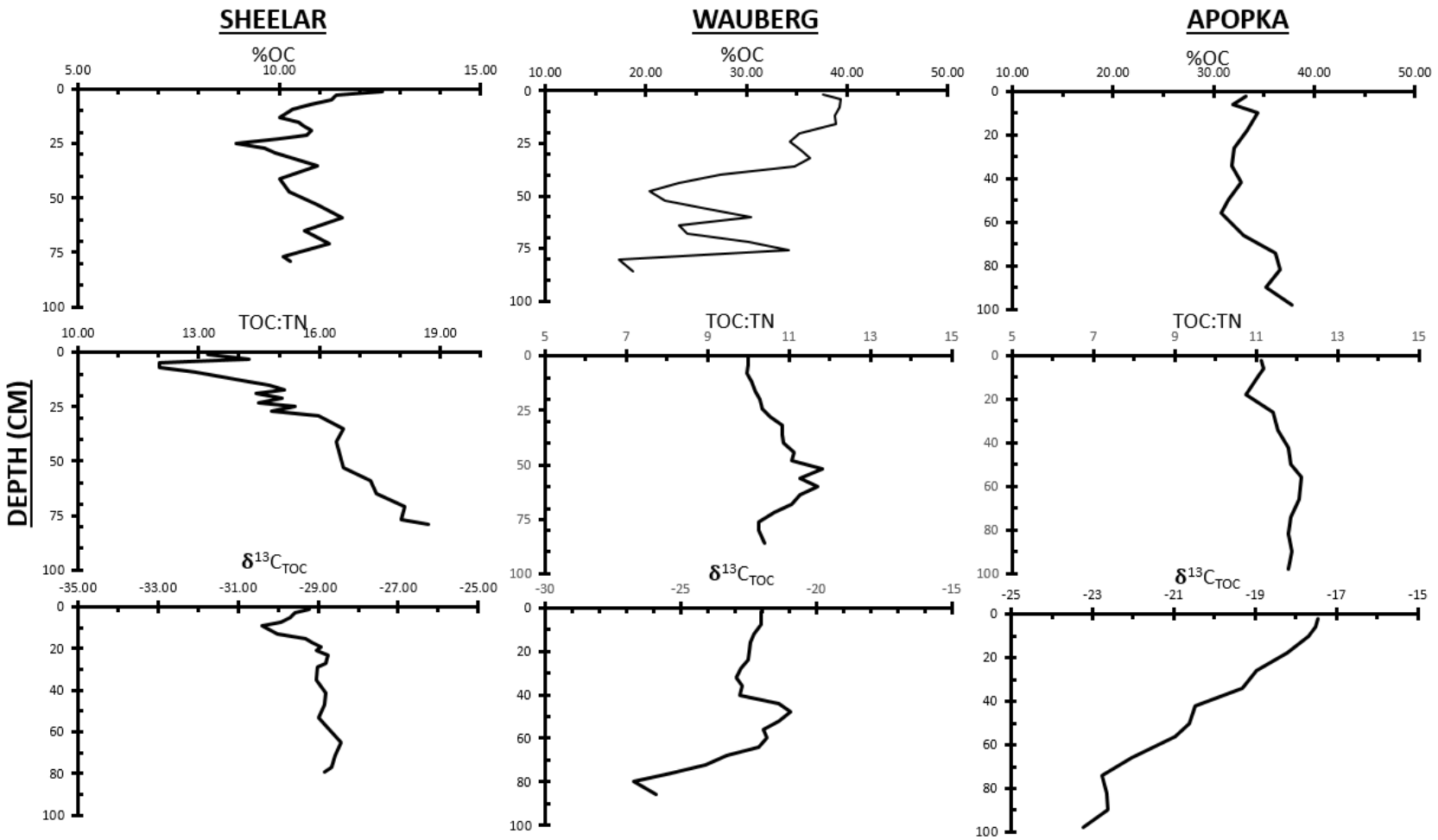

Figure 2-1. Down-core variability in bulk geochemical variables for lakes Sheelar, Wauberg, and Apopka.

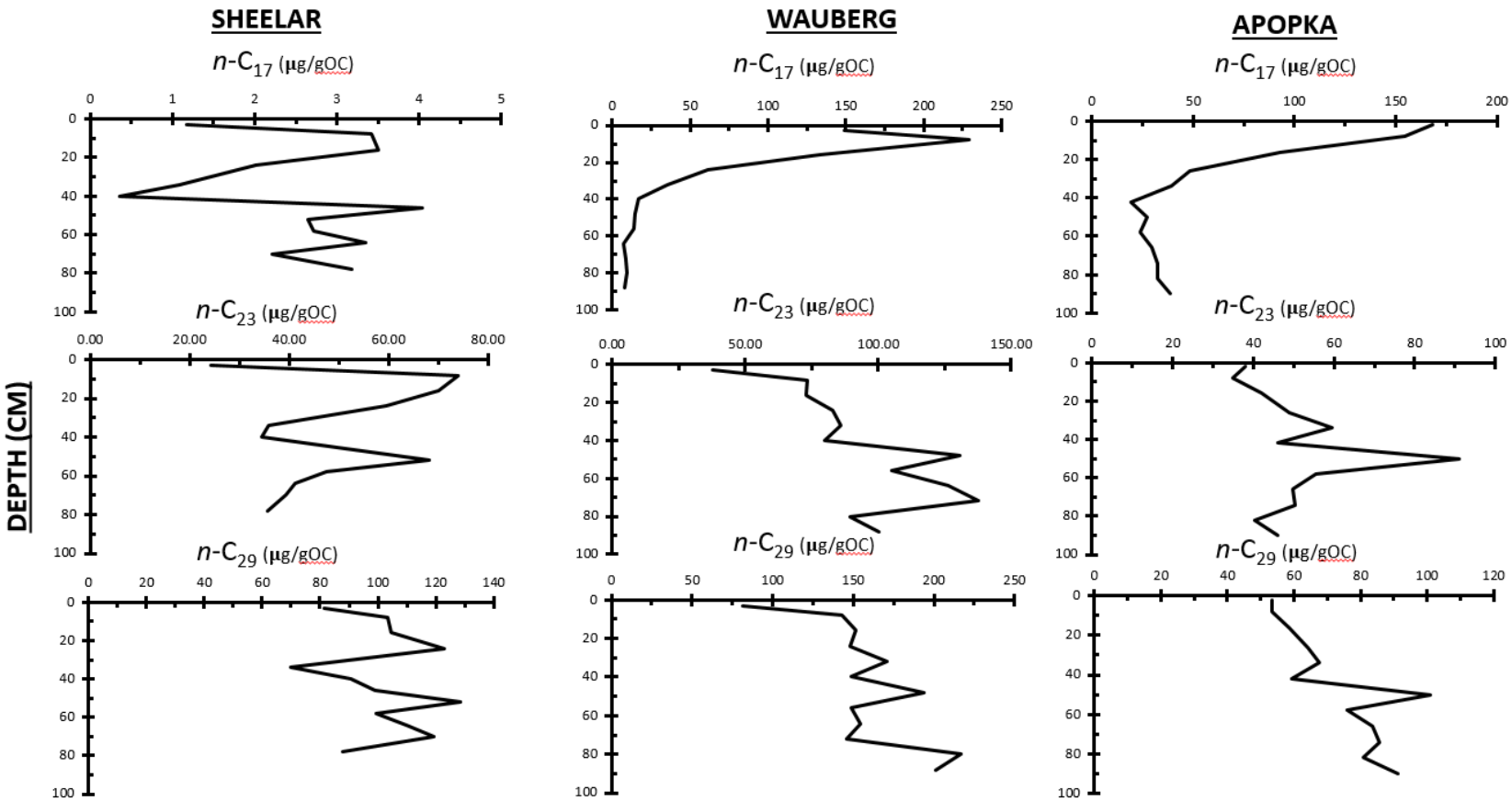

Figure 2-2. Down-core variability in select n-alkane chain lengths for Sheelar, Apopka, and Wauberg. The chain lengths are assigned to the following biological sources: *n*-C_{17} (algae), *n*-C_{23} (macrophytes), *n*-C_{29} (woody terrestrial vegetation).

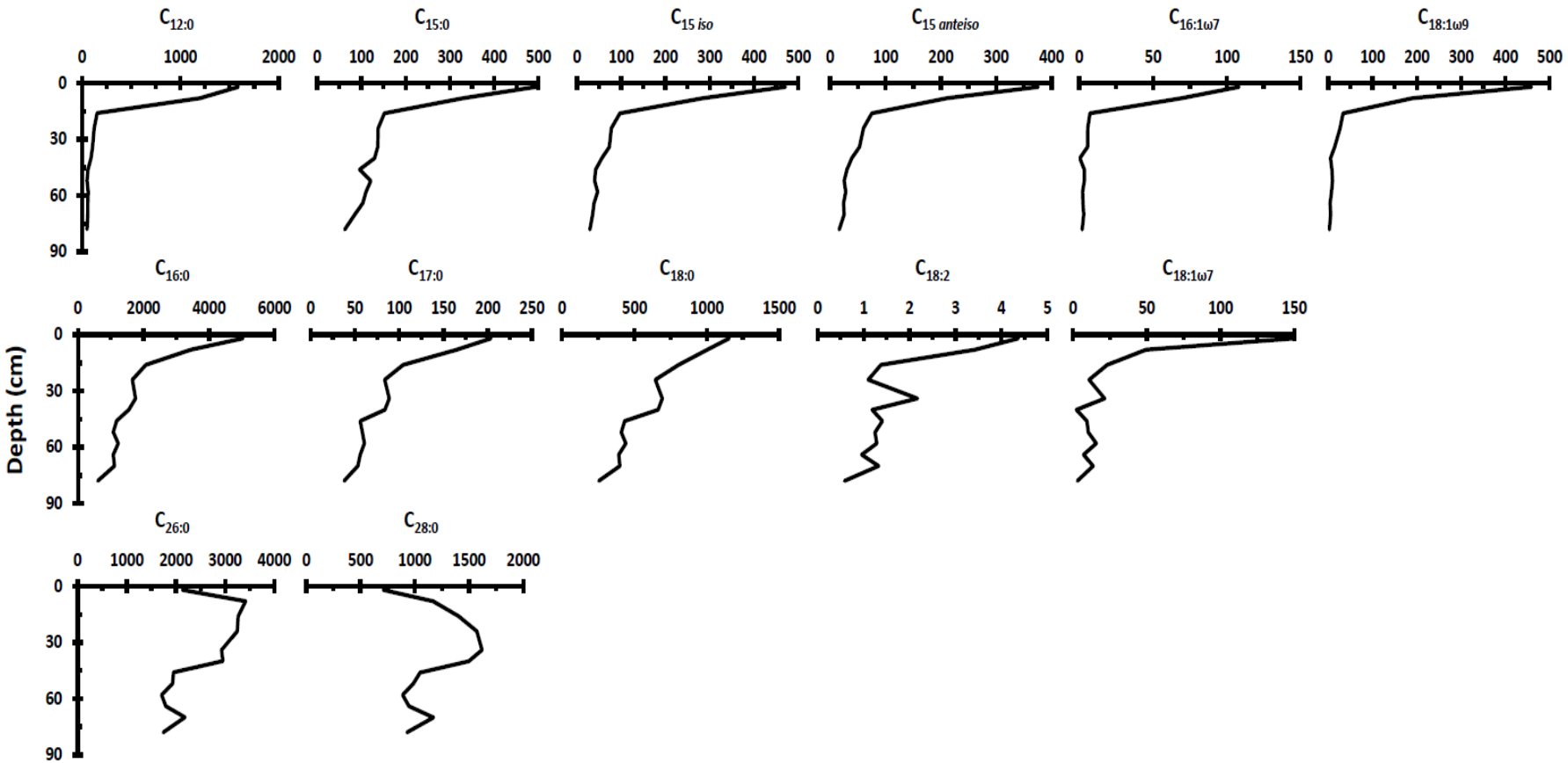

Figure 2-3. Down-core variability in select fatty acid chain lengths from Lake Sheelar. We grouped the bacterial derived fatty acids (BDFA) together with other non-BDFA chain lengths based upon similar down core concentration patterns. The first row includes saturated, branched *iso* and *anteiso*-$C_{15:0}$, $C_{16:1\omega7}$, and $C_{18:1\omega9}$ BDFA, and $C_{12:0}$, which follows a similar pattern. The second row includes $C_{17:0}$ and $C_{18:1\omega7}$ BDFA, and $C_{16:0}$, $C_{18:0}$, and $C_{18:2}$, which follow a similar pattern. In the final row are two representative LCFA. All concentrations are in µg/g OC.

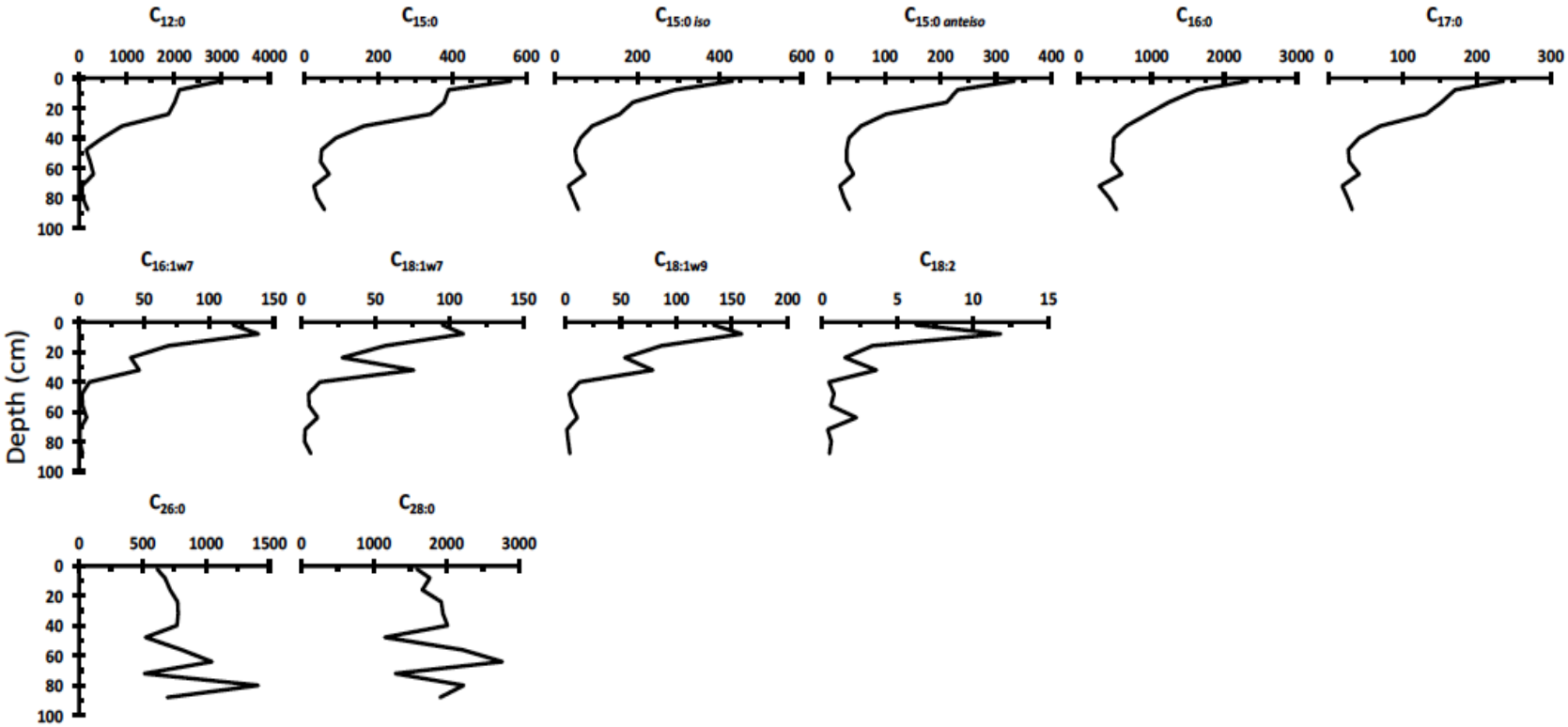

Figure 2-4. Down-core variability in select fatty acid chain lengths from Lake Wauberg. We grouped the bacterial derived fatty acids (BDFA) together with other non-BDFA chain lengths based upon similar down core concentration patterns. The first row includes saturated, branched *iso* and *anteiso*-$C_{15:0}$, $C_{16:1\omega7}$, and $C_{18:1\omega9}$ BDFA, and $C_{12:0}$, and $C_{16:0}$ which follow a similar pattern. The second row includes $C_{16:1\omega7}$, $C_{18:1\omega9}$, and $C_{18:2\omega7}$ BDFA, and $C_{18:2}$, which follows a similar pattern. In the final row are two representative LCFA. All concentrations are in µg/g OC.

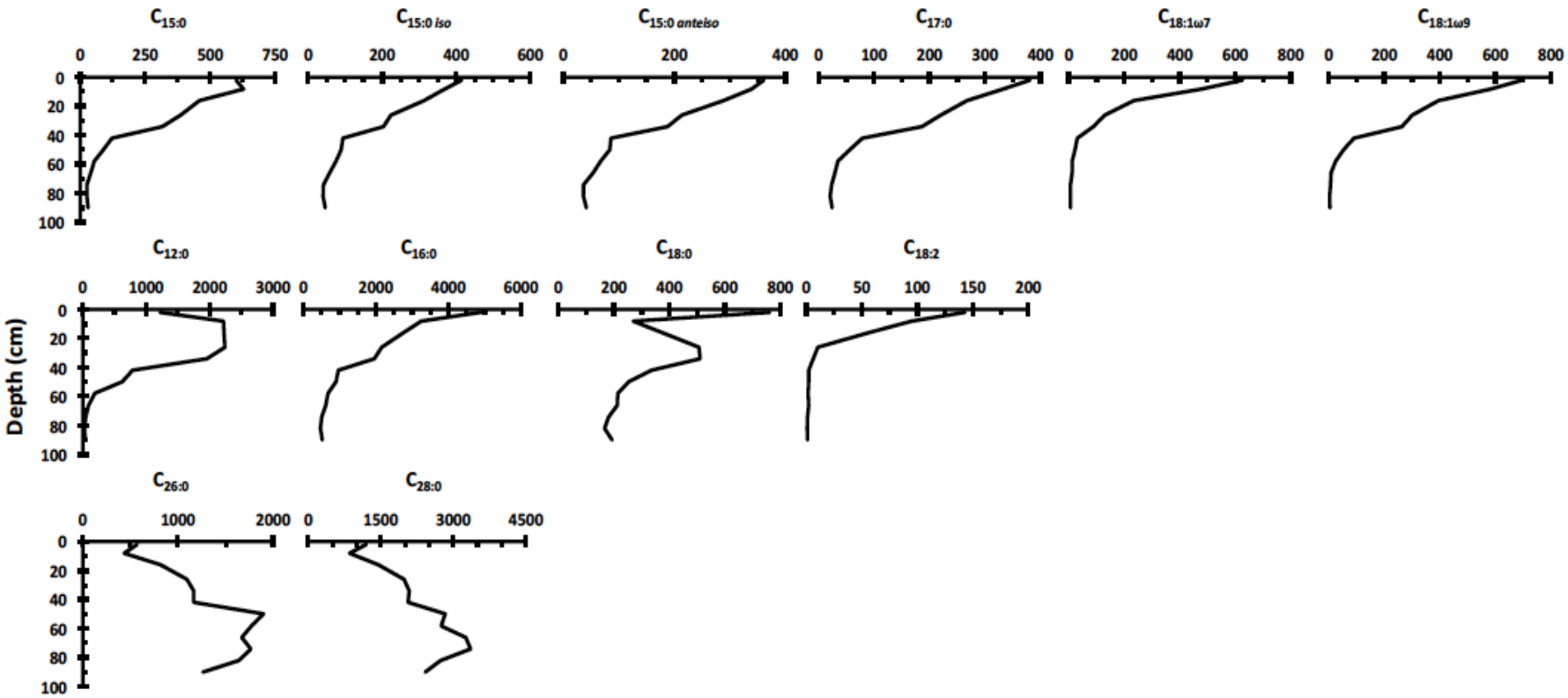

Figure 2-5. Down-core variability in select fatty acid chain lengths from Lake Apopka. All bacterial derived fatty acids (BDFA) displayed similar down core concentration patterns, shown in the first row. The second row displays representative SCFA, and the final row representative LCFA. All concentrations are in µg/g OC.

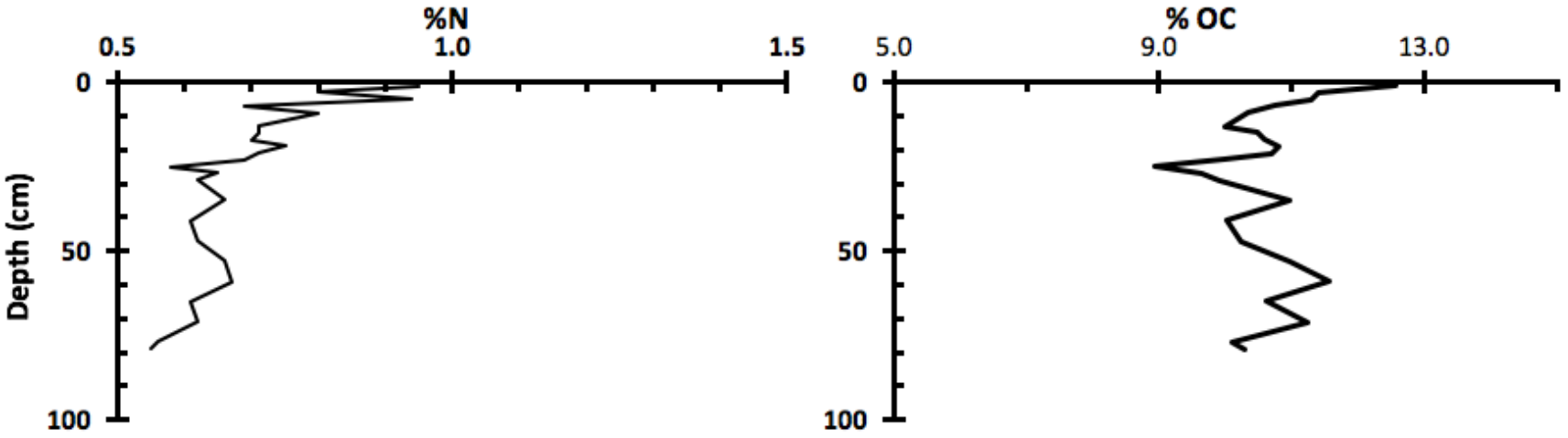

Figure 2-6. Relative abundances (wt/wt) of nitrogen and organic carbon from the Lake Sheelar core.

Table 2-1. Lake Sheelar alkane and fatty acid data: average chain length (ACL), Submerged to emergent/terrestrial vegetation ratio (P_{aq}), the ratio of long to short-chain hydrocarbons (TAR_{HC}), the sum of even-carbon fatty acid concentrations (μg/gOC) (LCFA), the sum of algal derived polyunsaturated fatty acids concentrations (μg/gOC) (PUFA), bacterial derived fatty acids concentrations (μg/gOC) (BDFA), and the ratio of long to short chain fatty acids (TAR_{FA})

Depth (cm)	ACL	P_{aq}	TAR_{HC}	LCFA	PUFA	BDFA	TAR_{FA}
2	28.81	0.36	88.06	5261.76	7.12	2262.08	0.53
8	28.31	0.51	21.61	7685.75	5.58	1299.64	1.08
16	28.13	0.53	17.37	8339.15	2.25	492.46	2.58
24	28.40	0.44	18.82	8570.78	1.79	410.92	3.31
34	28.14	0.50	21.10	8230.01	3.54	393.69	3.07
40	28.64	0.41	136.16	7785.54	1.94	316.72	3.32
46	28.31	0.47	18.22	5021.97	2.30	245.72	3.04
52	28.35	0.46	21.91	5207.13	2.04	268.53	3.26
58	28.42	0.44	24.97	4690.01	2.10	271.44	2.53
64	28.56	0.39	29.43	4871.15	1.56	236.24	2.96
70	28.63	0.38	42.66	5964.74	2.16	221.77	3.56
78	28.57	0.41	32.66	4571.05	0.95	153.56	4.90
Average	28.44	0.44	39.41	6349.92	2.78	547.73	2.84

Table 2-2. Lake Wauberg alkane and fatty acid data. See Table 2-1 for full description.

Depth (cm)	ACL	P_{aq}	TAR_{HC}	LCFA	PUFA	BDFA	TAR_{FA}
3	28.08	0.40	1.33	3149.72	10.53	1925.83	0.39
8	28.16	0.41	1.57	3588.62	20.09	1490.64	0.61
16	28.19	0.40	2.60	3581.50	5.67	1163.40	0.70
24	28.06	0.43	5.25	3885.90	2.54	851.43	0.91
32	28.21	0.40	7.38	3969.21	6.14	579.74	1.68
40	28.19	0.41	10.17	3929.50	0.79	257.81	2.76
48	28.17	0.44	8.24	2366.77	1.34	165.18	2.69
56	28.15	0.46	8.89	4154.41	0.94	169.19	4.31
64	28.05	0.48	13.65	5296.46	3.87	251.22	4.16
72	28.13	0.51	19.63	2395.42	0.63	100.42	5.11
80	28.21	0.41	27.10	4944.09	1.03	137.68	7.06
88	28.11	0.44	26.00	3321.36	0.80	192.89	3.64
Average	28.14	0.43	10.98	3715.25	4.53	607.12	2.84

Table 2-3. Lake Apopka alkane and fatty acid data. See Table 2-1 for full description.

Depth (cm)	ACL	P_{aq}	TAR_{HC}	LCFA	PUFA	BDFA	TAR_{FA}
2	28.14	0.48	0.75	2484.96	248.81	3639.91	0.29
8	28.08	0.47	0.82	1807.38	164.72	3147.25	0.23
16	28.08	0.49	1.46	3241.15	97.91	2190.96	0.42
26	28.06	0.49	2.62	4401.39	18.32	1636.55	0.66
34	28.06	0.51	3.14	4605.20	10.57	1379.17	0.78
42	27.99	0.50	5.10	4619.93	4.23	535.43	1.78
50	28.01	0.53	5.26	7142.13	3.35	413.36	3.03
58	27.97	0.50	4.32	6735.27	2.50	275.60	5.10
66	27.89	0.48	4.72	7073.56	4.08	206.46	7.07
74	27.91	0.48	4.60	6895.52	1.93	142.18	8.69
82	27.89	0.46	4.69	6870.40	1.51	132.78	9.40
90	27.89	0.46	4.41	5493.12	2.25	152.53	6.95
Average	28.00	0.49	3.49	5114.17	46.68	1154.35	3.70

CHAPTER 3
THE BIOGEOCHEMICAL EVOLUTION OF A SUBTROPICAL LAKE

Introduction: Lake Harris

Lakes are a critical component of terrestrial carbon cycling. Their sedimentary archives contain a history of changes in organic carbon sources within the lakes watershed (allochthonous) and the water column (autochtonous). They serve as a pool for sequestered organic carbon that is estimated to exceed that of the ocean by a factor of three (Dean and Gorham, 1998). Analysis of the organic carbon preserved within a lacustrine sedimentary archive can be used to reconstruct complex environmental changes throughout the lake's existence. In Florida, paleolimnological reconstructions with organic biomarkers have been used to document ecological successions (Watts and Hansen, 1994) and hydrology changes (reviewed in Castañeda and Schouten, 2011) during the transition from the last glacial period to the present.

These reconstructions routinely employ elemental C/N ratios and stable isotopes of TOC ($\delta^{13}C_{TOC}$) to distinguish sources of organic matter within lake sediments (Meyers, 1994; Silliman et al., 1996). Differences in C/N ratios arise from the absence of carbohydrate-rich structural components in algae (Meyers and Ishowatar, 1993), and values for vascular (C/N >20) and non-vascular plants (C/N between 4 and 10) have been used to gauge the relative contributions of the two end-member components to the organic sediment pool. The range in C/N values between algal and woody plant species demonstrates how basic bulk elemental data can be applied as a proxy for organic matter source. Analogously, $\delta^{13}C_{TOC}$ can be interpreted as a mixture of values from various end-member groups. The $\delta^{13}C$ values of plant and algal organic matter is primarily governed by the isotopic signature of the carbon substrate (atmospheric CO_2

or dissolved HCO_3^-) and the combined enzymatic fractionations associated with fixing that carbon (i.e. via RuBP) (O'Leary, 1988). Most terrestrial plants assimilate carbon through two photosynthetic pathways (C_3 or C_4), and thus, $\delta^{13}C$ signatures vary between these two groups (Farquhar et al., 1989). Although algae photosynthesize using the C_3 pathway, they are enriched in ^{13}C relative to C_3 plants in high-pH systems because dissolved HCO_3^- is enriched in ^{13}C relative to $CO_{2(aq)}$ by ~9‰ (O'Leary 1988).

Generalizations about carbon sources inferred from C/N ratios must be interpreted with caution. Recent studies have shown that C/N ratios vary considerably at the species level (Cloern et al., 2002), can be greater in N-limited systems (Bianchi and Canuel, 2011), and lower in systems where there is selective degradation of labile carbon sources (Aller, 1994). Similarly, interpretation of $\delta^{13}C_{TOC}$ signatures in relation to organic matter provenance is not unequivocal. In lake sediments, stratigraphic shifts toward more positive $\delta^{13}C$ values have been explained as reflecting greater input from algal material (Meyer, 1997), increased autotrophic carbon fixation (Brenner et al., 1999; Torres et al., 2012), or transitions from C_3 to C_4 terrestrial plant communities (Bianchi et al., 2002).

An alternative to analysis of bulk organic matter in lake sediments is the application of compound-specific isotope measurements of molecular biomarkers as a tool for tracking the source and history of organic matter within the lacustrine system. With biomarker-specific studies, reconstructions of complex hydrology changes have been carried out across millennial time scales (Filley et al., 2001). Carbon isotopic values of lipid compounds from lake sediments (Mud Lake, Florida, USA) were used by Filley et al. (2001) to document vegetation changes associated with Holocene climate

shifts. They found that shifts in alkane biomarkers corresponded to fluctuations in the regional water table that were caused by hydrological changes in the early Holocene. The changes recorded in the carbon isotopes of the *n*-alkanes mirrored similar changes from pollen-based environmental reconstructions from other Florida lakes (Watts et al., 1994).

A recent study of Lake Harris, FL, USA, used multiple geochemical proxies to identify prehistoric shifts in the primary producer community structure, from a sediment core dated to ~10,000 cal yrs BP (Kenney et al., 2016). A shift from carbonate-dominated to organic-dominated sediment occurred at approximately 5,540 yrs BP (Kenney et al., 2016). The timing of this shift may have been related to the onset of modern hydrological conditions in Florida, as inferred from pollen data (Watts el al. 1994), and core studies of basal peat layers form the Mississippi delta (Törnqvist et al., 2004).

The primary objectives of this study were two-fold: 1) to assess the major sources of organic matter to the sediments of Lake Harris from its nascent stages to the present, and 2) to determine the environmental and hydrological changes that drove the shifts in organic matter. We employed a suite of geochemical analyses throughout a complete Holocene sediment record from Lake Harris to evaluate these objectives quantitatively. The concentrations and stable isotope compositions of total sedimentary organic carbon (TOC), total nitrogen (TN), and select biomarker hydrocarbons, were used as proxies for measuring temporal trends in the primary producer communities. Geochemical analyses, including, concentrations and accumulation rates of carbonate ($CaCO_3$), biogenic silica (BioSi), and total organic carbon (TOC) were used as proxies

for hydrological changes, such as, increases or decreases in: groundwater input, lake level, and water table elevation. I hypothesize that the sources of organic matter (i.e. allochthonous vs. autochthonous) to the lake's sediments changed in concert with regional hydrologic and environmental events that occurred as the earth's climate stabilized in the mid-Holocene. Specifically, these climate events include: the steady rise in relative sea level in the Gulf of Mexico that began in the early Holocene and abruptly decreased at 7,000 yrs BP (Törnqvist et al., 2004), wetland formation and expansion in Florida at 5,000 yrs BP (Willard and Bernhardt, 2011), and the onset of the modern El Niño cycle at 3,000 yrs BP (Donders et al., 2008). The data demonstrate that sedimentary variables in Lake Harris responded to each of these events and showed a progressive trend towards eutrophication in the modern sediments.

Site Description: Lake Harris

Lake Harris is a relatively shallow (mean depth = 3.5m), productive lake (mean annual chlorophyll a = 57µg/L, total phosphorus = 38 µg/L, total nitrogen = 1707 µg/L), with a mean surface area of 75km^2 (Fulton and Smith, 2008). It is part of the Lake Harris chain of lakes located in the Upper Ocklawaha River Basin, Central Florida, USA. Flow through the system begins in a spring that emanates from the southwest section of hypereutrophic Lake Apopka and continues through four additional lakes and discharges into the Ocklawaha River (Kenney et al., 2010). Three other lakes in the chain, including Lake Harris, receive minimal flow from Lake Apopka and are all considered to be mesotrophic to eutrophic. The hydraulic retention time for Harris is relatively short (2.9 years) and can vary by orders of magnitude during periods of high and low flow (Fulton and Smith, 2008). Most of the lakes in the Harris chain receive surface and groundwater inputs that pass through organic- and mineral-rich soils, thus,

are hypothesized to be naturally productive and alkaline (Fulton and Smith, 2008). However, recent geochemical analyses of the same 5.9m sediment core from Lake Harris used in this study placed the lake on a trajectory towards increasing oligotrophication throughout the Holocene (Kenney et al., 2016). This trajectory was interrupted after AD 1950, when the human population around the region increased six-fold and the lake veered towards the highly productive end of the trophic state spectrum (Kenney et al., 2016).

Sediment Sampling: Lake Harris

We sampled sediment from the 5.9m core retrieved by Kenney et al. (2016). The upper portion of the core (first 1m) was dated using ^{210}Pb, and the remaining portion of the core was AMS-^{14}C dated using four charcoal, and three bulk sediment samples. For details of the chronology see Kenney et al. (2016).

The core was split in half, lengthwise, and one half of the core was sampled at 4-cm intervals for geochemical analyses. Wet subsamples were then frozen, freeze-dried, and ground and homogenized for analyses. $CaCO_3$, BioSi (both diatom- and sponge-spicule derived), TN, and %OM sampling methods are outlined in Kenney et al. (2016). TOC was measured as the difference between total carbon and inorganic carbon on a Carlo Erba NA1500 CNS elemental analyzer equipped with an auto-sampler. Dried sediment for $\delta^{13}C_{TOC}$ analyses was first pretreated with 1N HCl to remove inorganic carbon, and then measured on a Carlo Erba NA1500 CNS elemental analyzer interfaced with a Thermo Scientific Delta V Advantage isotope ratio mass spectrometer. Isotopic compositions were normalized to the VPDB scale, and reported in standard delta notation as follows:

$$\delta^{13}C = [(\delta^{13}C \text{ sample} / \delta^{13}C \text{ standard}) - 1] \times 1000 \quad (2\text{-}1)$$

Lipid Extraction and Quantification: Lake Harris

Lipids were extracted from 1g of freeze dried sediment with an Accelerated Solvent Extractor ASE200 (Dionex), using 2:1 (v/v) dichloromethane(DCM):methanol through three extraction cycles at 10.3 MPa (1500 psi) and 100°C. Between 1 and 2 g of sediment were used for lipid extraction. Total lipid extracts (TLE) were concentrated under a gentle stream of nitrogen, and the neutral lipid fraction was obtained after base saponification of the TLE. Neutral lipids were further separated, based on polarity, into compound classes by column chromatography, using 5% deactivated silica gel, according to methods modified from Nichols (2011). Hydrocarbons were eluted from the silica gel column with 4.5 ml of 9:1 Hexane:DCM, and saturated hydrocarbons were separated from alkenes on 5% Ag-impregnated silica gel (w/w) with 4 ml of hexane and ethyl acetate, respectively. Branched and cyclic saturated hydrocarbons were isolated from *n*-alkanes with triple urea adduction.

Alkane concentrations were measured and identified on a Thermo Scientific Trace 1310 gas chromatograph with a Supelco Equity 5 column, interfaced to a Thermo Scientific TSQ 8000 triple quadrupole mass spectrometer with electron ionization. The inlet was operated in splitless mode at 280°C. The column flow rate was set to 2.0 ml/min and the oven was programmed to an initial temperature of 60°C and held for 1 minute, then ramped to 140°C at 15°C/min, and to 320°C at 4°C/min and held for 25 minutes. Quantification was based on the calibration curves generated from the peak areas of external standards (C_7-C_{40}) with concentrations ranging from 5 to 250 μg/ml.

Compound-specific Isotope Measurements on *n*-Alkanes: Lake Harris

Compound-specific carbon isotope values for *n*-alkanes were measured on an Agilent 6890 GC connected to a Delta V Advantage IRMS interfaced with a GC-C combustion system. The GC flow rate was set to 2.0 ml/min, and the oven was programmed as follows: 60°C for 1 minute, then increased at a rate of 6°C/min to 320°C, and held for 20 minutes. Compounds were combusted over a nickel/platinum/copper wire with O_2 at 960°C. The isotope ratios of carbon in CO_2 were measured and normalized to the VPDB scale using the Uncertainty Calculator (Polissar and D'Andrea, 2014) and are reported in standard delta notation as above. Standard errors of the mean (SE) were calculated using the Uncertainty Calculator, which yielded a 1σ SE value of ± 0.39‰ (Polissar and D'Andrea, 2014).

Bulk Geochemistry and Isotopic Compositions: Lake Harris

The core was divided into three zones based on shifts in $\delta^{13}C_{TOC}$: from the bottom of the core to 403 cm is zone 3, from 402 to 241 cm is zone 2, and from 240 cm depth to the surface is zone 1 (Figure 3-1). Zone 3 is marked by an increase in $\delta^{13}C_{TOC}$ values upcore, from a minimum of -24.29‰ to a maximum of -15.78‰. Bulk carbon isotope values remain relatively stable in zone 2 (mean -14.79‰), before decreasing sharply in zone 1 from -13.27‰ to a minimum value of -22.18‰ at the surface. Organic carbon percentages remain below 15% throughout zone 3, while $\%CaCO_3$ decreases from a maximum value of 86% at 579 cm depth, to just under 30% at 418 cm, with an average value of ~60% throughout zone 3. Values of %TOC and $\%CaCO_3$ change suddenly at ~350 cm depth in zone 2: values of organic carbon increase from 2.7% to 38.1%, and carbonate drops to 1% and never increases above 25% in zone 2. In zone

1, %TOC remains at elevated levels and varies about its mean of 21.3%. Carbonate values never exceed 11% from 240 cm to the surface of the core and display average zone 1 values of 0.6%. In zone 3, TOC:TN values reach a maximum of 39.33 at 574 cm, before decreasing rapidly into zone 2 to a minimum value of 10.91. TOC:TN values continue to decrease slowly from zone 2 to zone 1 and reach a minimum value of 8.57 at 8 cm depth. Biogenic silica, both diatom- and sponge-derived, displays considerable variability throughout all zones. Of note is a dramatic increase in diatom silica at 144 cm, where concentrations increase from 11.96 to 51.96 mg/g. These values continue to rise in zone 1, reaching a maximum value of 147.30 mg/g at 52 cm.

Concentrations and Isotopic Compositions of Hydrocarbons: Lake Harris

Concentrations for select *n*-alkane chain lengths are displayed in Figure 3-3. Mean *n*-alkane concentrations for these chain lengths are displayed in Table 3-1. The *n*-alkane concentrations are dominated by long chain alkanes (i.e. >*n*-C_{25}). The most abundant *n*-alkane in our record is *n*-C_{27}, with an average concentration of 36.01 µg/g OC throughout the entire core. We calculated the average chain length (ACL) for all samples using the Eglinton and Hamilton (1967) equation:

$$ACL(C_{25}\text{-}C_{35}) = \frac{25C_{25}+27C_{27}+29C_{29}+31C_{31}+33C_{33}+35C_{35}}{C_{25}+C_{27}+C_{29}+C_{31}+C_{33}+C_{35}} \quad (2\text{-}2)$$

There is low variability in ACL throughout $\delta^{13}C_{TOC}$ zones 1 and 3 (ranges = 1.2 and 1.1, respectively), however ACL values in zone 2 vary by 2.8, with a high of 29.7 and a low of 26.9 (Table 3-2).

Carbon preference index (CPI) measures the maturity of the hydrocarbon source. We calculated CPI values from the equation of Bray and Evans (1961):

$$CPI = 0.5 \frac{C_{25}+C_{27}+C_{29}+C_{31}+C_{33}}{C_{26}+C_{28}+C_{30}+C_{32}+C_{34}} + \frac{C_{25}+C_{27}+C_{29}+C_{31}+C_{33}}{C_{24}+C_{26}+C_{28}+C_{30}+C_{32}} \quad (2\text{-}3)$$

The CPI values for all hydrocarbon samples averaged 3.68, with a maximum of 6.56 and a minimum of 2.14 (Table 3-2). All sample depths exhibit an odd-over-even predominance, which is indicative of vascular terrestrial plant sources. There is not a clearly discernible trend in CPI values throughout the three core zones.

Differences in alkane concentrations are apparent across each zone in the Lake Harris core (Figure 3-3). We subdivided alkanes into groups based upon their most probable source(s): cyanobacterial (7-methylheptadecane and diploptene), algal (*n*-C_{17}), emergent/submerged macrophytes (*n*-C_{23}), woody terrestrial vegetation (*n*-C_{27} and *n*-C_{29}), and mixed woody terrestrial/C_4 grasses (*n*-C_{35}), and related changes in these organic matter sources to regional environmental change. In broadest terms, there are three significant trends in alkane concentrations: 1) proliferation of algal and cyanobacterial biomarkers in the top 40 cm of the core, 2) a rapid increase in submerged macrophyte biomarker concentrations at 390 cm, which persisted until 330 cm, and 3) the dominance of terrestrial biomarkers throughout the rest of the core, with a concentration maximum at 530 cm.

More specifically, zone 3 is dominated by terrestrial alkane inputs: *n*-C_{27} and *n*-C_{29} concentrations are ~5x that of *n*-C_{23} and ~20x that of *n*-C_{17}. P_{aq} values are also indicative of primarily terrestrial inputs in this zone. A sudden increase in concentrations of *n*-C_{23}, *n*-C_{27}, *n*-C_{29}, and *n*-C_{35} occurs at 530 cm. Both terrestrial hydrocarbon biomarkers attain their maxima at this depth.

In zone 2 the average concentration of *n*-C_{17} decreases 8-fold, 7-methylheptadecane is nonexistent, and the terrestrial alkane concentrations are

approximately halved, although they remain the most abundant chain lengths in this zone. Of note is an increase in *n*-C_{23} concentrations from 6.23 µg/g OC at 340 cm to 32.51 µg/g OC at 330 cm, which then drops back down to 6.85 µg/g OC at 280 cm. A similar, albeit smaller increase in *n*-C_{17} concentrations also occurs during this interval (Figure 3-2). We measured the relative contributions of submerged and floating aquatic macrophytes to emergent terrestrial vegetation via the P_{aq} proxy (Ficken et al., 2000), described by the formula $(C_{23} + C_{25})/(C_{23} + C_{25} + C_{29} + C_{31})$. P_{aq} values from 330 cm to 290 cm range from 0.42 to 0.81, indicative of a freshwater, submerged vegetation source. This is the only portion of the Lake Harris core to have P_{aq} values that fall in the range of submerged vegetation.

The top zone of the core is characterized by a ~50-fold increase in the concentration of *n*-C_{17} and a ~40-fold increase in 7-methylheptadecane concentrations in the upper 40 cm of sediments. These are the hydrocarbons in the highest abundance in the top 40 cm of the core, but their concentrations drop to < 5 µg/g OC below 120 cm. At this depth, and throughout the rest of zone 1, the terrestrial biomarkers *n*-C_{27} and *n*-C_{29} become the most abundant hydrocarbons, with average concentrations of 52.32 µg/g OC and 43.25 µg/g OC, respectively.

A hydrocarbon proxy, known as the terrestrial to aquatic ratio (TAR_{HC}), was developed to distinguish between autochthonous and allochthonous sources of organic matter in sediments (Meyers, 1997). TAR_{HC} results, unsurprisingly, matched our comparative analyses of single-chain-length alkane concentrations (Table 3-2). Values <1 reflect a dominance of aquatic hydrocarbons, and are only observed in the top 15 cm of our core. TAR_{HC} are highly variable, but average 16.40, which indicates that

contributions from terrestrial plants dominate the record. The maximum TAR_{HC} (74.75) is found at 530 cm, whereas values <4 occur at 510, 400-360, 330-290, and 35 cm.

Isotopic compositions of selected chain lengths are shown in Figure 3-4. Based upon alkane concentrations, and organic matter source assignments, we interpreted only the following hydrocarbons in this study: 7-methylheptadecane, *n*-C_{17}, *n*-C_{23}, *n*-C_{27}, and *n*-C_{29}. Reliable carbon isotope ratios could not be measured on *n*-C_{17} and *n*-C_{23} below 415 cm depth.

The carbon isotopes of 7-methylheptadecane have the highest average value in our core. From 45 cm to the sediment surface, the $\delta^{13}C$ values of this branched alkane average -21.30‰, and vary by only 0.7‰ across those depths. The $\delta^{13}C$ signature of *n*-C_{17} decreases progressively across all zones from a maximum value of -22.3‰ at 380 cm depth, to a minimum value of 29.9‰ at the top of the core. From 400 to 313 cm (zone 2), $\delta^{13}C$ of *n*-C_{23} increases from -22.8‰ to 18.7‰, then stabilizes at a mean value of -19.9‰ throughout the rest of zone 2. In zone 1 carbon isotope values of *n*-C_{23} decrease from a maximum of -19.73‰ to a minimum value of -26.30‰ at 4 cm depth. From the bottom of the core to 400 cm (the base of zone 2) $\delta^{13}C$ values of vascular plant alkanes, *n*-C_{27} and *n*-C_{29}, both increase in a pattern that follows the enrichment of the $\delta^{13}C_{TOC}$. Carbon isotope signatures then rapidly decrease at 362 cm for *n*-C_{27}, and at 400 cm for *n*-C_{29}. These chain lengths return relatively invariable $\delta^{13}C$ values in core zone 1, with average values of 24.8‰ and 28.0‰ for *n*-C_{27} and *n*-C_{29}, respectively (Figure 3-4).

Discussion Overview

The shifts in geochemical variables measured in the sediments of Lake Harris coincide with major environmental events that transpired during the Holocene. Hydrocarbon biomarker data indicate a series of hydrological shifts that resulted from Northern Hemisphere deglaciation. These shifts in Lake Harris are temporally linked to records from other lakes in north and central Florida (Watts and Hansen, 1994; Filley et al., 2001; Donar et al., 2009). Broadly speaking, Lake Harris evolved from a marsh-like system in the early Holocene, to a shallow lake in the middle Holocene, and then deepened to its modern state after ~2,600 years BP. The carbon isotopes of the autochthonous and allochthonous organic matter pools are proxies for these changes, and reflect multiple sources of inorganic carbon utilization by the primary producer communities.

Concentrations of *n*-Alkanes and Shifts in Geochemical Biomarkers as Indicators of Organic Matter Source in Lake Harris

The biological sources of alkanes have been described in numerous publications (for review see Bianchi and Canuel, 2011). The *n*-$C_{27/29}$ homologues of *n*-alkanes represent organic matter sourced from woody terrigenous plants (Cranwell, 1982). C_4 graminoids contain *n*-C_{35} alkanes in their leaves at concentrations an order of magnitude greater than woody C_3 angiosperms (Garcin et al., 2014; Diefendorf and Freimuth, 2017). Submerged and emergent macrophytes are characterized by chain lengths of *n*-$C_{21/23}$ (Ficken et al., 2000), and algae synthesize alkanes with a predominant chain length of *n*-C_{17} (Cranwell 1982). Additionally, the branched alkanes, 7- and 8-methylheptadecane, are produced exclusively by cyanobacteria and account for 90% of their total branched alkanes (Han and Calvin, 1969). Although hydrocarbon

biomarkers are source-specific, they represent only a fraction of the total biochemical composition of bacteria and plants. The biomarker data gleaned from this study can supplement, and be supplemented by, bulk analyses, that represent larger fractions of the organic matter.

The earliest portion of the core (zone 3) is dominated by *n*-alkanes derived from terrestrial and, to a lesser extent, macrophyte sources, as well as high sponge-spicule-derived biogenic silica. Approximately 800 years (at 550 cm core depth) after the lake began to fill with water in the early Holocene (10,600 yrs BP), there was a pulse of *n*-C_{23}, *n*-C_{27}, and *n*-C_{29} to the sediments (Figure 3-3). This occurs shortly after TOC:TN values jump from 24 to 39 at 574 cm. TOC:TN values continue to increase towards maximum values, in agreement with terrestrial biomarker abundances. This is the earliest stage in the lake's evolution, when it was a shallow, low-productivity, marsh-like system that received abundant vascular plant input from littoral communities (e.g. *Taxodium* spp.), and supported macrophyte growth. The temporal correlation between the TOC:TN, sponge spicule, and terrestrial hydrocarbon biomarker increases is in strong agreement with palynological (Watts, 1975) and diatom-based paleolimnological reconstructions (Quillen et al., 2009) that describe central Florida lakes as low-nutrient, shallow-water systems during the early Holocene.

Zone 2 is highlighted by localized maxima of algae and macrophyte biomarkers (Figure 3-3). The increase in *n*-C_{23} begins at 358 cm (~6,700 yrs BP), which corresponds to a shift from predominantly $CaCO_3$ sediments to organic-rich sediments without measurable carbonate by 232 cm (~5,000 yrs. BP) (Figure 3-2). The carbonate collapse is coincident with the reduction in freshwater-sponge-derived biogenic silica,

ACL values below 27, and average P_{aq} values of 0.61 (Figure 3-2), are indicative of extensive macrophyte coverage in Lake Harris. Kenny et al. (2016) correlated these changes in geochemical proxies with the proliferation of *Pinus* pollen in Florida and the onset of wetter conditions in the middle Holocene (Watts and Hansen, 1994). During this interval, hydrologic inputs to Lake Harris shifted from a primarily groundwater source to a primarily meteoric source.

Lake Panasoffkee, in central FL, is a modern analogue to Lake Harris during the early to middle Holocene. Currently, Lake Panasoffkee receives substantial groundwater inputs and is a hard-water, macrophyte-dominated system (Brenner et al., 2006). TOC:TN values of submerged aquatic vegetation (SAV) measured in the Brenner et al. (2006) study (14-22) are only slightly greater than the average TOC:TN values in zone 2 of the Lake Harris core (12.1). From this, we can infer that sedimentary organic carbon in Lake Harris from ~8,000-5,000 yrs BP was a mixture of macrophytes and structurally poor, low TOC:TN, algae and periphyton. This reconstruction is further supported by vegetation studies from shallow, low-nutrient lakes that have primary producer communities dominated by SAV (Schelske et al., 2005). The *n*-alkane biomarker concentrations, with maxima of *n*-C_{17} (at ~400 and 330 cm) and *n*-C_{23} (at ~330 cm), the sponge-derived silica concentrations, and the TOC:TN data measured from modern SAV, periphyton, and algae, coincide with one another in this section of the core. Together they indicate a primarily groundwater-fed system with abundant submerged and emergent macrophyte populations.

The largest shift in any of the hydrocarbon concentrations occurs in zone 1, over the top ~40 cm of the core, where *n*-C_{17} and 7-methylheptadecane increase by 50-fold

and 40-fold, respectively. This rapid increase in algal and cyanobacterial biomarkers corresponds with the timing of an increase in trophic status of other Florida lakes and a six-fold population increase in the counties surrounding the Harris chain of lakes after AD ~1940 (Fulton and Smith, 2008). The 7-methylheptadecane concentrations, in particular, are indicative of a highly eutrophic, possibly N-limited lake that supports cyanobacteria proliferation (Dolman et al., 2012). Terrestrial (*n*-C_{27}) and macrophyte (*n*-C_{23}) biomarker concentrations fluctuate between high and low values, but display no discernible trend across zone 1. Biomarker concentrations from 40 cm depth to the bottom of zone 1 (240 cm) are more evenly distributed among the three major organic matter sources. Combined algal and macrophyte *n*-alkane concentrations equate to approximately half of the terrestrial *n*-alkane concentrations.

The observed trends in the biomarker data are not clearly borne out by the bulk geochemical data. The concentrations of algal and bacterial biomarkers are an order of magnitude greater than any terrestrial biomarker throughout the top 40 cm of the core, yet the TOC:TN values do not decrease as would be expected with an increase in non-vascular sources. Instead, TOC:TN values remain relatively stable throughout zone 1, with an average value of 10.16, indicative of a primarily algal source (Meyers, 2003). Post-depositional alteration of TOC:TN values occurs in sediments with oxic pore waters, which can result in artificially low values (Bianchi and Canuel, 2011). Organic matter decomposition can remove as much as 20% of the carbon that is buried on the lake bottom (Meyers, 2003; Gälman et al., 2008). Although such alteration is possible in Lake Harris, it is likely to occur during the winter when the water column loses its thermal stratification and bottom waters become oxygenated. Even if the lake is

thermally stratified, sediment trap studies have shown that much of the carbon in the water column is oxidized before leaving the epilimnion. In Lake Michigan, for instance, only 6% of the organic carbon formed via autochthonous production reached the sediment surface (Eadie et al., 1984). We cannot expect sinking particulate organic carbon to have similar exposure rates to oxidation in Lake Harris due to vast differences in water depth compared with Lake Michigan, but we can assume that a significant fraction is lost before being integrated into the sediment archive. Finally, algae are protein-rich, but carbohydrate- and lipid-poor. Lipids account for variable amounts of their biochemical composition, but are generally between 5-20% of the total constituents and hydrocarbons account for only 3-5% of the lipid fraction (Bianchi and Canuel, 2011). The limited *n*-alkane production from algae, coupled with carbon loss, is the most probable explanation for the incongruous TOC:TN and hydrocarbon concentration data.

Interpreting Carbon Isotope Variability in TOC and Hydrocarbon Biomarkers in Lake Harris

The carbon isotope value of the TOC fluctuates from low $\delta^{13}C_{TOC}$ values in the earliest part of the core, to the most enriched $\delta^{13}C_{TOC}$ values in the middle section, then back to depleted values in the latest section (Figure 3-1). This variability reflects the changing sources of carbon utilized by the primary producer communities. In the early Holocene, Lake Harris began to fill as the water table in the region started to rise in response to deglaciation (Watts and Stuiver, 1980). Most lakes in Florida began to accumulate sediment at this time, but remained as shallow marsh systems for millennia as precipitation and water table elevations were both lower during the early Holocene (Watts, 1971; Quillen et al., 2013). The carbon isotope values of *n*-C_{27} tracks $\delta^{13}C_{TOC}$

throughout zone 3. The $\delta^{13}C$ values of *n*-C_{27}, once adjusted for the 4.4‰ depletion during alkane synthesis, plot within the isotopic range of TOC values. The environmental reconstructions and carbon isotope data indicate that the major source of carbon to the lake sediments was from terrestrial plants that utilized atmospheric CO_2.

As Florida gradually became wetter during the middle Holocene (between 7,000 and 5,500 yrs BP, zone 2 in our record) the sclerophyllous oak and open prairie plant communities were replaced by modern vegetation communities, dominated by pine forests (Watts and Hansen, 1994; Donders et al., 2014). The first significant change in $\delta^{13}C_{TOC}$ values occurred at ~6,500 yrs BP (350 cm core depth) and corresponds to this environmental change. The enrichment in $\delta^{13}C_{TOC}$ by ~10‰ from zone 3 to 2 implies that a new source of carbon was being utilized by the primary producers. The average $\delta^{13}C_{TOC}$ values (14.8‰) fall within the range of C_4 vegetation, meaning a shift from C_3 to C_4 communities could be the cause of the $\delta^{13}C_{TOC}$ enrichment. This, however, is improbable for two reasons. First, C_4 plants are adapted to low pCO_2 and arid environments (Ehleringer et al., 1997), and the middle Holocene was a period of increasing precipitation and relatively high pCO_2. Second, our *n*-C_{35} record, which is a proxy for graminoid abundance (Diefendorf and Freimuth, 2017), and the record of C_3/C_4 changes from nearby Lake Tulane (Huang et al., 2006), do not indicate an increase in the relative abundance of C_4 plants during this time interval. It is also possible that the ^{13}C enrichment was a consequence of decreased carbon isotope discrimination among phytoplankton under highly eutrophic conditions. This has been observed in multiple high-productivity lacustrine systems in Florida (Gu et al., 2006; Torres et al., 2013), and has been attributed to recent cultural eutrophication in others

(Brenner et al., 1999). If this were the cause of the $\delta^{13}C_{TOC}$ enrichment, then Lake Harris would have been eutrophic during the middle Holocene, but Kenney et al. (2016) demonstrated that nutrient accumulation was much lower at that time compared to modern nutrient accumulation.

I propose that the $\delta^{13}C_{TOC}$ record in zone 2 reflects a shift to a more enriched carbon source for the in-lake primary producer community. The $\delta^{13}C$ signature of *n*-C_{23} is the only possible source for this enrichment, as: 1) this chain length exhibits the highest $\delta^{13}C$ values across the depth interval 350-250 cm, 2) these values, once corrected for the 3.2‰ offset during alkane synthesis, nearly overlap with the TOC isotope data, and 3) the *n*-C_{23} carbon isotope profile tracks the bulk isotope data throughout zone 2. Lake Harris had deepened as the modern hydrosphere began to develop. Algae initially filled this newly created niche. From 430 to 400 cm there is a ~15-fold increase in *n*-C_{17} concentrations. In Lake Griffin, which is part of the Harris chain of lakes, a similar mid-Holocene peak in algal abundance was recorded in cyanotoxins (Waters, 2016). I speculate that these findings indicate a relatively rapid rise in water levels that supported phytoplankton populations before the proliferation of macrophytes, indicated by a ~30-fold increase in *n*-C_{23} contributions to the sediment at 380 to 330 cm.

There are two possible explanations for the ^{13}C enrichment. First, the $CaCO_3$ levels recorded in the sediment from the beginning of the zone to 350 cm core depth indicate a well-buffered system with high pH (>9). Bicarbonate (HCO_3^-) is the major form of DIC at pH >9, and active uptake of this HCO_3- would enrich the phytoplankton and SAV biomass by 8‰ relative to $CO_{2(aq)}$ (Mook et al., 1974). This could explain the high

$\delta^{13}C$ values measured in *n*-C_{23}. Secondly, Brenner et al. (2006) measured modern $\delta^{13}C$ values in two SAV taxa (*Vallisineria* sp. and *Potamogeton* sp.) in nearby Lake Panasoffkee, and although variability was high within the group, their $\delta^{13}C$ range (-13.2‰ to -15.5‰) is enough to explain the elevated $\delta^{13}C$ of the bulk organic matter in zone 2 of Lake Harris. The enrichment of $\delta^{13}C$ in zone 2 indicates proliferation of *Vallisineria* sp. and *Potamogeton* sp. in the lake.

From 250 cm core depth to the present (zone 1), the organic matter becomes progressively more depleted in ^{13}C. This depletion coincides with a second stage of increased precipitation in Florida that occurred between 5,000 and 3,000 yrs BP (Donders, 2014). Pollen based reconstructions of summer precipitation show persistently wetter conditions after 3,000 yrs BP, which were related to the intensification of ENSO (Donders, 2014). During the latter period, south Florida transitioned from a wet prairie to swamp forest environment (Donders et al., 2005). Farther north, Quillen et al. (2013) linked changes in benthic diatom assemblages to an increase in water depth in Lake Annie around the same time that Donders et al. (2005) noted ENSO intensification. Our geochemical proxies indicate that Lake Harris also achieved its modern water depth around this time. Organic matter abundance stabilized at levels >50% and $CaCO_3$ dropped to trace levels after ~4,800 yrs BP (Figure 3-2). Diatom biogenic silica concentrations overtake sponge derived silica concentrations at ~2,800 yrs BP. Together these proxies track the transition from a primarily shallow, groundwater-fed lake, to a relatively deep lake, whose depth was controlled by precipitation and/or surface water inputs.

Our *n*-alkane data also support this interpretation. The shift towards more negative $\delta^{13}C_{TOC}$ values in zone 3 results from increased algal contributions to the sediment. The algal proxy *n*-C_{17} has the most depleted $\delta^{13}C$ values among all *n*-alkanes analyzed, and the transition to more negative values in the bulk isotope data signifies the rising contribution of algae to the organic matter pool. Interestingly, this is the opposite trend observed by Filley et al. (2001) in Mud Lake, Marion County, FL. In that study the most enriched $\delta^{13}C$ values were recorded in *n*-C_{17}. We argue that the photic zone to water column ratio is larger in Mud Lake, and therefore isotopic discrimination by the primary producers will have a greater impact on increasing the $\delta^{13}C_{TOC}$ signature. The dissolved inorganic carbon (DIC) pool in Lake Harris is larger, because it is deeper, thus primary productivity will have a less significant impact on altering the isotopic signature of the DIC pool.

The cyanobacteria biomarker, 7-methylheptadecane, is the biomarker in highest abundance in the top 35 cm of the core. It also exhibits the highest average $\delta^{13}C$ values among all hydrocarbons in zone 1. Despite this, the $\delta^{13}C_{TOC}$ values do not become more positive up-core, even though enriched $\delta^{13}C_{TOC}$ values would be expected as the lake became more eutrophic and cyanobacterial blooms thrived (Brenner et al., 1999). Currently, I have no explanation for the discrepancy between 7-methylheptadecane concentrations/isotopic values and $\delta^{13}C_{TOC}$ values. The average $\delta^{13}C$ values (-21.3‰) are nearly identical to values measured from 7-methylheptadecane (-21.9‰) in the top 30 cm of Mud Lake (Filley et al., 2001), implying accurate isotopic measurement. Diagenetic alteration of the cyanobacteria signal is unlikely as these compounds are

present in abundant concentrations in our record, and are major components in the surface sediments of other Florida lakes (Riedinger-Whitmore, 2005; Waters, 2016).

Conclusions: Lake Harris

The evolution of Lake Harris is recorded in the geochemical proxies preserved within its sediments. The lake began to fill with water ~10,000 yrs BP, when many lakes in Florida began to accumulate sediment in response to wetter conditions caused by deglaciation and eustatic sea level rise. From the bottom of the core to 403 cm depth (~7,800 yrs BP), terrestrial carbon inputs dominated the record, with limited input from macrophytes and algae, and the primary carbon source was atmospheric CO_2. Throughout the early Holocene, Lake Harris was a marsh-like system in a relatively dry, open-prairie environment. A rapid, positive shift in $\delta^{13}C_{TOC}$ values at 402 cm, and stabilization about these values at 350 cm, represents the onset of wetter conditions in Florida. Elevated $CaCO_3$ levels in the sediments indicate that Lake Harris was primarily fed by groundwater, and isotopic signatures of *n*-alkanes and bulk organic matter suggest that organic matter was primarily derived from macrophytes that utilize enriched HCO_3^- as their carbon source. It was during that time, between 7,000 and 5,000 yrs BP, that Florida transitioned from dry oak scrub vegetation to pine forests. Above 240 cm core depth, $\delta^{13}C_{TOC}$ values begin to decline, $CaCO_3$ levels in the sediments decrease to below trace levels, and organic carbon concentrations increase. Around that time (3,000 yrs BP) the effects of ENSO intensified, and many Florida lakes deepened to their current limnetic state. This is observed in Lake Harris at ~2,900 yrs BP, when diatom biogenic silica concentrations increase from 10 to 120 mg/g. Concentrations of algal and cyanobacteria biomarkers increase by orders of magnitude after about AD 1940 in response to human-induced eutrophication.

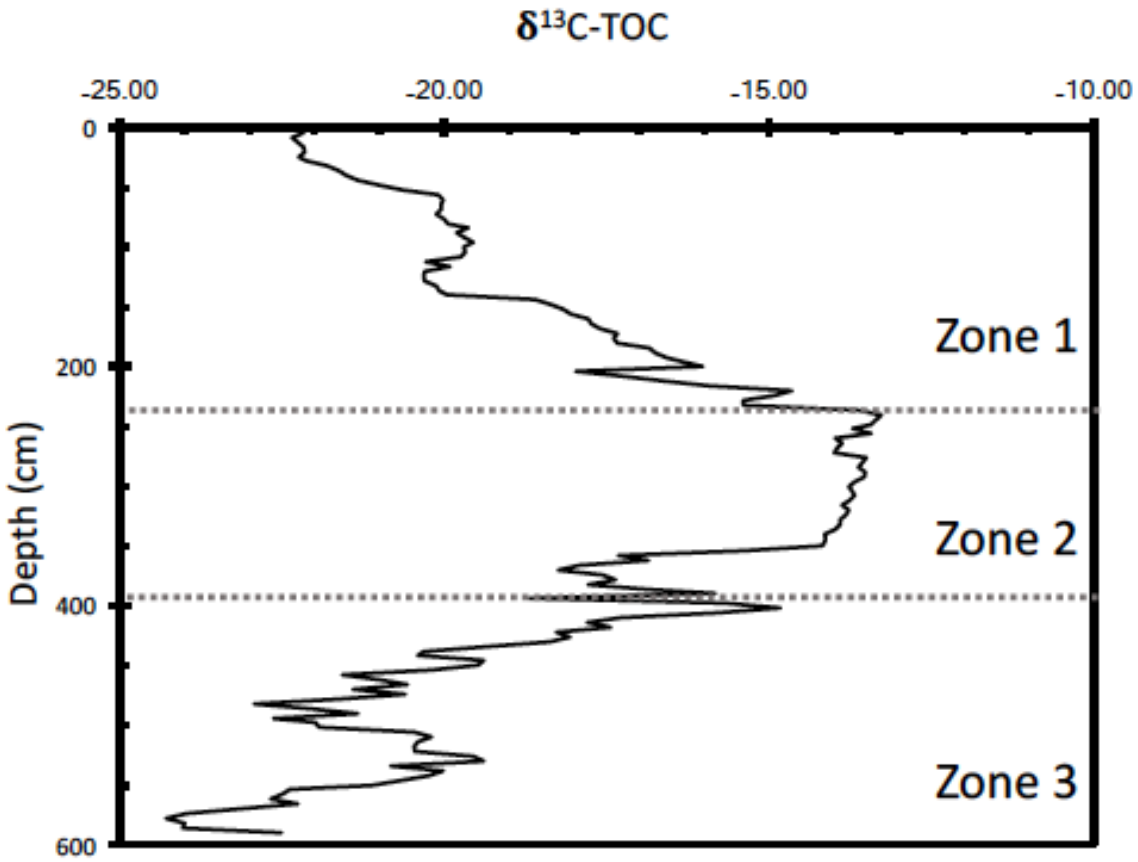

Figure 3-1. Down-core carbon isotope variability of TOC in the Lake Harris core. The three zones in the core are delineated by major shifts in $\delta^{13}C_{TOC}$ (shown in the figure as dashed lines). Zone 3 is from 590 to 403 cm, zone 2 is from 402 to 241 cm, and zone 1 extends from 240 cm to the core surface.

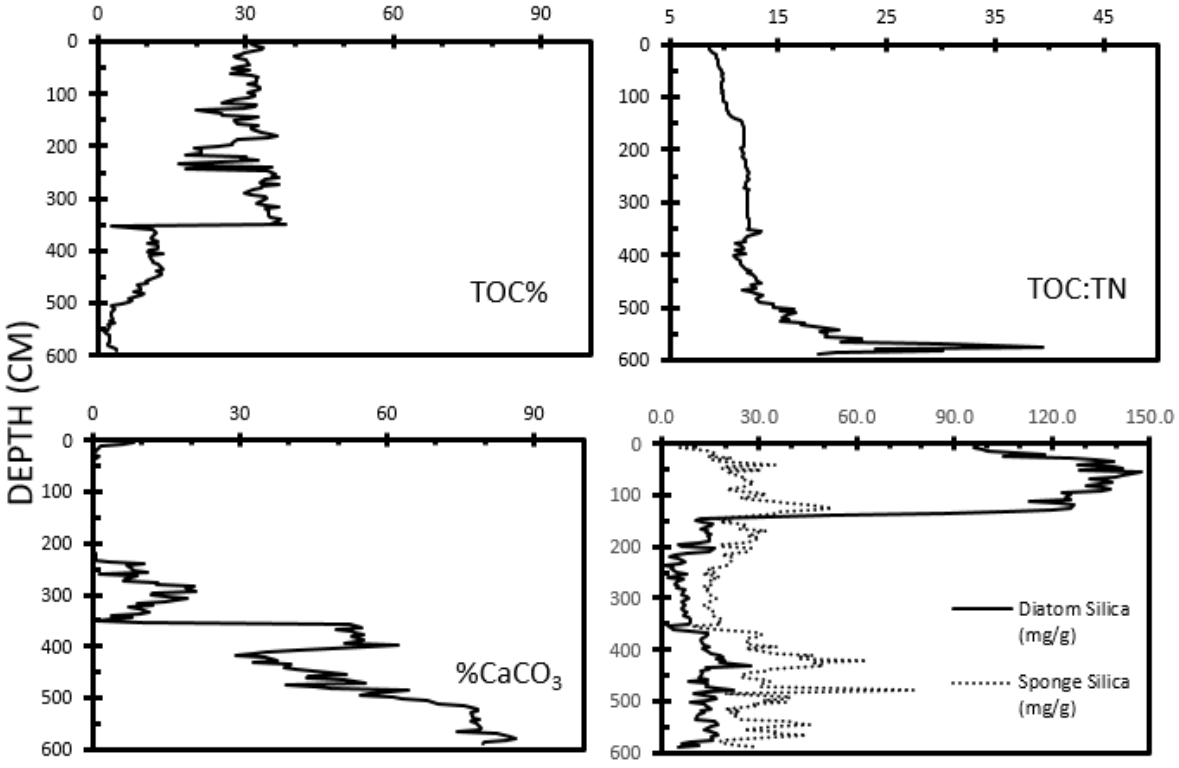

Figure 3-2. Bulk geochemical variability in the Lake Harris core.

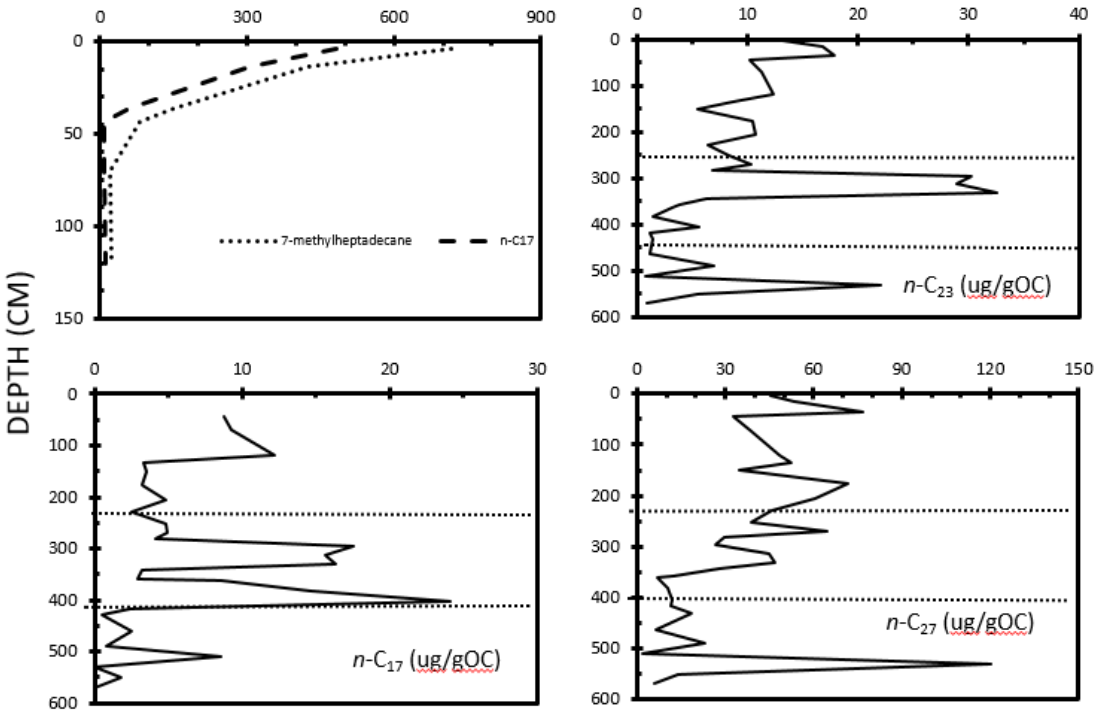

Figure 3-3. Select *n*-alkane chain length abundances in the Lake Harris core. Dashed lines delineate core zones 1-3.

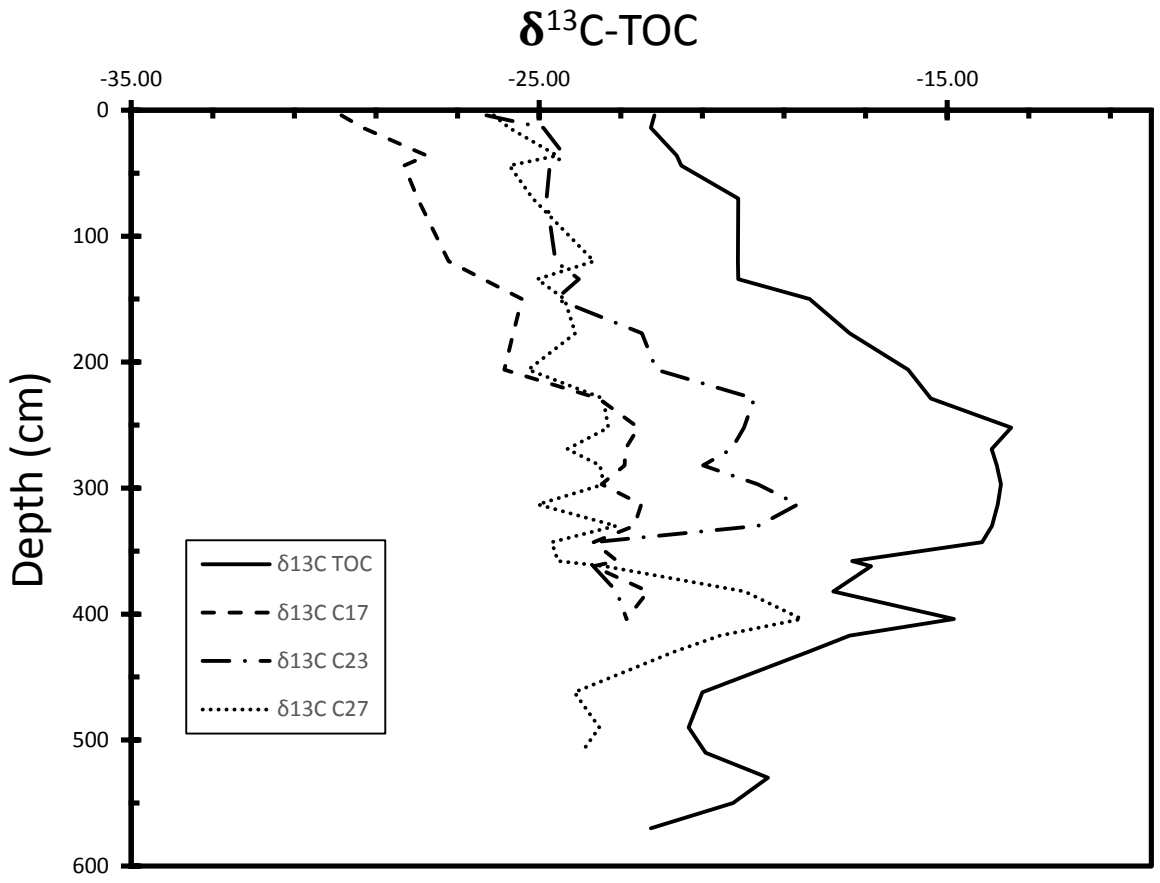

Figure 3-4. Carbon isotope variability in select *n*-alkane chain lengths in the Lake Harris core.

Table 3-1. Concentrations, maxima, minima, and ranges for the five *n*-alkane homologues used for organic matter source interpretation. Zones are delineated by $\delta^{13}C_{TOC}$ values.

n-alkane	C_{17} µg/gOC	C_{23} µg/gOC	C_{27} µg/gOC	C_{29} µg/gOC	C_{35} µg/gOC
Average	34.06	10.04	36.10	30.30	6.99
Max	482.57	32.51	120.00	79.70	50.45
Min	0.00	0.81	1.65	1.71	0.00
Range	482.57	31.70	118.35	77.99	50.45
Zone 1 Average	81.41	11.23	50.95	40.15	8.10
Zone 2 Average	10.63	12.50	29.22	26.28	4.59
Zone 3 Average	1.16	5.00	25.15	22.28	8.76

Table 3-2. Absolute values for carbon preference index (CPI), average chain length (ACL), and the ratio of submerged to emergent vegetation (Paq). Dates determined by the ^{210}Pb method are in Anno Domini (AD) and carbon-14 dated layers are in years before present (yrs BP), with BP set to 1950 AD, as is the convention.

Depth (cm)	CPI	ACL	P_{aq}	Age	Aging Method
4	3.53	28.72	0.47	2011.5	^{210}Pb-AD
14	6.56	29.67	0.29	1998.3	^{210}Pb-AD
36	4.01	29.27	0.30	1943.0	^{210}Pb-AD
44	2.74	28.99	0.38	1911.8	^{210}Pb-AD
70	3.36	29.17	0.30	900.0	C14-yrs BP
120	2.88	29.05	0.34	1916.7	C14-yrs BP
134	3.35	28.44	0.31	2398.0	C14-yrs BP
150	2.52	29.38	0.25	2775.9	C14-yrs BP
177	3.47	29.31	0.24	3565.4	C14-yrs BP
206	2.57	29.12	0.29	4770.1	C14-yrs BP
229	3.88	29.25	0.23	4843.2	C14-yrs BP
252	3.10	29.27	0.27	5199.8	C14-yrs BP
269	3.94	29.29	0.21	5449.5	C14-yrs BP
282	3.12	29.48	0.24	5620.0	C14-yrs BP
297	3.82	27.50	0.61	5840.5	C14-yrs BP
313	2.93	29.06	0.42	6049.6	C14-yrs BP
330	2.53	26.92	0.81	6252.4	C14-yrs BP
343	3.91	29.50	0.24	6425.4	C14-yrs BP
358	3.58	29.53	0.22	6741.6	C14-yrs BP
362	5.98	29.73	0.21	6826.3	C14-yrs BP
382	2.81	28.71	0.22	7770.0	C14-yrs BP
404	3.30	29.64	0.30	7845.3	C14-yrs BP
417	4.95	30.15	0.12	8019.3	C14-yrs BP
430	5.92	29.85	0.13	8167.3	C14-yrs BP
462	4.32	29.43	0.20	8477.8	C14-yrs BP
490	4.31	29.29	0.29	8827.0	C14-yrs BP
510	n/a	29.45	0.34	9300.0	C14-yrs BP
530	5.03	29.97	0.32	9472.3	C14-yrs BP
550	2.14	29.03	0.37	9832.4	C14-yrs BP
570	2.31	29.77	0.30	9900.0	C14-yrs BP

CHAPTER 4
SUBTROPICAL CLIMATE RESPONSE TO HEINRICH EVENTS IN THE NORTH ATLANTIC

Introduction: Lake Tulane and Heinrich Events

Lake Tulane is a relatively small (~36 ha), deep (z_{max} ~25 m) solution lake located in south-central Florida, USA. Its depth and location on a structural high, the Lake Wales Ridge, enabled continuous sediment accumulation since before the last glacial maximum. Palynological analysis on a sediment core from Lake Tulane indicated major shifts in plant communities over the past 60,000 years (Grimm et al., 1993). Of particular note are six peaks in *Pinus* (pine) pollen relative abundance, which coincide with the most intense cold phases of high-latitude Dansgaard–Oeschger (D-O) cycles and the Heinrich Events (HE) that terminate them. Alternating with *Pinus* peaks are zones with high relative percentages of *Quercus* (oak), *Ambrosia* (ragweed), *Lyonia* (staggerbush) and *Ceratiola* (rosemary) pollen, genera that today occupy the most xeric sites on the Florida landscape (Grimm et al., 2006). Additionally, the *Quercus* zones are replete with seeds from emergent aquatic plants, whereas all but one of the *Pinus* zones is devoid of such macrofossils. Lack of emergent macrofossils in *Pinus* phases suggests that the lake was too deep to support emergent vegetation close to the core site. Based on the quantitative similarity of the Pleistocene *Pinus* zones with modern/Holocene Florida vegetation, the *Pinus* peaks, and therefore the HE, were interpreted as warm and wet periods in Florida, whereas the *Quercus* zones were inferred to have been drier, and likely colder than the *Pinus* zones.

The assertion that the *Pinus* phases, and HE, represent warm and wet periods in the subtropics is contentious. HE are recorded in the sediment record of the North Atlantic as layers of ice-rafted debris (IRD), lithic fragments from rocks of continental

origin, which were derived from the calving and melting of large continental ice sheets (Bond et al., 1993). During Earth's last glacial interval, these episodic iceberg discharges perturbed global heat transport via reduction in the Atlantic meridional overturning circulation (AMOC) (Lynch-Stieglitz et al., 2014). Although the mechanism responsible for these events is still debated (Hemming, 2004; Marcott et al., 2011), teleconnections between HE and rapid climate oscillations have been recorded globally (Broecker, 2006). Their occurrence at the end of progressively cooler Greenland D-O interstadial cycles has led to the conclusion that HE were synchronous with lower temperatures and increased aridity over large regions of the Northern Hemisphere (Broecker et al., 1992; Zhao et al., 2003; Zhou et al., 2008). This hypothesis is supported by numerous lines of evidence, including: Iberian Margin sea-surface-temperature (SST) reconstructions derived from Mg/Ca ratios (Patton et al., 2011) and alkenone $U_{37}^{K'}$ records (Paillier and Bard, 2001), the relative abundance of the polar planktonic foraminiferan *Neogloboquadrina pachyderma* (sinistral) in the western Mediterranean (Cacho et al., 1999), and δ^{18}O records from marine sediment cores in the Icelandic and Irminger Seas (van Kreveld et al., 2000).

Although these studies indicated an in-phase relationship between SST and climate conditions in Greenland, there appears to be an anti-phase tendency in numerous other climate reconstructions, in particular, those from low to middle latitudes in the Atlantic (Hemming, 2004). Naafs et al.'s (2013) alkenone-based temperature reconstructions from the southernmost portions of the IRD belt (40-55°) indicate that surface waters were 2-4°C warmer during all six Heinrich Events. Farther south in the western Atlantic, temperatures approached modern values during HE1 (Weldeab et al.,

2006; Carlson et al., 2008) and HE5a (Schmidt et al., 2006), implying warm surface waters prior to transitions into interstadials. These results are in line with late-glacial circulation models, which produce warmer and more saline waters in middle latitudes of the western Atlantic when AMOC strength is at it's minimum, prior to the onset of HE farther north (Renold et al., 2009).

Reduced northward transport of heat just before and during HE, could be the source of the subtropical warming, hypothesized by Grimm et al. (2006) to be a prerequisite for *Pinus* proliferation. This idea was corroborated by coupled climate model simulations (Weaver et al., 2003), and pollen-climate inference models specific to Florida (Donders et al., 2011). Results from these modeling experiments demonstrate that a decrease in SST in the North Atlantic would increase the meridional temperature gradient, strengthen the trade winds and expand the Atlantic Warm Pool (AWP), resulting in more precipitation across the Florida Peninsula during HE (Donders et al., 2011).

Despite the results of modeling experiments, there are few empirical terrestrial records that document changes in temperature and precipitation across stadial/interstadial boundaries. In fact, the Grimm et al. (1993, 2006) studies of Lake Tulane represent the primary archive for terrestrial changes associated with HE in North America. Shortcomings of palynological reconstructions, however, which include inter-species differences in pollen production, dispersal, and preservation, make sedimentary pollen records potentially equivocal with respect to their ability to provide an accurate picture of plant community composition across the landscape (Bennet and Willis, 2002). Furthermore, pollen of different species within the genera *Pinus* and *Quercus* cannot be

distinguished, and today, taxa within each genus occupy different habitats across Florida's effective moisture spectrum, and this complicates assignment of plant genera to wet or dry environments. Given the lack of terrestrial records associated with HE, and potential problems associated with palynological reconstructions, additional lines of evidence are needed to test hypotheses regarding climate changes at low latitudes during HE.

Carbon Isotopes and Precipitation

Carbon isotopes of plant biomarkers in lake sediment cores have been used to infer shifts in precipitation and aridity over geologic timescales (e.g., Magill et al., 2013). Variations in the carbon isotopic composition of plant biomarkers, assuming no shifts in plant functional types or changes in the $\delta^{13}C$ of atmospheric CO_2, are caused primarily by changes in water-use efficiency (WUE = Assimilation/Transpiration) in plant communities as they respond to shifts in mean annual precipitation (MAP). A positive correlation (r= 0.74) between MAP and Δ_{leaf} values (as defined below) was demonstrated using data from the literature for >3,000 leaf samples from nine biomes with different MAP (Diefendorf et al., 2010). In areas with higher MAP, there was greater ^{13}C discrimination (Δ_{leaf}) by C_3 plants resulting in more negative plant $\delta^{13}C$ values.

The association between aridity (or decreased precipitation), and more enriched $\delta^{13}C_{leaf}$ values has been observed in many studies, with isotopic variability exceeding 6‰ at a single site (Ehleringer and Cooper, 1986; Stewart et al., 1995; Hartmann and Danin, 2010). Measurements from single *Pinus* species showed a ~2‰ decrease in $\delta^{13}C_{leaf}$ values across a 400-mm gradient of increasing precipitation in northeastern Spain (Ferrio et al., 2003), and values enriched by ~3‰ in water deficit treatments

(Waghorn et al., 2015). Taken together, these studies indicate that, once corrected for changes in $\delta^{13}C_{atmosphere}$ and carbon isotope discrimination, Δ_{leaf} is primarily driven by water availability (Diefendorf et al., 2010).

Hydrogen Isotopes and Precipitation

A strong positive correlation between δD of terrestrial plant lipids and δD of weighted mean annual precipitation has been demonstrated by various investigations (Sachse et al., 2004, 2012; Polissar and Freeman, 2010). Other studies have documented additional climatological (new precipitation sources and patterns), physiological (species-related photosynthetic offsets), or hydrological (precipitation amount) effects on δD values in leaf waxes (δD_{lipid}). Chief among these effects, however, is the evaporative enrichment of δD values in leaf water, which is primarily driven by relative humidity (Kahmen et al., 2008, 2013a, b).

Studies of leaf wax hydrogen isotope variability measured across precipitation gradients indicate that δD_{lipid} values are significantly enriched by transpiration in more arid environments (Smith and Freeman, 2006; Douglas et al., 2012). A study of *n*-alkanes from field-grown barley (*Hordeum vulgare*) showed that relative humidity influenced δD_{lipid} values, suggesting that hydrogen isotopes in leaf waxes yield a record of precipitation that is strongly modified by leaf water evaporation (Sachse et al., 2010). This effect is recorded in numerous other δD records that display decreased isotopic fractionation in lipids in sediments from arid sites (Polissar and Freeman, 2010), and among *n*-alkanes from plants across aridity gradients (Feakins and Sessions, 2010).

Thus, Δ_{leaf} and δD_{lipid} values in lake sediments should provide an indicator of past precipitation and these tools can be used to evaluate changes in Florida climate during HE. For example, during the hypothesized wet *Pinus* phases, Δ_{leaf} should be higher and

δD_{lipid} should be relatively lower, whereas during the dry *Quercus* periods, Δ_{leaf} should be lower and δD_{lipid} relatively higher. In this study we inferred temperature and precipitation changes across three HE (2-4) using the isotopic values ($\delta^{13}C$ and δD) in *n*-alkanes extracted from the same sediment core from Lake Tulane that Grimm et al. (2006) used to develop their pollen record. I hypothesize that precipitation in Florida was relatively greater during HE because of low-latitude warming associated with reduced AMOC strength. If, in fact, precipitation did change across stadial/interstadial boundaries, this change should be recorded in the carbon and hydrogen isotopes of plant leaf waxes.

Study Site and Sample Collection: Lake Tulane

Lake Tulane (Latitude 27°35'9"N; Longitude 81°30'13"W) occupies a surficial-groundwater-fed solution basin on the Lake Wales Ridge, an elongated, relict coastal ridge that has been above sea level since the early Pliocene (White, 1970). The sediments on the ridge are composed of coarse-grained quartz sands and gravels, often bound together with clays of fluvial origin (White, 1970). Lake Tulane is a relatively deep (z_{max} ~25m), oligotrophic water body (total phosphorus = 6 μg/L; Chl *a* = 3 μg/L) that is hydrologically isolated from the deep, Eocene-age limestone Floridan Aquifer, but receives seepage input through the shallow surficial aquifer. In spite of low aquatic productivity, the lake sediments are organic-rich (>10% organic matter). Despite its location above a limestone platform, the lake deposits lack carbonate.

A total of 24 sediment samples, four from each of *Pinus* zones 2-4 (TP 2-4) and *Quercus* zones 6-8 (TQ 6-8), were taken from the same core retrieved by Grimm et al. (2006) at 8-10 cm intervals. The core chronology is based on 55 AMS dates on bulk

sediments and, where available, terrestrial macrofossils. Our sampled interval (40,000-17,000 yr BP) fell within the range of radiocarbon dating. Grimm et al. (2006) calibrated samples < 20,000 ^{14}C yr BP using CALIB 5.0.2 with the INTCAL04 calibration curve, and for samples dated to 20,000-40,000 ^{14}C yr BP, the Fairbanks0805 calibration curve was applied (Fairbanks et al., 2005). See Grimm et al. (2006) for further details on calibration of the AMS dates.

Lipid Extraction, Purification, and Quantification: Lake Tulane

Sediment samples were freeze-dried and lipids were extracted with an Accelerated Solvent Extractor ASE200 (Dionex), using 2:1 (v/v) dichloromethane(DCM):methanol through three extraction cycles at 10.3 MPa (1500 psi) and 100°C. Between 1 and 2 g of sediment were used for lipid extraction. Total lipid extracts (TLE) were concentrated under a gentle stream of nitrogen, and the neutral lipid fraction was obtained after base saponification of the TLE. Neutral lipids were further separated, based on polarity, into compound classes by column chromatography, using 5% deactivated silica gel, according to methods modified from Nichols (2011). Hydrocarbons were eluted from the silica gel column with 4.5 ml of 9:1 Hexane:DCM, and saturated hydrocarbons were separated from alkenes on 5% Ag-impregnated silica gel (w/w) with 4 ml of hexane and ethyl acetate, respectively.

A Thermo Scientific Trace 1310 gas chromatograph with a Supelco Equity 5 column, interfaced to a Thermo Scientific TSQ 8000 triple quadrupole mass spectrometer with electron ionization, was used for compound identification. The split/splitless inlet was operated in splitless mode at 300°C with helium as the carrier gas. The column flow rate was 2.0 ml/min and the oven was held at an initial

temperature of 60°C for 1 minute, then ramped to 140°C at 15°C/min, and to 320°C at 4°C/min and held for 25 minutes. Alkane quantification was carried out on a Thermo Scientific Trace 1310 GC coupled with a flame ionized detector (GC-FID), using the same oven program as above. Androstane was added to sample vials prior to injection for use as an internal standard. Quantification was based on the calibration curves generated from the peak areas of external standards (C_7-C_{40}) with concentrations ranging from 5 to 250 μg/ml.

Compound-Specific Isotope Measurements: Lake Tulane

Compound-specific stable carbon isotope ratios were measured at Pennsylvania State University using a gas chromatograph coupled to an isotope ratio mass spectrometer interfaced with a GC-C combustion system. The *n*-alkanes were separated on a Varian model 3400 GC with a split/splitless injector operated in splitless mode. A fused silica capillary column (Agilent J&W DB-5; 30 m long, 0.32 mm I.D., 0.25 μm film thickness) was used with helium as the carrier gas and a column flow rate of 2.0 ml/min. The oven program began at a temperature of 60°C, was held for 1 minute, then increased at a rate of 6°C/min to 320°C, which was held for 20 minutes. Following GC separation, *n*-alkanes were combusted over nickel-platinum wire with O_2 in He (1%, v/v) at 1000°C. Isotope ratios of carbon in CO_2 were measured using a Finnigan Mat 252 isotope ratio mass spectrometer. Isotopic abundances were determined relative to a reference gas calibrated with Mix B (*n*-C_{16} to *n*-C_{30}; Arndt Schimmelmann, Indiana University). Carbon isotope values of samples were normalized to the VPDB scale using the Uncertainty Calculator (Polissar and D'Andrea, 2014) and are reported in standard delta notation as follows:

$$\delta^{13}C = [(({}^{13}C/{}^{12}C)_{sample}/({}^{13}C/{}^{12}C)_{standard}) - 1] \times 1000 \quad (3\text{-}1)$$

Standard errors of the mean (SE) were calculated using the Uncertainty Calculator, which yielded a 1σ SE value of ± 0.35‰ (Polissar and D'Andrea, 2014).

To eliminate possible confounding results associated with past changes in $\delta^{13}C$ values of atmospheric CO_2, all carbon isotope data are presented as Δ_{leaf} values (Farquhar et al, 1989), where:

$$\Delta_{leaf} = (\delta^{13}C_{atm} - \delta^{13}C_{leaf})/(1 + \delta^{13}C_{leaf}/1000) \quad (3\text{-}2)$$

Carbon isotope values for atmospheric CO_2 were taken from Leuenberger et al. (1992) and data were interpolated using a cubic spline. Carbon isotope values of atmospheric CO_2 ranged from -6.3‰ to -7.1‰ across the studied interval. By accounting for variations in carbon source, the Δ_{leaf} value primarily becomes a function of WUE, with lower Δ_{leaf} indicative of lower stomatal conductance and reduced precipitation (Diefendorf et al., 2010).

Compound-specific hydrogen isotopes were measured at the University of Cincinnati using a Thermo Trace GC Ultra coupled to a Thermo Electron Delta V Advantage IRMS instrument with an Isolink combustion furnace. A fused silica capillary column (Agilent J&W DB-5; 30 m long, 0.25 mm I.D., 0.25 μm film thickness) was used with helium as the carrier gas and a column flow rate of 1.5 ml/min using a split/splitless injector operated in splitless mode. The oven program was slightly modified from the schedule above: 80°C (2 min), then to 320°C (held 10 min) at 8°C/min. Hydrogen isotope abundances and standard errors were calculated as above for carbon isotopes. Reference gas values were calibrated with Mix A (*n*-C_{16} to *n*-C_{30}; Arndt Schimmelmann, Indiana University). The H_3^+ factor had a mean value of 6.244. Calculation of isotope

abundances and correction of δD values to the Vienna Standard Mean Ocean Water (VSMOW) scale was done in the same way as for carbon isotopes, and the pooled 1σ SE for all samples was ± 3.2‰. Hydrogen isotope values are reported in standard delta notation relative to VSMOW as follows:

$$\delta D = [((D/H)_{sample}/(D/H)_{standard}) - 1] \times 1000 \quad (3\text{-}3)$$

To estimate the environmental controls on hydrogen isotope ratios in leaf waxes, we first had to calculate the $\varepsilon_{l/w}$ values, defined as $[((D/H)_{lipid}/(D/H)_{water}) - 1]$, for C_{29} *n*-alkanes and different plant functional types (PFTs). The $\varepsilon_{l/w}$ values for terrestrial plants in this study were taken from Magill et al. (2013), who defined three primary PFTs on the basis of photosynthetic pathway and growth habit: C_4 graminoids [grasses] (−146‰ ± 8‰), C_3 herbs (−124‰ ± 10‰), and C_3 woody plants (−109‰ ± 8‰). Aquatic macrophyte $\varepsilon_{l/w}$ values were taken from Aichner et al. (2010), who calculated the biosynthetic offset between the C_{23} *n*-alkane from *Potamogeton* (pondweed) and lake water to be -82‰. After accounting for changes in $\varepsilon_{l/w}$, evapotranspiration (and aridity) can be estimated as the difference between the δD_{lipid} values of terrestrial and aquatic plants as follows:

$$\varepsilon_{(terr\text{-}aq)} = 1000 \times [(\delta D_{lipid}\ (C_{29}) + 1000)/(\ \delta D_{lipid}\ (C_{23}) + 1000) - 1)] \quad (3\text{-}4)$$

n-Alkane Concentrations and Chain Length Distributions

Concentrations for select *n*-alkane chain lengths are provided in Figure 4-1. The *n*-alkane chain lengths are dominated by the long-chain alkanes (i.e., > *n*-C_{25}), with *n*-C_{29} displaying the highest average abundance (120.3 µg/g OC) throughout the Lake Tulane sediment record. We calculated the average chain length (ACL) for all samples using the Eglinton and Hamilton (1967) equation:

$$ACL(C_{25}\text{-}C_{35}) = \frac{25C_{25}+27C_{27}+29C_{29}+31C_{31}+33C_{33}+35C_{35}}{C_{25}+C_{27}+C_{29}+C_{31}+C_{33}+C_{35}} \quad (3\text{-}5)$$

There is low variability in ACL throughout the record. The highest ACL value is 30.1 and the lowest is 29.2, with a mean ACL of 29.7 for the entire record (Table 4-1). All samples exhibit a strong odd over even predominance, consistent with vascular terrestrial plant sources. This is also in agreement with carbon preference index (CPI) values calculated from the equation of Bray and Evans (1961):

$$CPI = 0.5\,\frac{C_{25}+C_{27}+C_{29}+C_{31}+C_{33}}{C_{26}+C_{28}+C_{30}+C_{32}+C_{34}} + \frac{C_{25}+C_{27}+C_{29}+C_{31}+C_{33}}{C_{24}+C_{26}+C_{28}+C_{30}+C_{32}} \quad (3\text{-}6)$$

The *n*-alkane CPI values for all samples are >1, which indicates higher odd-chain *n*-alkane abundances. CPI values range from a maximum of 3.2 to a minimum of 2.0, with an average of 2.7 (Table 4-1).

Differences in mean *n*-alkane concentrations are apparent between *Pinus* and *Quercus* phases. Highest average abundances for carbon chain lengths *n*-C_{16}-C_{22} occurred during *Pinus* phases, whereas chain lengths *n*-C_{23}-C_{35} had the highest average abundances during *Quercus* phases. Alkanes derived from C_3 dicots (*n*-C_{27} and *n*-C_{29}) decreased in average abundance by 75% (*n*-C_{27}) and 70% (*n*-C_{29}) during the *Pinus* intervals. Furthermore, alkane biomarkers from mixed C_3/C_4 sources, *n*-C_{33} and *n*-C_{35}, were reduced by 64% and 62%, respectively, during the *Pinus* intervals. Although abundances of the submerged aquatic plant biomarker (*n*-C_{23}) were higher during *Quercus* phases by ~60%, the P_{aq} proxy (Ficken et al, 2000), described by the formula (C_{23} + C_{25})/(C_{23} + C_{25} + C_{29} + C_{31}), showed no significant change in the ratio of submerged to emergent/terrestrial vegetation across vegetation zones (Table 4-1).

Carbon Isotope Results: Lake Tulane

The Δ_{leaf} values for carbon chain lengths *n*-C_{27}-C_{35} are shown in Figure 4-2. Correlations between Δ_{leaf} values and *Pinus* pollen percentages are greater for shorter-chain-length alkanes *n*-C_{27} ($r = 0.62$, $n = 24$, $p < 0.001$) and *n*-C_{29} ($r = 0.54$, $n = 24$, $p < 0.01$), than for longer chain lengths *n*-C_{31} ($r = 0.44$, $n = 24$, $p < 0.05$) and *n*-C_{33} ($r = 0.40$, $n = 24$, $p < 0.05$), however, *n*-C_{35} ($r = 0.58$, $n = 24$, $p < 0.01$) is also more strongly correlated to *Pinus* pollen than the other long-chain *n*-alkanes. Mean Δ_{leaf} values for all *Pinus* zones were an average of 0.8‰ greater than means for *Quercus* zones and all chain length Δ_{leaf} values were significantly positively correlated with *Pinus* pollen percentages. Mean Δ_{leaf} values for all chain lengths are provided in Table 4-2. The *n*-alkanes with 31, 33, and 35 carbons displayed the greatest range in Δ_{leaf} values: 2.7‰ (max = 21.4‰, min = 18.7‰), 5.7‰ (max = 24.3‰, min = 18.6‰), and 4.7‰ (max = 21.3‰, min = 16.6‰), respectively, whereas the range in Δ_{leaf} values of *n*-alkanes with 27 and 29 carbons was 1.7‰ (max = 22.4‰, min = 20.7‰) and 2.0‰ (max = 21.9‰, min = 19.9‰), respectively.

Hydrogen Isotope Results: Lake Tulane

Hydrogen isotope profiles for select *n*-alkanes are displayed in Figure 4-3 and Table 4-3. For all chain lengths, the mean δD signature is higher during *Pinus* phases and lower during the *Quercus* zones. The greatest difference between means was recorded in the *n*-C_{23} (19.3‰), and all other chain lengths displayed differences in means (*Pinus*-*Quercus*) ranging from 2.6 to 8.2‰. Hydrogen isotope values begin to decrease prior to the end of each *Pinus* phase. As a result, δD profiles for all but one chain length (*n*-C_{23}) are not significantly correlated with *Pinus* pollen percentages (Figure 4-3). As with carbon isotope results, the longer-chain-length alkanes (*n*-C_{33} =

32.7‰, *n*-C_{35} = 25.8‰) exhibited greater δD ranges compared to shorter-chain-length alkanes (*n*-C_{27} = 20.5‰, *n*-C_{29} = 21.0‰), though the largest range in δD values was found in alkane *n*-C_{23} (43.5‰).

After adjusting the *n*-C_{23} ($\varepsilon_{l/w}$ = 82‰) and *n*-C_{29} ($\varepsilon_{l/w}$ = 109‰) δD signatures to account for fractionation during biosynthesis, $\varepsilon_{(terr\text{-}aq)}$ values were calculated as a proxy for evapotranspiration. Larger values are indicative of greater aridity and evapotranspiration. Overall, $\varepsilon_{(terr\text{-}aq)}$ is negatively correlated with percent *Pinus* pollen ($r = -0.79$, $n = 21$, $p < 0.001$), with $\varepsilon_{(terr\text{-}aq)}$ values, on average, 17.4‰ higher during *Quercus* phases (Figure 4-4). The $\varepsilon_{(terr\text{-}aq)}$ values had a mean of 15.4‰ and a range of 36.1‰.

Reconstructing Paleohydrology from Leaf Wax Carbon and Hydrology Isotopes

The late Pleistocene was characterized by periods of rapid climate fluctuations brought about by changes in ocean circulation and ice volume. These climate events have been studied extensively in sediment records from marine sites in the high-latitude north Atlantic, but rarely have they been documented in subtropical terrestrial sites. Carbon and hydrogen isotope leaf wax data from this study were used to reconstruct changes in paleohydrology at Lake Tulane, Florida (USA) and supplement the limited data on the effects of rapid climate change at low latitudes.

Both isotopes respond to changes in water availability, therefore vegetation transitions from *Pinus*-dominated to *Quercus*-dominated phases should have produced measurable differences in carbon and hydrogen stable isotope ratios. If variations in carbon source (i.e. $\delta^{13}C_{atms}$) are accounted for, the Δ_{leaf} value is primarily a function of WUE, with low Δ_{leaf} indicative of lower stomatal conductance and thus low precipitation (Diefendorf et al., 2010). Although our ranges in Δ_{leaf} values are small and their

correlation with *Pinus* percentages are all below r = 0.6, changes in water availability are still apparent across the studied section of the Lake Tulane sediment record. The *n*-C_{29} Δ_{leaf} profile exhibits the strongest positive correlation (r = 0.54) with changes in *Pinus* pollen relative abundance. This *n*-alkane, a primary component of leaf waxes in higher terrestrial angiosperms, was mainly derived from *Quercus*, with minor contributions from *Ambrosia*. These are the two dominant angiosperms in the Lake Tulane pollen record, accounting for ~50% of all pollen recorded during interstadials, and 10-25% during stadials. Despite the high *Pinus* pollen during stadials, very few *n*-alkanes were contributed by gymnosperms, as they are noted for their low alkane production (Diefendorf et al., 2011).

The small range (2‰) in *n*-C_{29} Δ_{leaf} values between *Pinus* and *Quercus* phases is in line with $\delta^{13}C$ ranges (~2‰) measured in modern experiments with a single taxon, during which *Pinus halepensis* received different amounts of water (Ferrio et al., 2003), and with natural variability among woody perennial plants (~3‰) that were sampled across rainfall gradients in the Mediterranean (Hartmann and Danin, 2010). I infer from higher Δ_{leaf} values during *Pinus* phases that WUE decreased and discrimination against ^{13}C increased. The interpretation of these data relies heavily on modern empirical studies of WUE in C_3 plants (e.g. Hartmann and Danin, 2010). Plants respond to water stress by reducing their stomatal conductance, which lowers the CO_2 concentration within leaves (internal leaf = c_i) relative to the concentration of CO_2 in the atmosphere (c_a), i.e. c_i/c_a. Partial closure of the stomata reduces the flux of CO_2 and H_2O, but the two fluxes are not reduced equally. Whereas the reduction in transpiration is proportional to the amount of stomatal closure, photosynthesis continues at a high rate,

and carbon assimilation thus declines less than transpiration. Because assimilation decreases slower than transpiration, WUE increases. Related to this, when c_i is low, plants are less able to discriminate against ^{13}C, and $\delta^{13}C_{leaf}$ values increase, and Δ_{leaf} values decrease (Marshall et al., 2007). From this I interpret *Pinus* zones (cold stadials) to have been wetter than *Quercus* zones (warm interstadials).

Although WUE is strongly correlated to $\delta^{13}C$ values in plants, it is not the only factor that can affect leaf wax carbon isotope signatures. A small amount of variability in the carbon isotope record could be the result of mixing of *n*-alkanes from different PFTs. Previous isotope and pollen research on the same sediment core from Lake Tulane showed that C_4 contributions to the organic carbon pool dropped from highs of ~50% during *Quercus* phases to nearly 0% during *Pinus* phases (Grimm et al., 2006; Huang et al., 2006). These results are in agreement with our *n*-alkane concentration data, which record a ~60% drop in *n*-C_{33} and *n*-C_{35} concentrations, but not in *n*-C_{27} and *n*-C_{29} concentrations in *Pinus* zones. The disparate behavior of *n*-$C_{27/29}$ and *n*-$C_{33/35}$ in the record is likely related to plant physiology: C_4 graminoids contain *n*-C_{33} and *n*-C_{35} alkanes in their leaves at concentrations an order of magnitude greater than in woody C_3 angiosperms (Garcin et al., 2014; Diefendorf and Freimuth, 2017). This bias towards longer-chain (greater than C_{31}) *n*-alkane synthesis in graminoids was also observed in a marine sediment core taken off the coast of equatorial Africa (Wang et al., 2013). The authors applied results from empirical isotope studies (e.g. Sasche et al., 2012) to their data to estimate the relative input of C_3/C_4 vegetation to their site over the past 37 ka. They found that *n*-C_{33-35} were mostly contributed by C_4 grasses that are depleted in deuterium and enriched in ^{13}C relative to the same *n*-alkane homologues from C_3 dicots.

The low Δ_{leaf} and δD values and reduced fractionation observed in the *n*-$C_{33\text{-}35}$ Δ_{leaf} record from this study suggests that these *n*-alkanes are primarily from C_4 sources. From the *n*-alkane concentration and isotope data we infer: 1) a negligible contribution of *n*-alkanes from C_4 grasses during HE, and 2) a limited contribution from grasses throughout the entire *n*-C_{29} record. The *n*-C_{29} data can be further classified as a terrestrial C_3 angiosperm biomarker based upon research on chain-length distributions and isotope values among different PFTs, which show that most gymnosperms do not produce *n*-alkanes in substantial quantities (Diefendorf et al., 2011).

Mixing of C_3/C_4 vegetation and variable input of conifer organic matter would not substantially influence the $\delta^{13}C$ values of the *n*-$C_{27/29}$ record, nor would the introduction of new plant species, as illustrated by Lake Tulane's pollen record (Grimm et al., 2006). Pollen counts showed that relative contributions of plant pollen changed significantly between stadial and interstadial periods, but relative pollen abundances were quite similar among all *Pinus* zones, and among all *Quercus* zones. Of the two major plant genera at the site, only *Quercus* produces *n*-$C_{27/29}$ in significant quantities, and palynological studies suggest that the most probable source of these homologues was from one or more *Quercus* species in Florida (Grimm et al., 2006). Therefore, changes in $\delta^{13}C$ values, unrelated to WUE, could be from physiological differences in carbon isotope fractionation among plants of the same functional type. Isotopic differences have been detected in *n*-alkanes sampled from angiosperms growing under identical environmental conditions and irrigated with the same water (Pedentchouck et al., 2008). Leaves measured from two species in that study, *Betula pendula* and *Populus tremuloides*, returned $\delta^{13}C$ values that were offset from one another by ~5‰, leading

the authors to conclude that different rates of stomatal conductance and carbon metabolism lead to isotopic differences among angiosperms (Pedentchouck et al., 2008). Furthermore, carbon isotope ratios measured in *n*-C_{29} alkanes from three species of *Quercus* returned values ranging from 33.3‰ to 34.8‰ (Chikaraishi and Naraoka, 2003), and bulk $\delta^{13}C$ measurements on individual *Q. chrysolepis* from a single study site ranged from -30‰ to -27‰ (Feakins and Sessions, 2010). Therefore, the *n*-$C_{27/29}$ Δ_{leaf} record responds to both changes in water availability, and to a lesser extent, to mixtures of *n*-alkanes from plants within the same genus and/or functional type.

This finding does not preclude our data from being used to reconstruct water availability. The relatively strong correlation between *Pinus* pollen relative abundance and *n*-$C_{27/29}$ indicates that water availability probably changed as the climate system in the northern hemisphere responded to HE. Because *n*-$C_{27/29}$ were least influenced by changes in relative contributions from different PFTs, δD of *n*-$C_{27/29}$ can be used as a robust indicator of precipitation changes across the study interval. The δD_{lipid} values of these chain lengths (and all other long-chain *n*-alkanes analyzed) decrease during the interstadial periods (*Quercus* zones) and reach maximum values during stadial (*Pinus* zones) (Figure 4-3). Kahmen et al. (2013b) demonstrated that the δD values of leaf waxes reflects the combined effects of aridity and precipitation δD values. When relative humidity is higher, both precipitation and leaf water δD values are lower. Assuming this is the case, δD profiles of terrestrial *n*-alkanes suggest greater aridity during the *Pinus* zones. The δD values recorded in the *n*-alkanes of terrestrial vegetation, however, does not solely track the effects of aridity, but rather reflects both aridity and variability in precipitation δD values. In the mid-latitudes, hydrogen isotope ratios in precipitation are

primarily controlled by temperature (Gat, 1996; Rach et al., 2014). Similar to the effect of increasing relative humidity, higher temperatures decrease δD values of precipitation. Central Florida's climate is subtropical, and during the last glacial period its climate likely shifted toward more temperate, i.e. cooler conditions. As such, the isotopic composition of precipitation was controlled more by temperature and less so by the amount effect. To separate the effects of aridity from condensation temperature on leaf wax δD values, we assigned $\varepsilon_{l/w}$ values to long-chain terrestrial and short-chain aquatic *n*-alkanes, and expressed the effect of aridity, or more specifically, evapotranspiration, as the difference between the terrestrial and aquatic lipid values ($\varepsilon_{(terr\text{-}aq)}$).

Even though we cannot exclude the possibility of multiple woody C_3 angiosperm sources in our *n*-$C_{27\text{-}29}$ record, we are confident these homologues represent negligible input from gymnosperms and C_4 grasses. Because *n*-C_{27} is less abundant throughout our record, we assigned a terrestrial $\varepsilon_{l/w}$ value of -109‰ to *n*-C_{29}, using Magill et al.'s (2013) calculation for woody C_3 plants. Determining $\varepsilon_{l/w}$ for submerged aquatic vegetation (SAV) is more challenging because few studies have addressed isotopic offsets between plants and lake water. We do know, however, that submerged vegetation contains a greater relative abundance of mid-chain-length, primarily *n*-C_{23}, alkanes (Ficken et al., 2000), and in a few studies, the offset between *n*-alkanes and their source water was calculated for SAV. For instance, Mügler et al. (2008) measured hydrogen isotope values of *n*-C_{23} in a suite of aquatic macrophytes from lakes on the Tibetan Plateau, and found $\varepsilon_{l/w}$ values with a mean of -111‰. This value, however, is ~30‰ lower relative to measurements on the submerged macrophyte *Potamogeton* ($\varepsilon_{l/w}$ = -82‰) made by Aichner et al. (2010), also in Tibet. In our record, δD values for mid-

chain-length *n*-C_{23} are higher by an average of ~20‰ relative to long-chain *n*-alkanes, despite the evaporative effect on δD values that would be expected to occur in the terrestrial isotope record. The greater δD values measured in *n*-C_{23} can be explained by its less negative $\varepsilon_{l/w}$ value, a value which is more like Aichner et al.'s (2010) *Potamogeton* measurements. This explanation is supported by *Potamogeton* macrofossil evidence within the Lake Tulane sediment core (Grimm et al., 2006), thus, we applied an $\varepsilon_{l/w}$ of -82‰ to the *n*-C_{23} alkane.

The $\varepsilon_{l/w}$-corrected δD values of the aquatic lipids record changes in the average δD value of annual precipitation, plus any evaporative enrichment of the lake water (Sachse et al., 2012; Rach et al., 2014). δD values of *n*-C_{23} decrease by an average of 21‰ during *Quercus* periods. The simplest explanation for this decrease in hydrogen isotope ratios invokes decreasing air temperature in the tropics during Greenland interstadials. We are confident that Lake Tulane's waters are only moderately affected by evaporative enrichment because of the lakes relatively great depth and the moderating effect of shallow groundwater inputs. This is supported by data from modern lake water studies that tracked isotopic shifts in Lake Tulane over a three-year period (Escobar et al., 2013). During that time span, the average intra-annual variability in $\delta^{18}O$ was 0.6‰, which is equivalent to 4.86‰ in δD space (Florea et al., 2010). We assumed that annual evaporative enrichment of lake waters was similar during the Pleistocene and had minimal influence on the isotope values of lake water. If, however, evaporative enrichment did increase during *Quercus* zones, the δD signature of *n*-C_{23} from SAV would also have increased. Instead, we measured an average depletion in the δD record during *Quercus* zones (Figure 4-3). This, of course, could be interpreted as a

decrease in aridity and an increase in precipitation during interstadial periods, but an interpretation of wetter conditions is at odds with: 1) our carbon isotope data, from which we infer greater WUE during *Quercus* periods, 2) the proliferation of C_4 grasslands during the Lake Tulane *Quercus* phases, which is suggestive of increased aridity (Huang et al., 2006), and 3) climate models and SST reconstructions that indicate ocean warming and relatively greater precipitation in the Gulf of Mexico region during *Pinus*, as opposed to *Quercus* zones (Flower et al., 2004; Schmidt et al., 2006; Donders et al., 2011). From this, we conclude that the isotopic variability in the *n*-C_{23} record reflects shifts in condensation and evaporation temperatures during cloud formation. During both evaporation of water from the source (ocean surface) and condensation of water vapor in the atmosphere, δD values of the resulting precipitation decrease with decreasing temperatures (Sharp, 2007). Then, the δD profile of *n*-$C_{23,}$ once corrected for the biological fractionation, is interpreted as a signal of temperature during precipitation. The higher δD values of *n*-C_{23} during *Pinus* periods are the result of higher temperatures, and the lower δD values during *Quercus* periods are from lower atmospheric temperatures.

Hydrogen isotope values of the terrestrial *n*-alkane (*n*-C_{29}) biomarker track precipitation, but are also influenced by evapotranspiration and mixing of plant communities with different $\varepsilon_{l/w}$ values (Smith and Freeman, 2006). When analyzed individually, the $\varepsilon_{l/w}$ corrected *n*-C_{29} record does not produce results that lead to meaningful paleo-hydrological interpretation. The ~5-10‰ enrichment in δD values during *Pinus* phases could be attributed to either climate variables, such as increased aridity and higher temperatures, or paleo-hydrological factors, such as shifts in the

source and timing of precipitation. When the *n*-C_{29} data are analyzed in conjunction with the $\varepsilon_{l/w}$-corrected *n*-C_{23} record, however, and expressed as the $\varepsilon_{(terr\text{-}aq)}$ value, changes in aridity between *Pinus* and *Quercus* zones can be quantified. On average, the values for our aridity proxy decrease by 17‰ during periods of increased *Pinus* pollen concentrations. These results are in line with model simulations that produce deuterium enrichment in *n*-alkanes by as much as 10-30‰ during evapotranspiration in temperate environments (Kahmen et al., 2013b).The negative correlation between $\varepsilon_{(terr\text{-}aq)}$ and *Pinus* zones ($r = -0.79$, $p<0.001$) (Figure 4-4) identifies these as zones of lower isotopic enrichment from evapotranspiration, and hence less aridity, which is defined as the ratio of annual precipitation to potential evapotranspiration (Maliva and Missimer, 2012). If both aridity and evapotranspiration decreased during *Pinus* zones, then precipitation in Florida must have increased when *Pinus* proliferated.

Implications of Rapid Climate Change Events in the Subtropics

Carbon and hydrogen isotope data from *n*-C_{29} and *n*-C_{23} indicate that evapotranspiration decreased and atmospheric temperatures increased during *Pinus* phases at Lake Tulane and HE/Greenland stadials. The independent chronology developed by Grimm et al. (2006) also found an inverse correlation between Greenland temperatures and the Lake Tulane pollen record. Multiple reconstructions of SST during HE indicate that surface waters south of the IRD belt warmed as temperatures over Greenland dropped (Flower et al., 2004; Schmidt et al., 2006; Weldeab et al., 2006), and temperature in the Gulf of Mexico also remained warm throughout Greenland stadials, implying persistence of the AWP around peninsular Florida (Carlson et al., 2008; Ziegler et al., 2008; Rasmussen and Thomsen, 2012). But what could have kept Florida and the Gulf of Mexico warm and wet during the extreme cold events in the

North Atlantic? Results of pollen-climate inference models (Donders et al., 2011) link a warm, persistent AWP with northward displacement of the ITCZ and increased precipitation across the Florida Peninsula during cold periods in the high-latitude North Atlantic. At present, the source and seasonal delivery of precipitation in Florida is similar to the late Pleistocene. The northward displacement of the ITCZ during the boreal summer increases trade wind strength over the subtropical North Atlantic, resulting in greater rainfall on the peninsula. Other studies showed that during Greenland stadials, the southward displacement of the polar front was associated with an expansion of the subpolar gyre and a westward movement of the subtropical gyre (Eynaud et al., 2009). The westward shift of the subtropical gyre results in a narrower Gulf Stream, and moves it closer to the continent (Hoogakker et al., 2013). This agrees with inferred stadial/interstadial shifts in the position of the Gulf Stream (Hoogakker et al., 2013), and warmer mid-latitude North Atlantic SSTs during stadial periods (Naafs et al., 2013). A narrower Gulf Stream with reduced northward heat transport, located closer to the Florida Peninsula, could explain why Florida remained warm and relatively wet during the Heinrich stadials.

Data from multiple studies (e.g. Kreveld et al., 2000) indicate that the duration and magnitude of the climate system response to HE6-1 was not uniform. Our $\varepsilon_{(terr\text{-}aq)}$ record spans a range of 36‰, and records multiple abrupt shifts in aridity. During HE4-3 departures towards negative $\varepsilon_{(terr\text{-}aq)}$ values indicate that these HE elicited the strongest response from the hydrological cycle, while HE2 produced a more muted response. It is not surprising that HE4 resulted in the largest shift toward less arid values as it is the largest of the six HE in terms of %IRD (Hemming 2004, Tierney et al., 2008). The

subdued response in our hydrogen isotope record during HE2, is also expected, as studies have demonstrated that there was no reduction in AMOC intensity across that interval (Lynch-Stieflitz et al., 2014; Parker et al., 2015). The pronounced response during HE3, however, does not match data that classify it as a low-foraminifera interval, with limited change in AMOC strength, rather than a true ice-rafting event (Hemming 2004; Lynch-Stieflitz et al., 2014). Tulane *Pinus* zone 3, which correlates to HE3, has lower values of *Pinus* pollen and higher values of *Ambrosia* than *Pinus* zones 1, 4, 5, and 6, suggesting cooler temperatures during HE3 (Grimm et al., 2006). If HE3 was not caused by a reduction in AMOC strength associated with freshening of the North Atlantic, another yet unidentified mechanism is needed to explain the hydrological changes during HE3. It is possible that ITCZ position and attendant atmospheric teleconnections remained similar during all six HE, even if the AMOC strength and sedimentary IRD percentages varied.

We converted our δD values to $\delta^{18}O$ space and applied the range of values to the Dansgaard (1964) temperature equation. Results showed a positive maximum temperature shift of 8.5˚C across stadial/interstadial periods in Florida - assuming all isotope variability for this chain length was temperature driven. Evaporation is a secondary mechanism that could contribute to the 21‰ enrichment in δD of *n*-C_{23}. If the effect of modern evaporative enrichment (a value of ~5‰) were deducted from our calculation, the maximum temperature shift would reduce to a 6.5˚C warming in Florida during stadials. The range in calculated temperatures from the warm stadials to the cool interstadials in Florida is comparable to the estimated 6-10˚C range inferred between the cold early deglacial and warmer Holocene in the lowlands of northern Guatemala

(Hodell et al., 2012). A TEX_{86}-derived surface air temperature record from Lake Tanganyika demonstrates a similar magnitude of warming (~5 ˚C) during HE1 and the YD (Tierney et al., 2008).

The fact that both temperature and precipitation at Lake Tulane responded in concert with rapid climatic variability in the high-latitude Northern Hemisphere demonstrates that glacial calving events have a strong influence on climate in the subtropics. Although these events produce cooling throughout much of the Northern Hemisphere, it is apparent that this was not the case in peninsular Florida. The antiphase relationship underscores the complex teleconnections linking atmospheric temperatures with oceanic SSTs and circulation patterns. The reduction in AMOC strength limited the amount of thermal energy that could be redistributed to the poles, but resulted in the persistence of the AWP and intensification of ocean currents and trade winds in the low-latitude North Atlantic that increased atmospheric temperatures and precipitation. Atmospheric warming is seen in other terrestrial records (e.g. Tierney et al., 2008) during HE, however warming never coincides with an increase in precipitation. Thus, the response to rapid climate change events is regional and, therefore, highly variable. The climate system's reaction depends on myriad factors, including, but not limited to: SST gradients, latent heat fluxes, and circulation patterns that influence regional atmospheric circulation patterns.

Conclusions: Lake Tulane

I presented a record of environmental change recorded in the sediments of Lake Tulane, Florida, which were deposited across HE 2-4. Carbon isotope (Δ_{leaf}) measurements from leaf waxes show the combined effects of WUE and mixing of PFTs. Correlations between carbon isotopes and *Pinus* pollen concentrations increase with

decreasing carbon chain length, indicating less mixing from multiple plant groups in shorter-chain-length *n*-alkanes. Terrestrial δD_{lipid} values from these chain lengths were paired with aquatic δD_{lipid} values to estimate aridity changes across HE and intervening interstadials. These $\varepsilon_{(terr\text{-}aq)}$ values correlate strongly with *Pinus* pollen relative abundance, and, like the Δ_{leaf} values from *n*-$C_{27\text{-}29}$, signify lower WUE and less aridity during Pinus phases. Aquatic δD_{lipid} values record an ~8.5˚C temperature increase in Florida during HE. Taken together, our results demonstrate that the subtropics responded out of phase with high-latitude environmental changes during at least three of the late Pleistocene stadial-interstadial transitions. The region remained warm and wet because of oceanic/atmospheric patterns that limited northward export of warm, saline water.

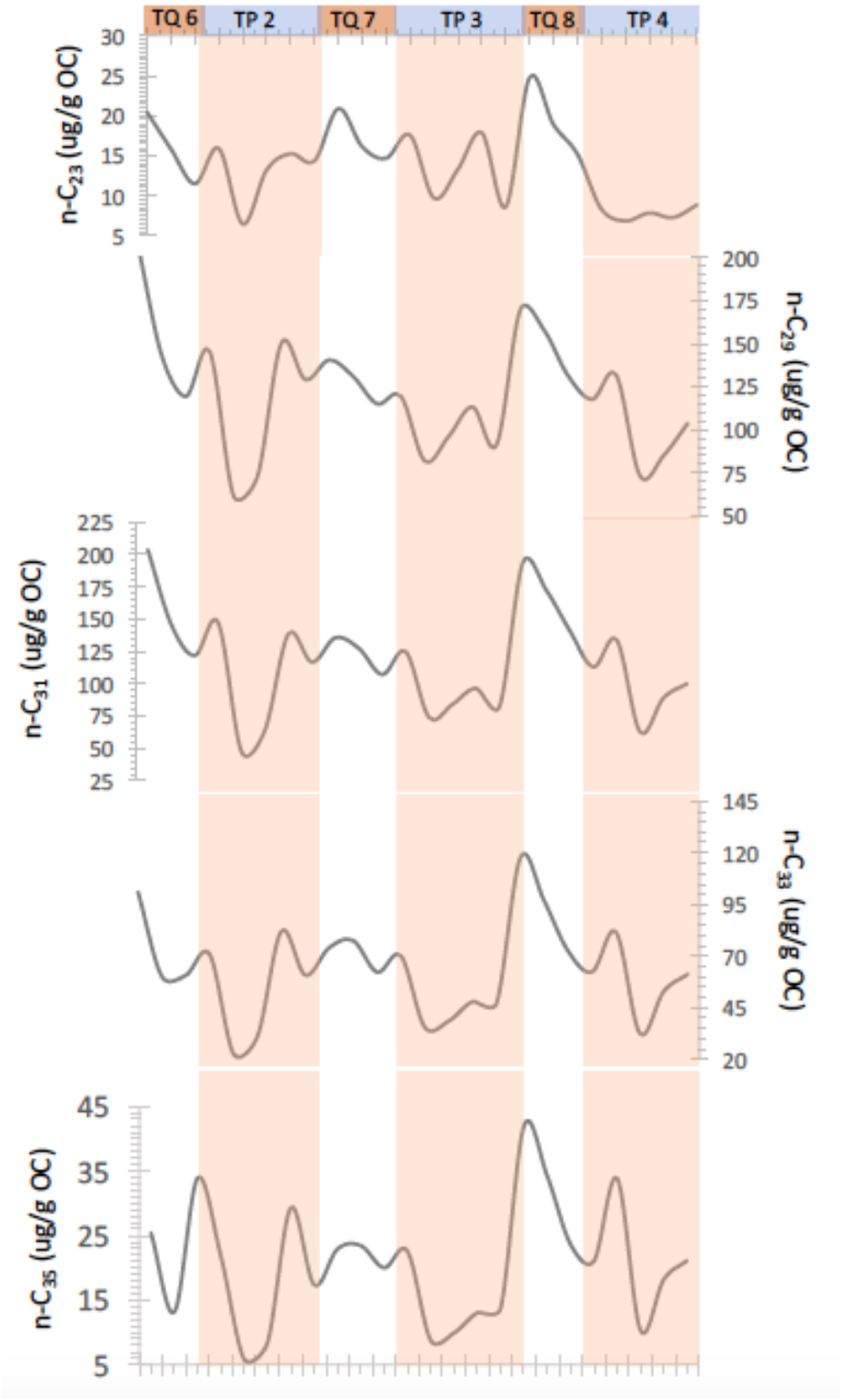

Figure 4-1. Concentrations of select *n*-alkane chain lengths. The vertical orange bars mark the extent of the *Pinus* zones, and both the *Pinus* (TP) and *Quercus* (TQ) zones are labeled at the top of the figure in blue, and red, respectively.

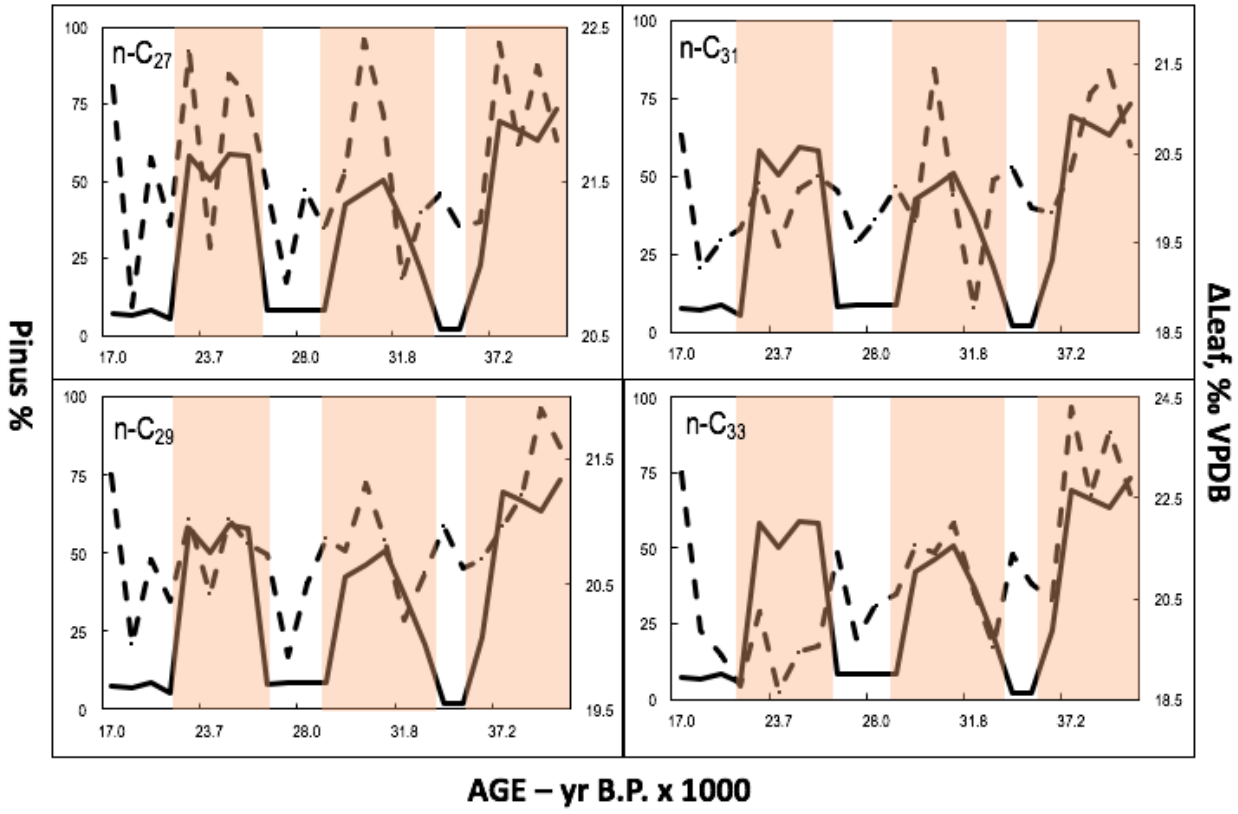

Figure 4-2. Select *n*-alkane chain lengths and their Δ_{leaf} values (dashed lines) plotted with the percent abundance of *Pinus* pollen (solid line). Tulane *Pinus* zones are represented with the orange bars. All data points have a 1σ SE value of ± 0.35‰

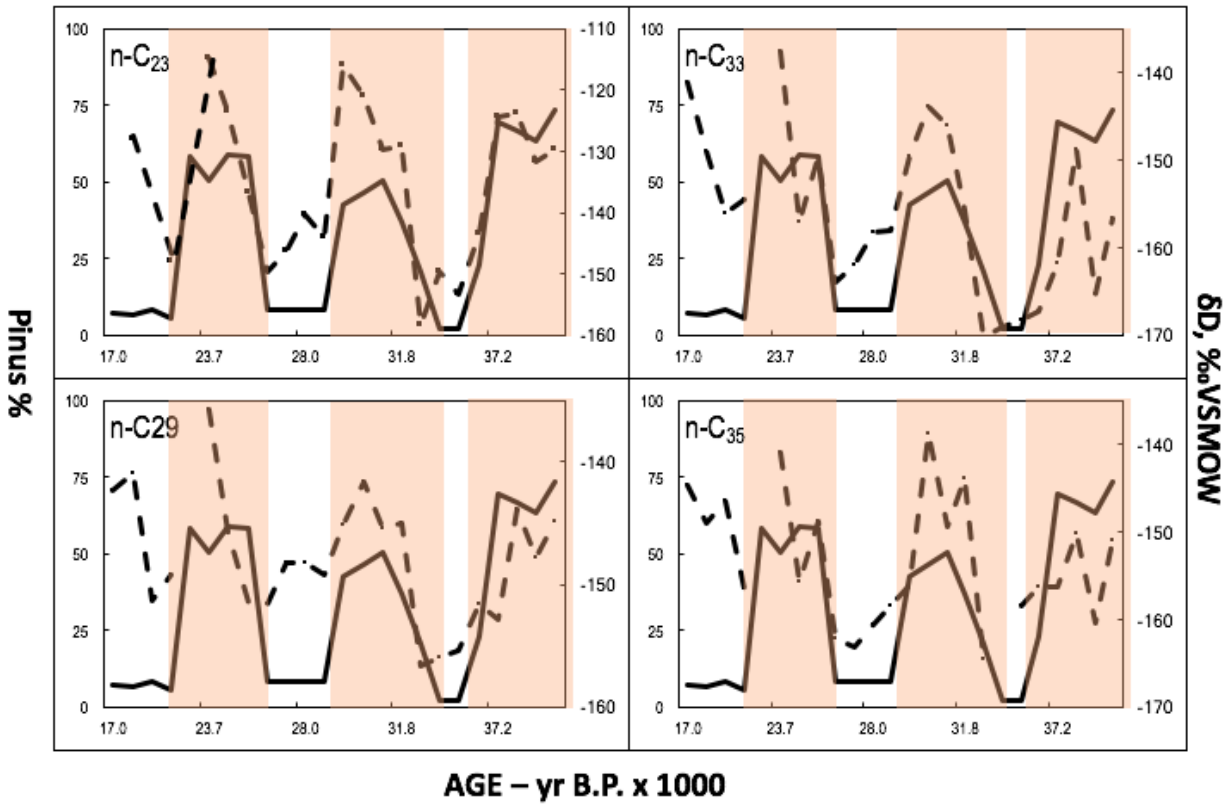

Figure 4-3. Select *n*-alkane chain lengths and their δD values (dashed lines) plotted with the percent abundance of *Pinus* pollen (solid line). Tulane *Pinus* zones are represented with the orange bars. The pooled 1σ SE for all samples was ± 3.2‰.

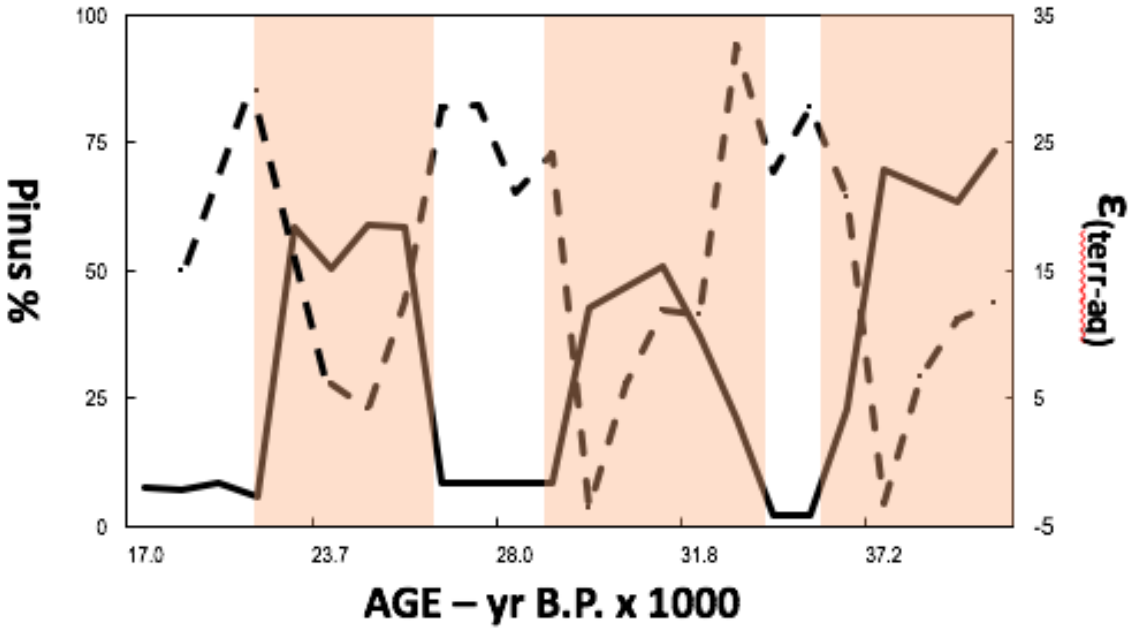

Figure 4-4. The $\varepsilon_{(terr\text{-}aq)}$ values (dashed line) plotted with the percent abundance of *Pinus* pollen (solid line). Tulane *Pinus* zones are represented with the orange bars. The $\varepsilon_{(terr\text{-}aq)}$ values are essentially an approximation of aridity, with higher values indicating more arid conditions. The pooled 1σ SE for all samples was ± 3.2‰.

Table 4-1. Values for the carbon preference index (CPI), average chain length (ACL), and submerged to emergent/terrestrial vegetation in the Lake Tulane core. The ages are calibrated following the methods outlined in Grimm et al. (2006), and the phases are Tulane *Quercus* (TQ) and Tulane *Pinus* (TP), which are also described in the Grimm et al. (2006) paper.

Age (cal. Yrs BP)	CPI	ACL25-35	P_{aq}	Phase
17038	3.21	29.64	0.17	TQ6
17345	2.97	29.54	0.18	TQ6
17655	0.84	29.94	0.16	TQ6
17965	2.04	29.73	0.17	TQ6
23522	2.75	29.23	0.21	TP2
23706	2.77	29.23	0.26	TP2
24447	2.81	29.69	0.19	TP2
25519	2.67	29.44	0.21	TP2
27716	2.63	29.48	0.24	TQ7
27925	2.90	29.63	0.22	TQ7
28030	2.89	29.64	0.21	TQ7
28134	2.76	29.68	0.22	TQ7
29693	3.09	29.55	0.18	TP3
30075	2.85	29.36	0.21	TP3
30457	2.93	29.31	0.24	TP3
31804	3.04	29.51	0.21	TP3
35511	2.27	30.00	0.19	TQ8
36068	2.35	30.04	0.15	TQ8
36207	2.33	29.93	0.15	TQ8
36347	2.71	29.84	0.14	TQ8
37180	2.38	30.13	0.11	TP4
38014	2.62	29.50	0.20	TP4
39386	2.66	29.96	0.16	TP4
39923	3.11	29.82	0.18	TP4

Table 4-2. Δ_{leaf} values for select *n*-alkane chain lengths extracted from the Lake Tulane core.

Age (cal yr BP)	C_{23} Δ-leaf	C_{27} Δ-leaf	C_{29} Δ-leaf	C_{31} Δ-leaf	C_{33} Δ-leaf	C_{35} Δ-leaf	Phase
17,038	23.73	22.11	21.38	20.70	23.00	19.10	TQ6
17,345	21.62	20.69	20.02	19.20	19.86	16.64	TQ6
17,655	23.85	21.65	20.70	19.52	19.38	17.17	TQ6
17,965	23.66	21.22	20.37	19.66	18.77	17.36	TQ6
23,522	n/a	22.34	21.01	20.16	20.26	20.15	TP2
23,706	22.53	21.07	20.42	19.46	18.64	n/a	TP2
24,447	22.57	22.19	21.01	20.10	19.45	18.88	TP2
25,519	22.39	22.05	20.83	20.24	19.56	18.68	TP2
27,716	21.19	21.46	20.74	20.08	21.41	18.99	TQ7
27,925	21.94	20.85	19.93	19.51	19.70	18.48	TQ7
28,030	22.54	21.44	20.50	19.75	20.37	18.51	TQ7
28,134	21.59	21.20	20.86	20.12	20.59	17.92	TQ7
29,693	n/a	21.56	20.76	19.73	21.57	n/a	TP3
30,075	24.55	22.41	21.31	21.44	21.40	n/a	TP3
30,457	24.42	21.93	20.85	20.02	22.02	n/a	TP3
31,804	23.01	20.87	20.21	18.77	20.61	n/a	TP3
35,511	21.00	21.29	20.58	20.20	19.55	17.84	TQ8
36,068	21.27	21.42	20.96	20.33	21.39	19.57	TQ8
36,207	20.96	21.20	20.63	19.89	20.80	19.47	TQ8
36,347	21.33	21.24	20.70	19.83	20.47	19.19	TQ8
37,180	n/a	22.39	20.96	20.33	24.30	20.61	TP4
38,014	21.94	21.73	21.22	21.18	22.56	18.67	TP4
39,386	22.80	22.24	21.90	21.43	23.82	21.30	TP4
39,923	21.82	21.76	21.60	20.60	22.59	19.88	TP4

Table 4-3. δD values for select *n*-alkane chain lengths extracted from the Lake Tulane core. Core phases are as follows: Tulane *Pinus* (TP), and Tulane *Quercus* (TQ).

Age (cal yr BP)	C_{23}- δD	C_{27}- δD	C_{29}- δD	C_{31}- δD	C_{33}- δD	C_{35}- δD	Phase
17,038	n/a	-137.80	-142.28	-151.42	-141.14	-144.74	TQ6
17,345	-127.91	-123.30	-140.89	-152.81	-148.98	-149.05	TQ6
17,655	n/a	-143.76	-151.31	-159.74	-156.16	-146.41	TQ6
17,965	-148.09	-138.05	-149.16	-157.94	-154.56	-156.54	TQ6
23,522	n/a	n/a	-144.21	n/a	n/a	n/a	TP2
23,706	-114.94	-124.69	-135.69	-153.80	-137.55	-140.93	TP2
24,447	-123.48	-132.01	-145.74	-155.02	-157.02	-155.75	TP2
25,519	-136.61	-133.97	-151.40	-157.44	-149.56	-148.89	TP2
27,716	-149.54	-138.46	-151.62	-161.61	-163.89	-162.25	TQ7
27,925	-146.19	-132.48	-148.22	-158.86	-161.96	-163.15	TQ7
28,030	-140.46	-134.38	-148.25	-158.89	-158.29	-160.51	TQ7
28,134	-144.15	-136.46	-149.27	-156.72	-158.06	-158.40	TQ7
29,693	-116.02	-136.45	-145.11	-153.21	-149.52	-156.03	TP3
30,075	-120.97	-130.33	-141.67	-151.62	-143.82	-138.71	TP3
30,457	-129.80	-138.57	-145.44	-151.97	-146.13	-149.46	TP3
31,804	-129.09	-139.11	-145.03	-157.99	-155.74	-143.82	TP3
35,511	-158.47	-135.15	-156.69	-169.64	-170.28	-164.54	TQ8
36,068	-149.61	-132.87	-155.91	-170.89	-169.13	n/a	TQ8
36,207	-153.24	-140.69	-155.34	-166.87	-168.35	-158.48	TQ8
36,347	-143.48	-143.49	-151.53	-168.93	-167.26	-156.18	TQ8
37,180	-124.40	-131.83	-152.92	-159.72	-161.84	-156.31	TP4
38,014	-123.74	-135.23	-143.84	-155.64	-148.83	-150.23	TP4
39,386	-131.76	-137.69	-147.86	-162.96	-165.22	-160.37	TP4
39,923	-129.70	-135.56	-144.90	-161.02	-156.71	-150.97	TP4

CHAPTER 5
CONCLUSIONS

Based upon analyses of bulk geochemical variables and alkyl lipid concentrations, I found that both Lakes Wauberg and Apopka became increasingly more productive and derived more of their organic matter from algal sources immediately after anthropogenic influences disturbed their watersheds. In Lake Apopka, this occurred in the mid-1940s, after nearby wetlands were converted to muck farms, and in Lake Wauberg, algal abundances increased in the 1980s, after major residential development began around the lake. Lake Sheelar has remained a low-productivity system since at least the turn of the 20th century, and algae contribute only minor amounts of organic matter to the sediments.

The evolution of Lake Harris, the focus of my second study, is recorded in the geochemical variables preserved within its sediments. The lake evolved from a shallow marsh-like system in the early Holocene (~10,000 yrs BP), when many lakes in Florida began to fill with water in response to deglaciation, to a shallow lake in the middle Holocene (7,000-5,000 yrs BP) as Florida transitioned from dry oak scrub vegetation to pine forests. Around 3,000 yrs BP, the effects of ENSO intensified, and Lake Harris achieved its modern limnetic state. In the modern era (after ca. AD 1950), concentrations of algal and cyanobacteria biomarkers increased by orders of magnitude in response to human-induced eutrophication.

Temporal patterns of carbon and hydrogen isotope signatures of *n*-alkanes extracted from Pleistocene-age sediments in Lake Tulane show correlations to Heinrich Events in the North Atlantic. During periods of cold sea-surface temperatures in the North Atlantic, hydrogen isotope ratios indicate that Florida remained relatively warm.

Combined hydrogen and carbon isotope values from multiple *n*-alkane chain lengths demonstrate that aridity increased during warm phases in the North Atlantic and decreased during cold phases, i.e. Heinrich Events. In paper 3, I conclude that Florida was likely buffered by warm sea surface temperatures that resulted from the reduced flow of the Atlantic meridional overturning circulation.

LIST OF REFERENCES

Aichner, B., Herzschuh, U., Wilkes, H., Vieth, A., & Böhner, J. (2010). δD values of n-alkanes in Tibetan lake sediments and aquatic macrophytes–A surface sediment study and application to a 16ka record from Lake Koucha. *Organic Geochemistry*, *41*(8), 779-790.

Aller, R. C. (1994). Bioturbation and remineralization of sedimentary organic matter: effects of redox oscillation. *Chemical Geology*, *114*(3-4), 331-345.

Anderson, D. M., Glibert, P. M., & Burkholder, J. M. (2002). Harmful algal blooms and eutrophication: nutrient sources, composition, and consequences. *Estuaries*, *25*(4), 704-726.

Appleby, P. G., & Oldfield, F. (1983). The assessment of 210Pb data from sites with varying sediment accumulation rates. In *Paleolimnology* (pp. 29-35). Springer Netherlands.

Bennett, K. D., & Willis, K. J. (2002). Pollen. In *Tracking environmental change using lake sediments* (pp. 5-32). Springer Netherlands.

Bianchi, T. S., & Canuel, E. A. (2011). *Chemical biomarkers in aquatic ecosystems*. Princeton University Press.

Bianchi, T. S., Mitra, S., & McKee, B. A. (2002). Sources of terrestrially-derived organic carbon in lower Mississippi River and Louisiana shelf sediments: implications for differential sedimentation and transport at the coastal margin. *Marine Chemistry*, *77*(2), 211-223.

Binford, M. W. (1990). Calculation and uncertainty analysis of 210Pb dates for PIRLA project lake sediment cores. *Journal of Paleolimnology*, *3*(3), 253-267.

Bond, G., Broecker, W., Johnsen, S., McManus, J., Labeyrie, L., Jouzel, J., & Bonani, G. (1993). Correlations between climate records from North Atlantic sediments and Greenland ice. *Nature*, *365*(6442), 143-147.

Bray, E. E., & Evans, E. D. (1961). Distribution of n-paraffins as a clue to recognition of source beds. *Geochimica et Cosmochimica Acta*, *22*(1), 2-15.

Brenner, M., Hodell, D. A., Leyden, B. W., Curtis, J. H., Kenney, W. F., Gu, B., & Newman, J. M. (2006). Mechanisms for organic matter and phosphorus burial in sedimentsof a shallow, subtropical, macrophyte-dominated lake. *Journal of Paleolimnology*, *35*(1), 129-148.

Brenner, M., Whitmore, T. J., Curtis, J. H., Hodell, D. A., & Schelske, C. L. (1999). Stable isotope ($\delta^{13}C$ and $\delta^{15}N$) signatures of sedimented organic matter as indicators of historic lake trophic state. Journal of Paleolimnology, 22(2), 205-221.

Broecker, W. S. (2006). Abrupt climate change revisited. *Global and Planetary Change*, *54*(3), 211-215.

Broecker, W., Bond, G., Klas, M., Clark, E., & McManus, J. (1992). Origin of the northern Atlantic's Heinrich events. *Climate Dynamics*, *6*(3-4), 265-273.

Cacho, I., Grimalt, J. O., Pelejero, C., Canals, M., Sierro, F. J., Flores, J. A., & Shackleton, N. (1999). Dansgaard-Oeschger and Heinrich event imprints in Alboran Sea paleotemperatures. *Paleoceanography*, *14*(6), 698-705.

Carlson, A. E., Oppo, D. W., Came, R. E., LeGrande, A. N., Keigwin, L. D., & Curry, W. B. (2008). Subtropical Atlantic salinity variability and Atlantic meridional circulation during the last deglaciation. *Geology*, *36*(12), 991-994.

Carr, A.F. (1934). The plankton and carbon dioxide-oxygen cycle in Lake Wauberg, Florida. Master's Thesis, University of Florida, Gainesville.

Castañeda, I. S., & Schouten, S. (2011). A review of molecular organic proxies for examining modern and ancient lacustrine environments. *Quaternary Science Reviews*, *30*(21), 2851-2891.

Chikaraishi, Y., & Naraoka, H. (2003). Compound-specific δD–δ 13 C analyses of n-alkanes extracted from terrestrial and aquatic plants. *Phytochemistry*, *63*(3), 361-371.

Cloern, J. E., Canuel, E. A., & Harris, D. (2002). Stable carbon and nitrogen isotope composition of aquatic and terrestrial plants of the San Francisco Bay estuarine system. *Limnology and oceanography*, *47*(3), 713-729.

Correll, D. L. (1998). The role of phosphorus in the eutrophication of receiving waters: A review. *Journal of Environmental Quality*, *27*(2), 261-266.

Craft, C. B., & Richardson, C. J. (1997). Relationships between soil nutrients and plant species composition in Everglades peatlands. *Journal of Environmental Quality*, *26*(1), 224-232.

Craft, C. B., Vymazal, J., & Richardson, C. J. (1995). Response of Everglades plant communities to nitrogen and phosphorus additions. *Wetlands*, *15*(3), 258-271.

Cranwell, P. A. (1982). Lipids of aquatic sediments and sedimenting particulates. *Progress in lipid research*, *21*(4), 271-308.

Cranwell, P. A., Eglinton, G., & Robinson, N. (1987). Lipids of aquatic organisms as potential contributors to lacustrine sediments—II. *Organic Geochemistry*, *11*(6), 513-527.

Dansgaard, W. (1964). Stable isotopes in precipitation. *Tellus*, *16*(4), 436-468.

Dean, W. E., & Gorham, E. (1998). Magnitude and significance of carbon burial in lakes, reservoirs, and peatlands. *Geology*, *26*(6), 535-538.

Diefendorf, A. F., Freeman, K. H., Wing, S. L., & Graham, H. V. (2011). Production of n-alkyl lipids in living plants and implications for the geologic past. *Geochimica et Cosmochimica Acta*, *75*(23), 7472-7485.

Diefendorf, A. F., & Freimuth, E. J. (2017). Extracting the most from terrestrial plant-derived n-alkyl lipids and their carbon isotopes from the sedimentary record: A review. *Organic Geochemistry*, *103*, 1-21.

Diefendorf, A. F., Mueller, K. E., Wing, S. L., Koch, P. L., & Freeman, K. H. (2010). Global patterns in leaf 13C discrimination and implications for studies of past and future climate. *Proceedings of the National Academy of Sciences*, *107*(13), 5738-5743.

Dolman, A. M., Rücker, J., Pick, F. R., Fastner, J., Rohrlack, T., Mischke, U., & Wiedner, C. (2012). Cyanobacteria and cyanotoxins: the influence of nitrogen versus phosphorus. *PloS one*, *7*(6), e38757.

Donar, C., Stoermer, E. F., & Brenner, M. (2009). The Holocene paleolimnology of Lake Apopka, Florida. *Nova Hedwigia*, 57-70.

Donders, T. H. (2014). Middle Holocene humidity increase in Florida: Climate or sea-level?. *Quaternary Science Reviews*, *103*, 170-174.

Donders, T. H., de Boer, H. J., Finsinger, W., Grimm, E. C., Dekker, S. C., Reichart, G. J., & Wagner-Cremer, F. (2011). Impact of the Atlantic Warm Pool on precipitation and temperature in Florida during North Atlantic cold spells. *Climate Dynamics*, *36*(1-2), 109-118.

Donders, T. H., Wagner, F., Dilcher, D. L., & Visscher, H. (2005). Mid-to late-Holocene El Nino-Southern Oscillation dynamics reflected in the subtropical terrestrial realm. *Proceedings of the National Academy of Sciences of the United States of America*, *102*(31), 10904-10908.

Donders, T. H., Wagner-Cremer, F., & Visscher, H. (2008). Integration of proxy data and model scenarios for the mid-Holocene onset of modern ENSO variability. Quaternary Science Reviews, 27(5), 571-579.

Douglas, P. M., Pagani, M., Brenner, M., Hodell, D. A., & Curtis, J. H. (2012). Aridity and vegetation composition are important determinants of leaf-wax δD values in southeastern Mexico and Central America. *Geochimica et Cosmochimica Acta*, *97*, 24-45.

Eadie, B. J., Chambers, R. L., Gardner, W. S., & Bell, G. L. (1984). Sediment trap studies in Lake Michigan: Resuspension and chemical fluxes in the southern basin. *Journal of Great Lakes Research*, *10*(3), 307-321.

Eglinton, G., & Hamilton, R. J. (1967). Leaf epicuticular waxes. *Science*, *156*(3780), 1322-1335.

Ehleringer, J. R., Cerling, T. E., & Helliker, B. R. (1997). C4 photosynthesis, atmospheric CO2, and climate. *Oecologia*, *112*(3), 285-299.

Ehleringer, J. R., & Cooper, T. A. (1988). Correlations between carbon isotope ratio and microhabitat in desert plants. *Oecologia*, *76*(4), 562-566.

Escobar, J., Buck, D. G., Brenner, M., Curtis, J. H., & Hoyos, N. (2009). Thermal stratification, mixing, and heat budgets of Florida lakes. *Fundamental and Applied Limnology/Archiv für Hydrobiologie*, *174*(4), 283-293.

Eynaud, F., De Abreu, L., Voelker, A., Schönfeld, J., Salgueiro, E., Turon, J. L., ... & Malaizé, B. (2009). Position of the Polar Front along the western Iberian margin during key cold episodes of the last 45 ka. *Geochemistry, Geophysics, Geosystems*, *10*(7).

Farquhar, G. D., Ehleringer, J. R., & Hubick, K. T. (1989). Carbon isotope discrimination and photosynthesis. *Annual review of plant biology*, *40*(1), 503-537.

Fairbanks, R. G., Mortlock, R. A., Chiu, T. C., Cao, L., Kaplan, A., Guilderson, T. P., ... & Nadeau, M. J. (2005). Radiocarbon calibration curve spanning 0 to 50,000 years BP based on paired 230 Th/234 U/238 U and 14 C dates on pristine corals. *Quaternary Science Reviews*, *24*(16), 1781-1796.

Feakins, S. J., & Sessions, A. L. (2010). Controls on the D/H ratios of plant leaf waxes in an arid ecosystem. *Geochimica et Cosmochimica Acta*, *74*(7), 2128-2141.

Ferrio, J. P., Voltas, J., & Araus, J. L. (2003). Use of carbon isotope composition in monitoring environmental changes. *Management of Environmental Quality: An International Journal*, *14*(1), 82-98.

Ficken, K. J., Li, B., Swain, D. L., & Eglinton, G. (2000). An n-alkane proxy for the sedimentary input of submerged/floating freshwater aquatic macrophytes. *Organic geochemistry*, *31*(7), 745-749.

Filley, T. R., Freeman, K. H., Bianchi, T. S., Baskaran, M., Colarusso, L., & Hatcher, P. G. (2001). An isotopic biogeochemical assessment of shifts in organic matter input to Holocene sediments from Mud Lake, Florida. *Organic Geochemistry*, *32*(9), 1153-1167.

Fisher, M. M., Brenner, M., & Reddy, K. R. (1992). A simple, inexpensive piston corer for collecting undisturbed sediment/water interface profiles. *Journal of Paleolimnology*, *7*(2), 157-161.

Florida Department of Environmental Protection (FDEP). (2008). Integrated Water Quality Assessment for Florida: 2008 305(b) Report and 303(d) List Update.

Florida LAKEWATCH. (2003). Florida LAKEWATCH Annual Data Summaries 2002. Department of Fisheries and Aquatic Sciences, University of Florida/Institute of Food and Agricultural Sciences. Library, University of Florida. Gainesville, Florida.

Flower, B. P., Hastings, D. W., Hill, H. W., & Quinn, T. M. (2004). Phasing of deglacial warming and Laurentide Ice Sheet meltwater in the Gulf of Mexico. *Geology*, *32*(7), 597-600.

Florea, L. J., & McGee, D. K. (2010). Stable isotopic and geochemical variability within shallow groundwater beneath a hardwood hammock and surface water in an adjoining slough (Everglades National Park, Florida, USA). *Isotopes in environmental and health studies*, *46*(2), 190-209.

Fulton III, R. S., & Smith, D. (2008). Development of phosphorus load reduction goals for seven lakes in the upper Ocklawaha river basin, Florida. Lake and Reservoir Management, 24(2), 139-154.

Gälman, V., Rydberg, J., de-Luna, S. S., Bindler, R., & Renberg, I. (2008). Carbon and nitrogen loss rates during aging of lake sediment: Changes over 27 years studied in varved lake sediment. *Limnology and Oceanography*, *53*(3), 1076-1082.

Garcin, Y., Schefuß, E., Schwab, V. F., Garreta, V., Gleixner, G., Vincens, A., ... & Sachse, D. (2014). Reconstructing C 3 and C 4 vegetation cover using n-alkane carbon isotope ratios in recent lake sediments from Cameroon, Western Central Africa. *Geochimica et Cosmochimica Acta*, *142*, 482-500.

Gat, J. R. (1996). Oxygen and hydrogen isotopes in the hydrologic cycle. *Annual Review of Earth and Planetary Sciences*, *24*(1), 225-262.

Grimm, E. C., Jacobson, G. L., Watts, W. A., Hansen, B. C., & Maasch, K. A. (1993). A 50,000-year record of climate oscillations from Florida and its temporal correlation with the Heinrich events. *SCIENCE-NEW YORK THEN WASHINGTON-*, *261*, 198-198.

Grimm, E. C., Watts, W. A., Jacobson, G. L., Hansen, B. C., Almquist, H. R., & Dieffenbacher-Krall, A. C. (2006). Evidence for warm wet Heinrich events in Florida. *Quaternary Science Reviews*, *25*(17), 2197-2211.

Gu, B., Chapman, A. D., & Schelske, C. L. (2006). Factors controlling seasonal variations in stable isotope composition of particulate organic matter in a soft water eutrophic lake. *Limnology and Oceanography*, *51*(6), 2837-2848.

Gu, B., Schelske, C. L., & Brenner, M. (1996). Relationship between sediment and plankton isotope ratios (δ13C and δ15N) and primary productivity in Florida lakes. *Canadian Journal of Fisheries and Aquatic Sciences*, *53*(4), 875-883.

Gu, B., Schelske, C. L., & Hodell, D. A. (2004). Extreme $\delta^{13}C$ enrichments in a shallow hypereutrophic lake: Implications for carbon cycling. *Limnology and Oceanography*, *49*, 1152-1159.

Han, J., & Calvin, M. (1969). Hydrocarbon distribution of algae and bacteria, and microbiological activity in sediments. *Proceedings of the National Academy of Sciences*, *64*(2), 436-443.

Hartman, G., & Danin, A. (2010). Isotopic values of plants in relation to water availability in the Eastern Mediterranean region. *Oecologia*, *162*(4), 837-852.

Hasler, A. D. (1947). Eutrophication of lakes by domestic drainage. *Ecology*, *28*(4), 383-395.

Hemming, S. R. (2004). Heinrich events: Massive late Pleistocene detritus layers of the North Atlantic and their global climate imprint. *Reviews of Geophysics*, *42*(1).

Ho, E. S., & Meyers, P. A. (1994). Variability of early diagenesis in lake sediments: evidence from the sedimentary geolipid record in an isolated tarn. *Chemical Geology*, *112*(3-4), 309-324.

Hodell, D. A., Turchyn, A. V., Wiseman, C. J., Escobar, J., Curtis, J. H., Brenner, M., ... & Brown, E. T. (2012). Late Glacial temperature and precipitation changes in the lowland Neotropics by tandem measurement of δ 18 O in biogenic carbonate and gypsum hydration water. *Geochimica et Cosmochimica Acta*, *77*, 352-368.

Hoogakker, B. A. A., Downy, F., Andersson, M. A., Chapman, M. R., Elderfield, H., McCave, I. N., ... & Gruetzner, J. (2013). Gulf Stream–subtropical gyre properties across two Dansgaard–Oeschger cycles. *Quaternary Science Reviews*, *81*, 105-113.

Huang, Y., Shuman, B., Wang, Y., Webb, T., Grimm, E. C., & Jacobson, G. L. (2006). Climatic and environmental controls on the variation of C 3 and C 4 plant abundances in central Florida for the past 62,000 years. *Palaeogeography, Palaeoclimatology, Palaeoecology*, *237*(2), 428-435.

Kahmen, A., Hoffmann, B., Schefuß, E., Arndt, S. K., Cernusak, L. A., West, J. B., & Sachse, D. (2013b). Leaf water deuterium enrichment shapes leaf wax n-alkane δD values of angiosperm plants II: Observational evidence and global implications. *Geochimica et Cosmochimica Acta*, *111*, 50-63.

Kahmen, A., Schefuß, E., & Sachse, D. (2013a). Leaf water deuterium enrichment shapes leaf wax n-alkane δD values of angiosperm plants I: Experimental evidence and mechanistic insights. *Geochimica et Cosmochimica Acta*, *111*, 39-49.

Kahmen, A., Simonin, K., Tu, K. P., Merchant, A., Callister, A., Siegwolf, R., ... & Arndt, S. K. (2008). Effects of environmental parameters, leaf physiological properties and leaf water relations on leaf water δ18O enrichment in different Eucalyptus species. *Plant, Cell & Environment*, *31*(6), 738-751.

Kenney, W. F., Brenner, M., Curtis, J. H., Arnold, T. E., & Schelske, C. L. (2016). A Holocene Sediment Record of Phosphorus Accumulation in Shallow Lake Harris, Florida (USA) Offers New Perspectives on Recent Cultural Eutrophication. *PloS one*, *11*(1), e0147331.

Kenney, W. F., Brenner, M., Curtis, J. H., & Schelske, C. L. (2010). Identifying sources of organic matter in sediments of shallow lakes using multiple geochemical variables. *Journal of Paleolimnology*, *44*(4), 1039-1052.

Kreveld, S. V., Sarnthein, M., Erlenkeuser, H., Grootes, P., Jung, S., Nadeau, M. J., ... & Voelker, A. (2000). Potential links between surging ice sheets, circulation changes, and the Dansgaard-Oeschger cycles in the Irminger Sea, 60–18 kyr. *Paleoceanography*, *15*(4), 425-442.

Landsberg, J. H., Flewelling, L. J., & Naar, J. (2009). Karenia brevis red tides, brevetoxins in the food web, and impacts on natural resources: Decadal advancements. *Harmful Algae*, *8*(4), 598-607.

Leuenberger, M., Siegenthaler, U., & Langway, C. (1992). Carbon isotope composition of atmospheric CO 2 during the last ice age from an Antarctic ice core. *Nature*, *357*(6378), 488-490.

Lynch-Stieglitz, J., Schmidt, M. W., Henry, L. G., Curry, W. B., Skinner, L. C., Mulitza, S., ... & Chang, P. (2014). Muted change in Atlantic overturning circulation over some glacial-aged Heinrich events. *Nature Geoscience*, *7*(2), 144-150.

Magill, C. R., Ashley, G. M., & Freeman, K. H. (2013). Water, plants, and early human habitats in eastern Africa. *Proceedings of the National Academy of Sciences*, *110*(4), 1175-1180.

Maliva, R., & Missimer, T. (2012). Aridity and drought. In *Arid lands water evaluation and management* (pp. 21-39). Springer Berlin Heidelberg.

Marcott, S. A., Clark, P. U., Padman, L., Klinkhammer, G. P., Springer, S. R., Liu, Z., ... & He, F. (2011). Ice-shelf collapse from subsurface warming as a trigger for Heinrich events. *Proceedings of the National Academy of Sciences*, *108*(33), 13415-13419.

Marshall, J. D., Brooks, J. R., & Lajtha, K. (2007). Sources of variation in the stable isotopic composition of plants. *Stable isotopes in ecology and environmental science*, *2*, 22-60.

Meyers, P. A. (1994). Preservation of source identification of sedimentary organic matter during and after deposition. *Chemical Geology*, *144*(3/4), 289-302.

Meyers, P. A. (1997). Organic geochemical proxies of paleoceanographic, paleolimnologic, and paleoclimatic processes. *Organic geochemistry*, *27*(5), 213-250.

Meyers, P. A. (2003). Applications of organic geochemistry to paleolimnological reconstructions: a summary of examples from the Laurentian Great Lakes. *Organic geochemistry*, *34*(2), 261-289.

Meyers, P. A., & Ishiwatari, R. (1993). Lacustrine organic geochemistry—an overview of indicators of organic matter sources and diagenesis in lake sediments. *Organic geochemistry*, *20*(7), 867-900.

Mook, W. G., Bommerson, J. C., & Staverman, W. H. (1974). Carbon isotope fractionation between dissolved bicarbonate and gaseous carbon dioxide. *Earth and Planetary Science Letters*, *22*(2), 169-176.

Mügler, I., Sachse, D., Werner, M., Xu, B., Wu, G., Yao, T., & Gleixner, G. (2008). Effect of lake evaporation on δD values of lacustrine n-alkanes: a comparison of Nam Co (Tibetan Plateau) and Holzmaar (Germany). *Organic Geochemistry*, *39*(6), 711-729.

Muri, G., & Wakeham, S. G. (2006). Organic matter and lipids in sediments of Lake Bled (NW Slovenia): source and effect of anoxic and oxic depositional regimes. *Organic Geochemistry*, *37*(12), 1664-1679.

Naafs, B. D. A., Hefter, J., Gruetzner, J., & Stein, R. (2013). Warming of surface waters in the mid-latitude North Atlantic during Heinrich events. *Paleoceanography*, *28*(1), 153-163.

Nichols, J. E. (2011). Procedures for extraction and purification of leaf wax biomarkers from peats. Mires and Peat, 7(13), 1-7.

O'Leary, M. H. (1988). Carbon isotopes in photosynthesis. *Bioscience*, *38*(5), 328-336.

Pailler, D., & Bard, E. (2002). High frequency palaeoceanographic changes during the past 140 000 yr recorded by the organic matter in sediments of the Iberian Margin. *Palaeogeography, Palaeoclimatology, Palaeoecology*, *181*(4), 431-452.

Palomo, L., & Canuel, E. A. (2010). Sources of fatty acids in sediments of the York River estuary: relationships with physical and biological processes. *Estuaries and coasts*, *33*(3), 585-599.

Parker, A. O., Schmidt, M. W., & Chang, P. (2015). Tropical North Atlantic subsurface warming events as a fingerprint for AMOC variability during Marine Isotope Stage 3. *Paleoceanography*, *30*(11), 1425-1436.

Parkes, R. J., & Taylor, J. (1983). The relationship between fatty acid distributions and bacterial respiratory types in contemporary marine sediments. *Estuarine, Coastal and Shelf Science*, *16*(2), 173IN5175-174189.

Patton, G. M., Martin, P. A., Voelker, A., & Salgueiro, E. (2011). Multiproxy comparison of oceanographic temperature during Heinrich Events in the eastern subtropical Atlantic. *Earth and Planetary Science Letters*, *310*(1), 45-58.

Pedentchouk, N., Sumner, W., Tipple, B., & Pagani, M. (2008). δ 13 C and δD compositions of n-alkanes from modern angiosperms and conifers: an experimental set up in central Washington State, USA. *Organic Geochemistry*, *39*(8), 1066-1071.

Peterson, B. J., & Fry, B. (1987). Stable isotopes in ecosystem studies. *Annual review of ecology and systematics*, *18*(1), 293-320.

Polissar, P. J., & D'Andrea, W. J. (2014). Uncertainty in paleohydrologic reconstructions from molecular δD values. *Geochimica et Cosmochimica Acta*, *129*, 146-156.

Quillen, A. K. (2009). Diatom-based paleolimnological reconstruction of quaternary environments in a Florida Sinkhole Lake.

Quillen, A. K., Gaiser, E. E., & Grimm, E. C. (2013). Diatom-based paleolimnological reconstruction of regional climate and local land-use change from a protected sinkhole lake in southern Florida, USA. *Journal of paleolimnology*, *49*(1), 15-30.

Rach, O., Brauer, A., Wilkes, H., & Sachse, D. (2014). Delayed hydrological response to Greenland cooling at the onset of the Younger Dryas in western Europe. *Nature Geoscience*, *7*(2), 109-112.

Rasmussen, T. L., & Thomsen, E. (2012). Changes in planktic foraminiferal faunas, temperature and salinity in the Gulf Stream during the last 30,000 years: influence of meltwater via the Mississippi River. *Quaternary Science Reviews*, *33*, 42-54.

Riedinger-Whitmore, M. A., Whitmore, T. J., Smoak, J. M., Brenner, M., Moore, A., Curtis, J., & Schelske, C. L. (2005). Cyanobacterial proliferation is a recent response to eutrophication in many Florida lakes: a paleolimnological assessment. *Lake and Reservoir Management*, *21*(4), 423-435.

Renold, M., Raible, C. C., Yoshimori, M., & Stocker, T. F. (2010). Simulated resumption of the North Atlantic meridional overturning circulation–Slow basin-wide advection and abrupt local convection. *Quaternary Science Reviews*, *29*(1), 101-112.

Sachse, D., Billault, I., Bowen, G. J., Chikaraishi, Y., Dawson, T. E., Feakins, S. J., ... & Polissar, P. (2012). Molecular paleohydrology: interpreting the hydrogen-isotopic composition of lipid biomarkers from photosynthesizing organisms. *Annual Review of Earth and Planetary Sciences*, *40*, 221-249.

Sachse, D., Gleixner, G., Wilkes, H., & Kahmen, A. (2010). Leaf wax n-alkane δD values of field-grown barley reflect leaf water δD values at the time of leaf formation. *Geochimica et Cosmochimica Acta*, *74*(23), 6741-6750.

Sachse, D., Radke, J., & Gleixner, G. (2004). Hydrogen isotope ratios of recent lacustrine sedimentary n-alkanes record modern climate variability. *Geochimica et Cosmochimica Acta*, *68*(23), 4877-4889.

Schelske, C. L. (1997). Sediment and phosphorus deposition in Lake Apopka.

Schelske, C. L., Lowe, E. F., Battoe, L. E., Brenner, M., Coveney, M. F., & Kenney, W. F. (2005). Abrupt biological response to hydrologic and land-use changes in Lake Apopka, Florida, USA. *AMBIO: A Journal of the Human Environment*, *34*(3), 192-198.

Schelske, C. L., Peplow, A., Brenner, M., & Spencer, C. N. (1994). Low-background gamma counting: applications for210Pb dating of sediments. *Journal of Paleolimnology*, *10*(2), 115-128.

Schmidt, M. W., Vautravers, M. J., & Spero, H. J. (2006). Rapid subtropical North Atlantic salinity oscillations across Dansgaard–Oeschger cycles. *Nature*, *443*(7111), 561-564.

Sharp, Z. (2007). *Principles of stable isotope geochemistry* (p. 344). Upper Saddle River, NJ: Pearson education.

Shumate, B. C., Schelske, C. L., Crisman, T. L., & Kenney, W. F. (2002). Response of the cladoceran community to trophic state change in Lake Apopka, Florida. *Journal of Paleolimnology*, *27*(1), 71-77.

Silliman, J. E., Meyers, P. A., & Bourbonniere, R. A. (1996). Record of postglacial organic matter delivery and burial in sediments of Lake Ontario. *Organic Geochemistry*, *24*(4), 463-472.

Silliman, J. E., & Schelske, C. L. (2003). Saturated hydrocarbons in the sediments of Lake Apopka, Florida. *Organic Geochemistry*, *34*(2), 253-260.

Smith F. A., & Freeman, K.H. (2006). Influence of physiology and climate on delta D of leaf wax n-alkanes from C-3 and C-4 grasses. *Geochimica Cosmochimica Acta*, 70, 1172–1187.

Stewart, G. R., Turnbull, M. H., Schmidt, S., & Erskine, P. D. (1995). 13C natural abundance in plant communities along a rainfall gradient: a biological integrator of water availability. *Functional Plant Biology*, *22*(1), 51-55.

Swain, E. B. (1985). Measurement and interpretation of sedimentary pigments. *Freshwater Biology*, *15*(1), 53-75.

Tierney, J. E., Russell, J. M., Huang, Y., Damsté, J. S. S., Hopmans, E. C., & Cohen, A. S. (2008). Northern hemisphere controls on tropical southeast African climate during the past 60,000 years. *Science*, *322*(5899), 252-255.

Törnqvist, T. E., González, J. L., Newsom, L. A., van der Borg, K., de Jong, A. F., & Kurnik, C. W. (2004). Deciphering Holocene sea-level history on the US Gulf Coast: A high-resolution record from the Mississippi Delta. Geological Society of America Bulletin, 116(7-8), 1026-1039.

Torres, I. C., Inglett, P. W., Brenner, M., Kenney, W. F., & Reddy, K. R. (2012). Stable isotope (δ13C and δ15N) values of sediment organic matter in subtropical lakes of different trophic status. Journal of paleolimnology, 47(4), 693-706.

Waghorn, M. J., Whitehead, D., Watt, M. S., Mason, E. G., & Harrington, J. J. (2015). Growth, biomass, leaf area and water-use efficiency of juvenile Pinus radiata in response to water deficits. *New Zealand Journal of Forestry Science*, *45*(1), 3.

Wakeham, S. G., Forrest, J., Masiello, C. A., Gélinas, Y., Alexander, C. R., & Leavitt, P. R. (2004). Hydrocarbons in Lake Washington sediments. A 25-year retrospective in an urban lake. *Environmental science & technology*, *38*(2), 431-439.

Wang, Y. J., Cheng, H., Edwards, R. L., An, Z. S., Wu, J. Y., Shen, C. C., & Dorale, J. A. (2001). A high-resolution absolute-dated late Pleistocene monsoon record from Hulu Cave, China. *Science*, *294*(5550), 2345-2348.

Wang, Y. V., Larsen, T., Leduc, G., Andersen, N., Blanz, T., & Schneider, R. R. (2013). What does leaf wax δD from a mixed C 3/C 4 vegetation region tell us?. *Geochimica et Cosmochimica Acta*, *111*, 128-139.

Waters, M. N. (2016). A 4700-year history of cyanobacteria toxin production in a shallow subtropical lake. *Ecosystems*, *19*(3), 426-436.

Watts, W. A. (1971). Postglacial and interglacial vegetation history of southern Georgia and central Florida. *Ecology*, *52*(4), 676-690.

Watts, W. A. (1975). A late Quaternary record of vegetation from Lake Annie, south-central Florida. *Geology*, *3*(6), 344-346.

Watts, W. A., & Hansen, B. C. S. (1994). Pre-Holocene and Holocene pollen records of vegetation history from the Florida peninsula and their climatic implications. *Palaeogeography, Palaeoclimatology, Palaeoecology*, *109*(2-4), 163-176.

Watts, W. A., & Stuiver, M. (1980). Late Wisconsin climate of northern Florida and the origin of species-rich deciduous forest. *Science*, *210*(4467), 325-327.

Weaver, A. J., Saenko, O. A., Clark, P. U., & Mitrovica, J. X. (2003). Meltwater pulse 1A from Antarctica as a trigger of the Bølling-Allerød warm interval. *Science*, *299*(5613), 1709-1713.

Weldeab, S., Schneider, R. R., & Kölling, M. (2006). Deglacial sea surface temperature and salinity increase in the western tropical Atlantic in synchrony with high latitude climate instabilities. *Earth and Planetary Science Letters*, *241*(3), 699-706.

White, W. A. (1970). The geomorphology of the Florida peninsula. GSA Bulletin, 51, 1-172.

Whiticar, M. J. (1999). Carbon and hydrogen isotope systematics of bacterial formation and oxidation of methane. *Chemical Geology*, *161*(1), 291-314.

Willard, D. A., & Bernhardt, C. E. (2011). Impacts of past climate and sea level change on Everglades wetlands: placing a century of anthropogenic change into a late-Holocene context. Climatic Change, 107(1-2), 59-80.

Zhang, X., Bianchi, T. S., & Allison, M. A. (2015). Sources of organic matter in sediments of the Colville River delta, Alaska: A multi-proxy approach. *Organic Geochemistry*, *87*, 96-106.

Zhao, J. X., Wang, Y. J., Collerson, K. D., & Gagan, M. K. (2003). Speleothem U-series dating of semi-synchronous climate oscillations during the last deglaciation. *Earth and Planetary Science Letters*, *216*(1), 155-161.

Zhou, H., Zhao, J., Feng, Y., Gagan, M. K., Zhou, G., & Yan, J. (2008). Distinct climate change synchronous with Heinrich event one, recorded by stable oxygen and carbon isotopic compositions in stalagmites from China. *Quaternary Research*, *69*(2), 306-315.

Ziegler, M., Nürnberg, D., Karas, C., Tiedemann, R., & Lourens, L. J. (2008). Persistent summer expansion of the Atlantic Warm Pool during glacial abrupt cold events. *Nature Geoscience*, *1*(9), 601-605.

BIOGRAPHICAL SKETCH

Thomas Elliott Arnold was born in Lancaster, PA. He graduated with a B.S. degree from Pennsylvania State University and with a PhD degree from the University of Florida in 2017. Dr. Arnold plans to continue his work in the field of organic geochemistry at the University of Pittsburgh. Although he learned a lot at the University of Florida, if he could do it all over again, he would pursue a career in theater and set design.